Master Thesis

Master's degree in Smart Electrical Networks and Systems (SENSE)

Thesis Topic

Resonance Impact on Inter-Area Oscillations of the Nordic Power System

Author: Dimitrios Dimitropoulos

Supervisor (RISE): Emil Hillberg
Examiner (UPC): Oriol Gomis Bellmunt

Summon: September 2019

ABSTRACT

Maintaining the robustness and stability of the Nordic power system is an essential task nowadays. The Nordic electricity network has the characteristics of bearing heavy generation in the northern region while supplying large consumption in the southern region through long transmission lines. Therefore, its operation might become more complex which in fact can lead to operational issues that did not exist in the past and might lead to major problems of the network.

The resonance interaction caused by forcing oscillations occurring at frequencies near the inter-area mode frequencies is such an issue and is studied thoroughly in this thesis project. Small signal stability analysis is the basis for the research of this phenomenon, as the inter-area modes need to be calculated.

For verifying this phenomenon, simulations were implemented in DigSilent PowerFactory software. The Nordic 32 test model is utilized, as it reflects the original Nordic system. Initially, the modes of the system are calculated, and the inter-area modes of interest are identified based on their frequency and damping ratio value. The observability, controllability and participation factors of the modes are considered for picking the modes of interest for further analysis. Then, forced oscillations in the form of load variations are implemented to study the resonance impact with the inter-area modes. As a mean to quantify the resonance impact, the active power flow of tie lines in the system is used.

A sensitivity study was performed to study how various factors of the forced oscillations influence the resonance impact. The sensitivity study considered the following aspects of the forced oscillations: frequency, amplitude, location, and type.

The amplification of the resulting oscillations seems to be affected by the value of controllability of the mode whose frequency couples with the inter-area frequency. This connection is evaluated in the simulations of this project and interesting results occur for further analysis.

Keywords

Small signal stability, electromechanical oscillations, forced oscillations, inter-area oscillations, damping ratio, controllability, observability, participation factor, resonance, Nordic 32 test system

ACKNOWLEDGEMENTS

After bringing in my memory the whole process for completing this thesis project – especially the time and effort required – I definitely need to thank some people with whom I collaborated and who contributed to this final outcome.

I would like to thank Dr. Emil Hilberg, my supervisor from RISE Research Institutes of Sweden for giving me the opportunity to work on this very interesting project. His constant guidance, his advice and the support he provided me were crucial for successfully completing this project. My gratitude also goes to Professor Mehrdad Ghandhari from KTH, who made me aware of that project at the very beginning. He also helped me whenever needed in case I had to work at the KTH computer room before I obtain the DigSilent PowerFactory license.

I would like to thank my rest co-supervisors, Dr. Bertil Beggren from KTH and Dr. Robert Eriksson from Svenska Kraftnät. Bertil's technical advice regarding the PowerFactory software and the test model I worked on was very valuable, especially at the beginning phase. In addition, Robert's comments during our planned meeting were very punctual and gave me the opportunity guide my research to an even deeper level. Fingrid's specialists Jukka Turunen and Antti-Juhani Nikkilä did also attend many of the planned meetings for my project and gave me useful advice on how to proceed, so I want to thank them, too.

Many thanks to Dr. Amin Nasri from the RISE office in Stockholm. He helped me to adjust to the office environment a lot, and our discussions regarding my project were truly fruitful.

I would like also to thank my supervisor at UPC, Barcelona, Professor Oriol Gomis for our great cooperation in this thesis work, the help he provided me to obtain the license for DigSilent PowerFactory software, as well as for the advice he gave me throughout the duration of the project.

I want now to thank my friends in Stockholm and in Barcelona. Their constant support throughout my master's programme was very important for me, as this period was very demanding and stressful, and we shared the same concerns. The time we spent was an escape from the daily routine – which consisted of studying mainly – and gave me the courage to keep on working till now.

My girlfriend Despoina needs a special reference here. I have lived with Despoina through most of the duration of my master's programme. I owe a lot to her for the constant support she gave me, for her tolerance and for the mental strength she provided me through her character. I have shared almost all my student life with her, and I will probably continue to do so after the completion of this master's programme, as she is the only person that can drive me to achieve my future goals.

Last but not least, I need to thank my family. The constant encouragement my parents gave me throughout these two years was the motivation I needed for completing this effort successfully. Especially, I want to dedicate this work to my mother who is giving a hard fight this period against a serious health problem, which I am sure she will overcome.

Dimitrios Dimitropoulos

Stockholm, September 2019

Table of Contents

List of Figures

1. Introduction

1.1 Background

Faults or load changes, which actually consist small disturbance of the system, lead to the creation of electromechanical oscillations. These might be either local or inter-area oscillations. There is a risk that these oscillations may lead to blackouts of the power system, since their damping limits the power system capacity. This is the case especially when power is being transferred through long transmission lines from a small system to a larger one.

The Transmission System Operators (TSOs) have the responsibility of the system and obtain real-time information about its stability state. Thus, they ought to monitor the oscillation modes continuously in order to estimate the damping ratios as well as the mode frequencies. The monitoring and the analysis of the power system events - by implementing simulations – are of vital importance for the TSOs in order to prepare in advance the actions that need to be taken in real case stability incidents.

Forced oscillations, which can be introduced to the system from external mechanisms - like mechanical aspects of generators or cyclic loads – can lead to catastrophic resonance phenomena for the power system and its components by interacting with low frequency inter-area modes. The concept of resonance is well known in physics. Resonance is the tendency of a system to oscillate with greater amplitude at some frequencies than the others. Therefore, in case an inter-area mode is poorly damped, and if forced oscillations are injected at a frequency close to the system mode frequency at a location where the inter-area mode is participating, then resonance can occur. This will lead to oscillations that are much larger than that of the source. Because of their geographically widespread nature, inter-area modes have proven to be more vulnerable than local modes to such interactions with forced oscillations.

The detection of the appearance of forced power oscillations and of their interactions with the system modes is a major challenge. At the moment, the number of installed phasor measurement units (PMUs) has been increased, making it feasible to detect forced oscillations and forecast resonance by utilizing measurement-based framework, and some methods have already been developed for this purpose.

1.2 Main Objectives

The main objective of this thesis project is to increase the current knowledge of resonance impact on inter-area oscillations, to identify scenarios where such events may occur, and to propose how measurements can be used to identify forced oscillations and their origins. The activities and the goals of the project are the following:

- Study of resonance theory and the interaction between forced oscillations and inter-area oscillations. This study is based on theory on small-signal stability, linearization, eigen-value and modal analysis
- Technical & mathematical description of the phenomena related to resonance
- Method description of suitable modal analysis to identify scenarios with risk for resonance

- Development of test model based on Nordic 32 test model and performing simulation study. The Nordic 32 test model is simulated by utilizing the software PowerFactory
- Assessment of the obtained results and reporting

1.3 Thesis Outline

The project is split in two parts. The first part covers the theoretical background of the resonance phenomena on the power system. The inter-area oscillations and forced power are analyzed, the resonance theory is explained. In the second part, the Nordic 32 test system is presented along with the simulation results which are obtained. The outline of the thesis project is given below:

- **Chapter 1** gives a short background of the resonance impact on the power systems by the interaction of forced oscillations and inter-area mode oscillations. Overall, the project is introduced, and the main goals and objectives are outlined.
- **Chapter 2** introduces the small signal stability theory which is the theoretical basis of the project
- **Chapter 3** gives an insight on inter-area oscillations and forced oscillations, and introduces the resonance theory
- **Chapter 4** describes the Swedish test system Nordic32 which is utilized for the simulations
- **Chapter 5** presents the simulation results obtained by utilizing the software DigSilent PowerFactory after following certain scenarios for the Nordic32 test system
- **Chapter 6** gives the summary of the project. The conclusion obtained are presented along with plans for future work.

2. Small Signal Stability

The small signal stability analysis consists the ability of the power system to maintain its synchronism while subjected to small disturbances. This analysis is applied to linearized system models and provides useful information about the inherent dynamic characteristics of the system. Analysis of small signal stability is usually performed in the frequency-domain, however, information gained by time-domain simulation can also be utilized. [1]

Small disturbances, like the normal small fluctuations in the system loads or small changes of the set values of some parameters, are always present in a power system. They normally result in power (or electromechanical) oscillations that are stable; in other words, the oscillations are positively damped and decay with time. On the other hand, these spontaneous oscillations may occasionally grow in amplitude with time, because of insufficient damping. This leads to sustained low frequency oscillations that cause loss of synchronism.

The low frequency oscillations of the inter-area mode of the system are investigated in depth, since their interaction with forced oscillation can lead to resonance phenomena. For that purpose, modal analysis and linearization techniques are of great importance, as they set the basis of the low frequency oscillations. The purpose of this chapter is to describe the theoretical background of these concepts.

2.1 Modal Analysis

The Linear Time-Invariant (LTI) system is considered, with the following form [3]:

$$\begin{aligned} \dot{\boldsymbol{x}}(\boldsymbol{t}) &= \boldsymbol{A}\boldsymbol{x}(\boldsymbol{t}) + \boldsymbol{B}\mathcal{U}(\boldsymbol{t}) \\ \mathcal{Y}(\boldsymbol{t}) &= \boldsymbol{C}\boldsymbol{x}(\boldsymbol{t}) \end{aligned} \quad \textbf{(1)}$$

where

- x is a vector that contains the system's state variables of order $(n_x \times 1)$ where n_x: number of state variables.
- $\mathcal{Y}$ is a vector that contains the system outputs or measured values of order of $(m \times 1)$ where m : number of system outputs.
- $\mathcal{U}$ is a vector that contains the system inputs or control variables of order $(r \times 1)$ where r : number of system inputs.
- A is the state matrix of the system, as defined before, of order $(n_x \times n_x)$.
- B is the input matrix of the system of order $(n_x \times r)$.
- C is the output matrix of the system of order $(m \times n_x)$.

Considering the unforced LTI system, after letting $\mathcal{U}$ equal to zero, then the form of LTI I shown below:

$$\dot{\boldsymbol{x}}(\boldsymbol{t}) = \boldsymbol{A}\boldsymbol{x}(\boldsymbol{t}) \quad \textbf{(2)}$$

2.1.1 Eigenvalues

The eigenvalues of A can be defined as the $\boldsymbol{n_x}$ solutions of $\boldsymbol{\lambda = \lambda_1, \dots, \lambda_{n_x}}$. These solutions satisfy the equation

$$\boldsymbol{det(A - \lambda I) = 0} \quad \textbf{(3)}$$

where “det” stands for determinant, and **I** is the identity matrix.

The eigenvalues can be real or complex numbers. Commonly, each eigenvalue $\boldsymbol{\lambda_i}$ corresponds to a mode of the system. The stability of an equilibrium point can be determined based on the eigenvalues of the system. A real eigenvalue corresponds to a non-oscillatory mode. A negative real eigenvalue represents a decaying mode whereas a positive real eigenvalue monotonic instability. The larger the magnitude of the eigenvalue is, the faster the decay will be. [1]

If A is real, then eigenvalues are complex numbers that always occur in conjugate pairs. Each pair corresponds to an oscillatory mode (the eigenvalues are distinct), and is expressed (for the i-th mode) by [1]

$$\boldsymbol{\lambda_i = \sigma_i \pm j\omega_{pi}} \quad \textbf{(4)}$$

The damping of the i-th mode is given by the real component $\boldsymbol{\sigma_i}$. A negative σ represents a damped oscillatory mode, however a positive σ represents an oscillatory instability. The imaginary component $\boldsymbol{\omega_{pi}}$ gives the oscillation frequency of the i-th mode, and is expressed by [1]

$$\boldsymbol{f_{pi} = \frac{\omega_{pi}}{2\pi}} \quad \textbf{(5)}$$

The damping ratio of the i-th mode is given below [1]

$$\boldsymbol{\zeta_i = \frac{-\sigma_i}{\sqrt{{\sigma_i}^2 + {\omega_{pi}}^2}}} \quad \textbf{(6)}$$

and the decay rate of the oscillation amplitude is determined by a positive damping ratio.

2.1.2 Eigenvectors

The right eigenvector of A corresponding to the eigenvalue $\boldsymbol{\lambda_i}$ matches any non-zero vector V_i^r which satisfies

$$\boldsymbol{AV_i^r = \lambda_i V_i^r} \quad \textbf{(7)}$$

and V_i^r is a column vector of order $n_x x 1$.[3]

Likewise, the left eigenvector of A corresponding to the eigenvalue $\boldsymbol{\lambda_i}$ matches any non-zero vector V_i^l which satisfies

$$\boldsymbol{V_i^l A = \lambda_i V_i^l} \quad \textbf{(8)}$$

and V_i^l is a row vector of order $1 x n_x$.

It can be easily concluded that

$$\boldsymbol{V_i^l V_j^r = 0} \quad \textbf{(9)}$$
$$\boldsymbol{V_i^l V_i^r = C_i \neq 0}$$

It must be noted that $\boldsymbol{V_i^r}$ (or $\boldsymbol{V_i^l}$) is not a unique solution. In fact, $\boldsymbol{kV_i^l}$ (where k is a scalar) can also be a solution. Because of this property, the normalization of the right and left eigenvectors is feasible so that [3]

$$\boldsymbol{V_i^l V_i^r} = \begin{bmatrix} \boldsymbol{u_{i1}^l} & \boldsymbol{u_{21}^l} & \dots & \boldsymbol{u_{in_x}^l} \end{bmatrix} \begin{bmatrix} \boldsymbol{u_{1i}^r} \\ \boldsymbol{u_{2i}^r} \\ \vdots \\ \boldsymbol{u_{n_x i}^r} \end{bmatrix} = \mathbf{1} \tag{10}$$

Physically, the right eigenvector describes how each mode of oscillation is distributed among the systems states. It is sometimes called mode shape. The left eigenvector, together with the input coefficient matrix and the disturbance determines the amplitude of the mode. [2]

2.1.3 Modal Matrices

It is convenient – for modal analysis purposes - to introduce the following modal matrices [3]:

$$\begin{aligned} \boldsymbol{V^R} &= \begin{bmatrix} \boldsymbol{V_1^r} & \boldsymbol{V_2^r} & \dots & \boldsymbol{V_{n_x}^r} \end{bmatrix} \\ &= \begin{bmatrix} \boldsymbol{u_{11}^r} & \boldsymbol{u_{12}^r} & \dots & \boldsymbol{u_{1n_x}^r} \\ \boldsymbol{u_{21}^r} & \boldsymbol{u_{22}^r} & \dots & \boldsymbol{u_{2n_x}^r} \\ \vdots & \vdots & \ddots & \vdots \\ \boldsymbol{u_{n_x 1}^r} & \boldsymbol{u_{n_x 2}^r} & \dots & \boldsymbol{u_{n_x n_x}^r} \end{bmatrix} \end{aligned} \tag{11}$$

$$\begin{aligned} \boldsymbol{V^L} &= \begin{bmatrix} \left(\boldsymbol{V_1^l}\right)^{\boldsymbol{T}} & \left(\boldsymbol{V_2^l}\right)^{\boldsymbol{T}} & \dots & \left(\boldsymbol{V_{n_x}^l}\right)^{\boldsymbol{T}} \end{bmatrix}^{\boldsymbol{T}} \\ &= \begin{bmatrix} \boldsymbol{u_{11}^l} & \boldsymbol{u_{12}^l} & \dots & \boldsymbol{u_{1n_x}^l} \\ \boldsymbol{u_{21}^l} & \boldsymbol{u_{22}^l} & \dots & \boldsymbol{u_{2n_x}^l} \\ \vdots & \vdots & \ddots & \vdots \\ \boldsymbol{u_{n_x 1}^l} & \boldsymbol{u_{n_x 2}^l} & \dots & \boldsymbol{u_{n_x n_x}^l} \end{bmatrix} = \left(\boldsymbol{V^R}\right)^{-\mathbf{1}} \end{aligned} \tag{12}$$

as well as the diagonal matrix

$$\boldsymbol{\Lambda} = \begin{bmatrix} \boldsymbol{\lambda_1} & \mathbf{0} & \dots & \mathbf{0} \\ \mathbf{0} & \boldsymbol{\lambda_2} & \dots & \mathbf{0} \\ \vdots & \vdots & \ddots & \vdots \\ \mathbf{0} & \mathbf{0} & \dots & \boldsymbol{\lambda_{n_x}} \end{bmatrix} \tag{13}$$

Based on the above matrices, equation (3) from which the right eigenvector is defined can also be expressed as

$$\boldsymbol{AV^R} = \boldsymbol{V^R \Lambda} \tag{14}$$

and the matrix A can be diagonalized by its modal matrix $\boldsymbol{V^R}$.

2.1.4 Modes of the system

The state matrix A is not a diagonal matrix and the dynamic of each state variable of the unforced LTI system (2) is a linear combination of the other state variables. Therefore, the identification of the parameters that have significant impact on the dynamic of each state variable is a demanding task. To overcome this difficulty, the

system (2) is transformed to an LTI system whose state matrix is diagonalized as follows (based on the modal matrices).

First, a new state vector ξ is established by the transformation [3]

$$\boldsymbol{\xi(t) = V^L x(t) = \left(V^R\right)^{-1} x(t)} \quad \textbf{(15)}$$

and

$$\boldsymbol{x(t) = V^R \xi(t)} \quad \textbf{(16)}$$

The combination of this transformation with the original system (2) results in the following transformed system

$$\begin{aligned} \boldsymbol{V^R \dot{\xi}(t) = A V^R \xi(t) \Rightarrow} \\ \boldsymbol{\dot{\xi}(t) = \left(V^R\right)^{-1} A V^R \xi(t)} \\ \boldsymbol{= \Lambda \xi(t)} \end{aligned} \quad \textbf{(17)}$$

Thus, we now have an LTI system whose state matrix is diagonal, i.e. Λ. The dynamic system (17) represents $\boldsymbol{n_x}$ uncoupled first-order differential equations of the form [3]

$$\boldsymbol{\dot{\xi}(t) = \lambda_i \xi_i(t)} \qquad \boldsymbol{for\ i = 1, \ldots, n_x} \quad \textbf{(18)}$$

whose solutions are given by

$$\boldsymbol{\dot{\xi}(t) = \xi_i(0) e^{\lambda_i t}} \qquad \boldsymbol{for\ i = 1, \ldots, n_x} \quad \textbf{(19)}$$

where, $\boldsymbol{\xi_i(0)}$ is the initial value of $\boldsymbol{\xi_i(t)}$ at t = 0.

From (15), we have [3]

$$\boldsymbol{\xi_i(0) = V_i^l x(0)} \quad \textbf{(20)}$$

which is a scalar and will be denoted by $\boldsymbol{a_i}$. Moreover, $\boldsymbol{x(0)}$ is the initial values of all the original state variables $\boldsymbol{x(t)}$ at t = 0.

Next, thanks to the expression for x in (15) and also equations (19) and (20), the solution of the original dynamic system (2) is given below [3]

$$\begin{aligned} \boldsymbol{x(t)} &= \boldsymbol{\sum_{i=1}^{n_x} V_i^r \left[V_i^l x(0)\right] e^{\lambda_i t}} \\ &= \boldsymbol{\sum_{i=1}^{n_x} V_i^r\ a_i e^{\lambda_i t}} \end{aligned} \quad \textbf{(21)}$$

or for the k-th state variable

$$\boldsymbol{x_k(t) = \sum_{i=1}^{n_x} u_{ki}^r\ a_i e^{\lambda_i t}} \quad \textbf{(22)}$$

Equation (19) gives the dynamic modes (corresponding to $e^{\lambda_i t}$) of the system with magnitude a_i. Still, the dynamic response of each state variable is given by equation (22) which is a linear combination of n_x dynamic modes.

From equations (16) and (21) it is obvious that that the right eigenvector V_i^r describes the distribution of each dynamic mode among the system states x that describe the mode shape. In addition, from equation (20) we can see that the left eigenvector V_i^l weighs the contribution of the initial condition $x(0)$ to the i-th mode. Therefore, the k-th element of V_i^r measures the activity of the state variable $\boldsymbol{x_k}$ in the i-th mode, and the k-th element of V_i^l weighs the contribution of this activity to the i-th mode. [3]

2.1.5 Participation Factor

It is of utmost importance to measure properly the participation of state variables within a mode i for small-signal stability and control. The right eigenvector $\boldsymbol{V_i^r}$ is a possible choice for this issue as its elements measure the activity of the state variables in the mode i. The participation factor $\boldsymbol{p_{ki}}$ **,** which combines the right and left eigenvectors, measures the relative participation of the k-th state variable in the i-th mode, and vice versa. It is given by [3]

$$\boldsymbol{p_{ki} = u_{ik}^l u_{ki}^r = u_{ki}^r u_{ik}^l} \quad \textbf{(23)}$$

Since the $\boldsymbol{u_{ki}^r}$ measures the activity of the state variable $\boldsymbol{x_k}$ in the i-th mode and the $\boldsymbol{u_{ik}^l}$ weighs the contribution of this activity to the mode, the product $\boldsymbol{p_{ki}}$ measures the net participation.

For small-signal analysis purposes, it is convenient to introduce a matrix $\boldsymbol{P}$ containing all participation factors. This matrix is named participation matrix and has the following form [3]

$$\boldsymbol{P} = [\boldsymbol{P_1} \quad \dots \quad \boldsymbol{P}_{n_x}] \quad \textbf{(24)}$$

2.1.6 Modal controllability and observability

Consider the LTI system (1). By applying the transformation (16) to (1), the following formulas can be obtained [3]

$$\dot{\boldsymbol{\xi}}(\boldsymbol{t}) = \boldsymbol{\Lambda \xi}(\boldsymbol{t}) + \boldsymbol{V^L B}\mathcal{U}(\boldsymbol{t}) \quad \textbf{(25)}$$

$$\mathcal{Y}(\boldsymbol{t}) = \boldsymbol{C V^R \xi}(\boldsymbol{t}) \quad \textbf{(26)}$$

Equation (25) can be written as n_x uncoupled equations

$$\dot{\boldsymbol{\xi}}(\boldsymbol{t}) = \boldsymbol{\lambda_i \xi_i}(\boldsymbol{t}) + \sum_{\boldsymbol{j=1}}^{\boldsymbol{r}} \boldsymbol{V_i^l B_j} u_j(\boldsymbol{t}) = \boldsymbol{\lambda_i \xi_i}(\boldsymbol{t}) + \sum_{\boldsymbol{j=1}}^{\boldsymbol{r}} \boldsymbol{c_{ij}} u_j(\boldsymbol{t}) \qquad \boldsymbol{for\ i = 1, \dots, n_x} \quad \textbf{(27)}$$

where, $\boldsymbol{c_{ij} = V_i^l B_j}$, $\boldsymbol{V_i^l}$ is the i-th row of $\boldsymbol{V^L}$, $\boldsymbol{B_j}$ is the j-th column of B and $\mathrm{u}_j(\boldsymbol{t})$ is the j-th element of $\mathcal{U}(\boldsymbol{t})$.

Obviously, the effect of the input u_j on the i-th mode is insignificant if $\boldsymbol{c_{ij}}$ is equal to zero. Thus, the i-th mode is controllable if and only if there is any $c_{ij} \neq 0$.

The $n_x \times r$ matrix $\boldsymbol{V^L B}$ consists the **mode controllability matrix** whose element in the i-th row and j-th column is c_{ij}. By inspecting this matrix, the controllable (or

uncontrollable) modes can be identified. For example, the i-th mode is uncontrollable in case the i-th row of this matrix is zero.

Equation (26) can also be written as [3]

$$\mathcal{Y}_i(\boldsymbol{t}) = \sum_{\boldsymbol{j=1}}^{\boldsymbol{r}} \boldsymbol{C_j V_i^r}\, \xi_i(\boldsymbol{t}) = \sum_{\boldsymbol{j=1}}^{\boldsymbol{r}} \boldsymbol{o_{ij}}\, \xi_i(\boldsymbol{t}) \qquad \boldsymbol{for\ j = 1, \ldots., m} \quad \textbf{(28)}$$

where, $\boldsymbol{o_{ij}} = \boldsymbol{C_j V_i^r}$, $\boldsymbol{C_j}$ is the j-th row of C and $\boldsymbol{V_i^r}$ is the i-th column of $\boldsymbol{V^R}$. Also, the i-th mode cannot be observed in the j-th output variable (i.e. $\mathcal{Y}_i(\boldsymbol{t})$) if $\boldsymbol{o_{ij}}$ is equal to zero. Thus, the i-the mode is observable if and only if there is any $c_{ij} \neq 0$.

The $\mathrm{m} \times n_x$ matrix $\boldsymbol{CV^R}$ consists the **mode observability matrix** whose element in the j-th row and i-th column is $\boldsymbol{o_{ij}}$. By inspecting this matrix, the observable (or unobservable) modes can be identified. For example, the i-th mode is unobservable in case the i-th column of this matrix is zero. [3]

2.2 Linearization of the system

The dynamic of a non-linear power system is given in the following formulas [3]

$$\begin{aligned} \dot{\boldsymbol{x}} &= \boldsymbol{f}(\boldsymbol{x}, \boldsymbol{y}) \\ 0 &= \boldsymbol{g}(\boldsymbol{x}, \boldsymbol{y}) \end{aligned} \qquad \textbf{(29)}$$

The system is linearized around an operating point $(\boldsymbol{x_0}, \boldsymbol{y_0})$**.** Then, small signal stability can be utilized to this system. The linearized system is given below: [3]

$$\Delta\dot{\boldsymbol{x}} = \boldsymbol{f_x}\Delta\boldsymbol{x} + \boldsymbol{f_y}\Delta\boldsymbol{y} \qquad \textbf{(30)}$$

$$0 = \boldsymbol{g_x}\Delta\boldsymbol{x} + \boldsymbol{g_y}\Delta\boldsymbol{y} \qquad \textbf{(31)}$$

where the Jacobian matrices f_x, f_y, g_x, g_y are calculated by the following mathematical expressions

$$\boldsymbol{f_x} = \left[\frac{\partial \boldsymbol{f}(\boldsymbol{x}, \boldsymbol{y})}{\partial \boldsymbol{x}}\right]_{\boldsymbol{x=x_0, y=y_0}} \qquad \boldsymbol{f_y} = \left[\frac{\partial \boldsymbol{f}(\boldsymbol{x}, \boldsymbol{y})}{\partial \boldsymbol{y}}\right]_{\boldsymbol{x=x_0, y=y_0}}$$

$$\boldsymbol{g_x} = \left[\frac{\partial \boldsymbol{g}(\boldsymbol{x}, \boldsymbol{y})}{\partial \boldsymbol{x}}\right]_{\boldsymbol{x=x_0, y=y_0}} \qquad \boldsymbol{g_y} = \left[\frac{\partial \boldsymbol{g}(\boldsymbol{x}, \boldsymbol{y})}{\partial \boldsymbol{y}}\right]_{\boldsymbol{x=x_0, y=y_0}}$$

After solving equation (31) for $\Delta\boldsymbol{y}$**,** the following mathematical expression is obtained [3]

$$\Delta\boldsymbol{y} = -\left(\boldsymbol{g_y}\right)^{-1}\boldsymbol{g_x}\Delta\boldsymbol{x} \qquad \textbf{(32)}$$

Then, by utilizing equation (30), and after assuming that $\left(\boldsymbol{g_y}\right)^{-1}$ is non-singular, the following mathematical expression is obtained which describes the linearized system of the non-linear power system in (29) [3]

$$\Delta\dot{\boldsymbol{x}} = \left(\boldsymbol{g_y}\right)\Delta\boldsymbol{x} = \boldsymbol{A_S}\Delta\boldsymbol{x} \qquad \textbf{(33)}$$

where $\boldsymbol{A_S}$ describes the overall system state matrix. The eigenvalues of the linearized system are calculated by equation (3) where the state matrix $\boldsymbol{A}$ is now replaced by $\boldsymbol{A_S}$.

2.3 Summary

The main aspects of Small Signal Stability are of utmost importance for the purpose of this thesis project. The modal analysis of the linearized system is crucial in order to calculate the eigenvalues and eigenvectors of all the modes. Then, the modes of interest (inter-area modes) are identified, based on their frequency and their damping ratio values.

The observability, controllability and participation of each mode are crucial for the location of the forced oscillation. In fact, the observability plot of each mode identifies the areas of the system where the generators oscillate in different direction. Based on the controllability and participation, the bus on which the forced oscillation is applied can be identified. Then, the resonance impact is visible and can be investigated in many different cases.

3. Inter-Area Mode, Forced oscillations and Resonance phenomena

Electromechanical oscillations in power systems can be classified into two main groups:

- “Natural” system mode oscillations
- Forced oscillations

“Natural” system mode oscillations are caused by random load fluctuations which represent continuous small disturbances to the system. These disturbances excite poorly damped modes causing permanent low amplitude oscillations in the system. Forced oscillations are the result of different phenomena in power systems, such as cyclic loads, control loops in power plants, diesel generators etc. Therefore, this type of oscillations is not a result of the general dynamics of the power system, rather they are caused by particular system elements with a distinctive oscillatory behavior.

The interactions of low frequency inter-area modes and forced oscillations are of great interest and are studied in this thesis project. In fact, because of their geographically widespread nature, inter-area modes are very vulnerable to resonance from forced oscillations. In case an inter-area mode is poorly damped and at the same time forced oscillations are injected at a frequency close to the system mode frequency, then resonance can occur leading to oscillations that are much larger than that of the source. So, this chapter studies in depth and includes theoretical background on the aspects of forced oscillations, inter-area oscillations and resonance, which are later tested through simulations.

3.1 Inter-area Oscillations

The electromechanical modes of a system are normally categorized as either local or inter-area in nature. In case a single generator or plant swings against the system, then local modes occur. On the other hand, an inter-area mode occurs when several generators in an area swing against generators in another area. Since local modes are characterized by larger inertias and lower impedance paths, their frequencies have a tendency to be higher. Actually, local modes tend to be in the 1–2 Hz range while inter-area modes tend to be in the 0.2–1.0 Hz range. [9]

Normally, the inter-area modes are more troublesome. In fact, inter-area oscillations correspond to the inter-area modes and refer to the dynamics of the swing between groups of machines in one area against groups of machines in another area. This interaction is implemented via the transmission system. Possible causes can be small disturbances such as changes in loads or may occur as an aftermath of large disturbances. This form of instability (small-signal rotor-angle instability) in interconnected power systems is mostly led by low frequency inter-area oscillations. These oscillations maybe result from small disturbances, if this is the case, their effects might not be instantaneously noticed. Though, over a period, they may grow in amplitude and lead to the collapse of the system. [10]

Cases of inter-area oscillations have been reported for many decades. One of the most prominent cases is the WECC breakup in 1996. Mode properties of low frequency inter-area oscillations in large interconnected systems depend on the power network configuration, types of generator excitation systems and their locations, and load

characteristics. Furthermore, the natural frequency and damping of inter-area modes depend on the weakness of inter-area ties and on the power transferred through them.[10]

After applying modal analysis on the system, inter-area modes can easily be identified by the frequency values of the modes (5) and the damping ratios (6). After that identification, they are further investigated to ensure the resonance impact on them by forced oscillations with the same frequency.

3.1.1 Nordic Power system and Inter-area oscillations

The power networks in Finland, Sweden, Norway and eastern Denmark consists the Nordic synchronous power system. Several oscillatory modes exist between regions of the system. One inter-area mode of the system has a natural frequency that varies 0.3–0.4 Hz and where generators in southern Finland oscillate against generators in southern Sweden and southern Norway. The oscillating generators have some 2000 km between them. In the south, only HVDC connections exists and connects Finland and Sweden under the sea (Gulf of Bothnia).

The transmission capacity is limited in case of 0.3–0.4 Hz oscillations when power is exported from Finland to Sweden via AC-lines in the north. That fact enhances the importance of monitoring the frequency, amplitude, and damping of this mode. The oscillations of the 0.3–0.4 Hz mode are well observable on the AC tie-lines between Finland and Sweden.

The inter-area oscillations of the Nordic system, due to the resonance with forcing oscillation, seems to be becoming a major issue related to the power system oscillations. The worst case consists of a situation when simultaneously the system has low damping, the frequencies of the forced and natural oscillation are close, and the source location has high controllability on the oscillations. [7]

Figure 3.1 presents the Nordic power system

Figure 3. 1: The Nordic power system in 2019 [8]

3.2 Forced Oscillations

Forced oscillation phenomena in power system exist in the literature over the last decades. There are different sources of these oscillations. The regulation system of steam turbines may be the cause of such oscillatory behavior. In addition, the impact of cyclic loads in the system as well as of diesel generators consist possible causes for forced low-frequency oscillations.

All types of forced oscillations have some common characteristics – no matter their cause – that can be utilized for their identification. A forced oscillation is a permanent oscillation and has a specific frequency. Its range is described by a very narrow high amplitude peak. This characteristic can be determined from the fact that undamped sine signal is represented by the Dirac delta function in frequency domain.

Most of the spectral content of a forced oscillation is concentrated in one small frequency bin. However, the spectral content of a system mode is spread around the main peak. In Fig. 3.2, the spectral response of a forced oscillation at 1 Hz has all its

spectral content in a single frequency bin, while a damped oscillation has a more spread spectral content centered at 1 Hz as shown in Fig. 3.3. The resulting spectrum from the combination of the two above oscillations is presented in Fig. 3.4. This is similar to the spectrum which one should expect from a forced oscillation overlaying a true system mode. The understand of this characteristic is crucial when estimating power system damping. [4]

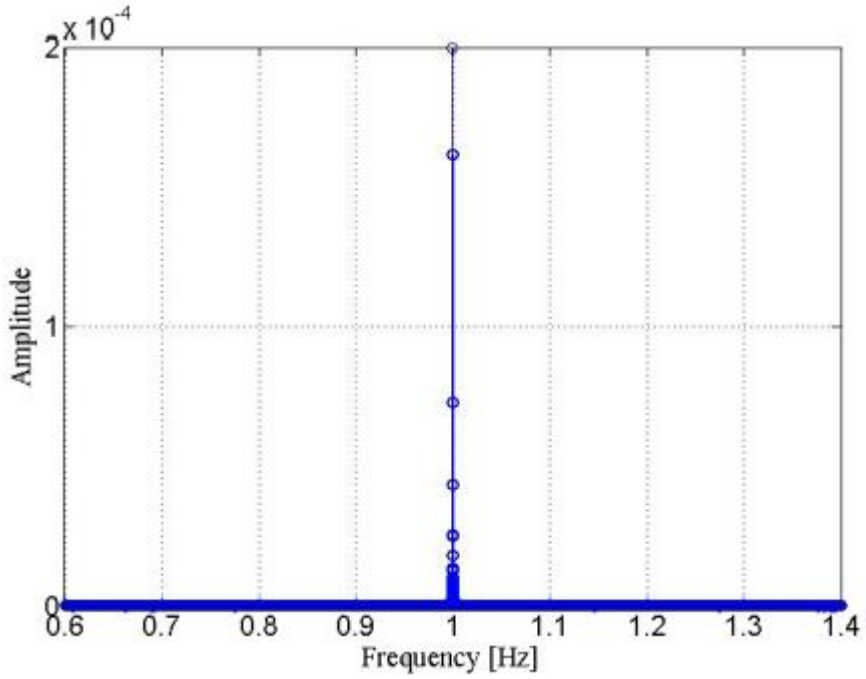

Figure 3. 2: FFTs computed with simulated data showing forced oscillation [4]

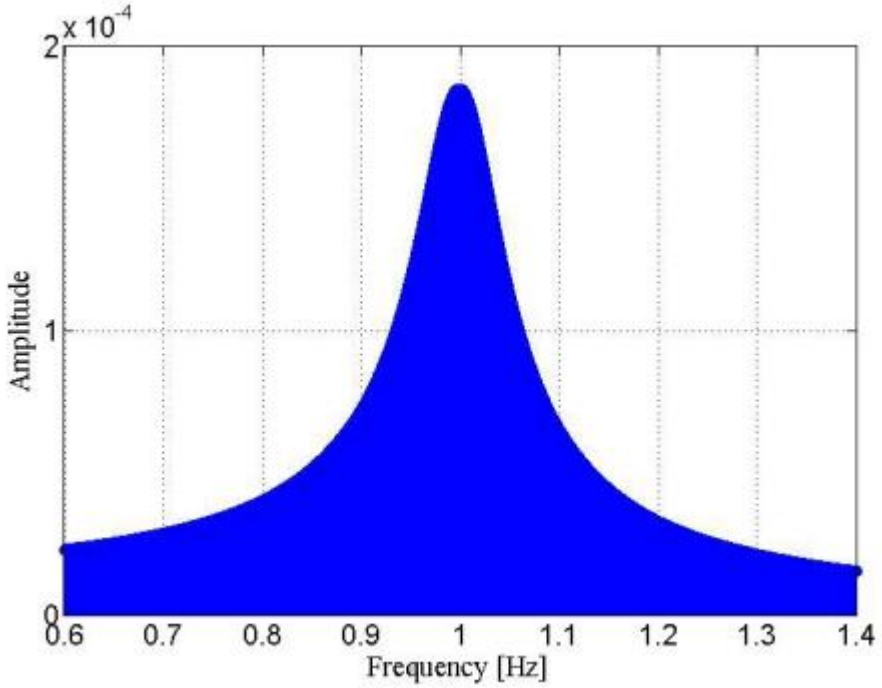

Figure 3. 3: FFTs computed with simulated data showing damped oscillation [4]

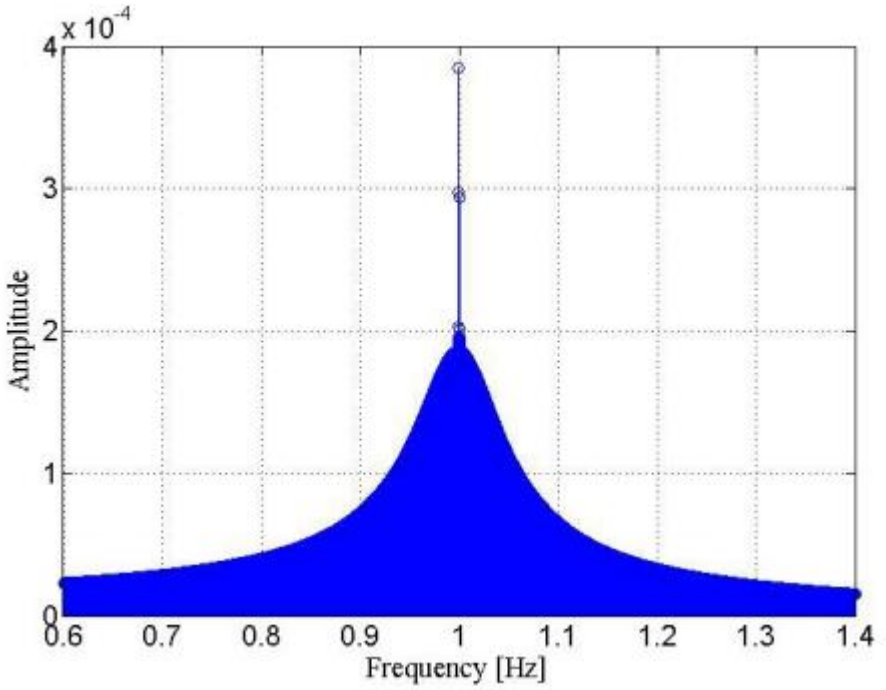

Figure 3. 4: FFTs computed with simulated data showing combination of a damped and forced oscillation [4]

3.2.1 Forced Oscillations Location

Forced oscillations lead to undesirable mechanical vibrations in electric devices, potentially increasing the probability of equipment failure and maintenance costs, as well as reducing of equipment lifespan. Therefore, it has become highly desirable for system operators to detect, locate, and mitigate potential forced oscillations in a nearly real-time fashion. Several methods on detecting and locating forced oscillations have been created and are presented below.

Multivariate Time Series Classification

A machine learning approach that utilizes phasor measurement unit (PMU) measurements of generator rotor angle and active power in power grids to locate the source of forced oscillation geographically down to the substation level is proposed. It is assumed that at least one PMU measurement is available for each power plant, and the model of the power system is also available.

Fig. 3.5 shows the flowchart of this method. In case of a forced oscillation, the response of generators is distinct for different oscillation source locations. Based on this intuition, dynamics of generators under various scenarios of forced oscillation source locations are generated through time domain simulation. Simulated PMU measurements of rotor angles and active power of generators are utilized to construct signature multivariate time series. Mahalanobis distance is trained offline through metric learning. If a forced oscillation is noticed, the same coefficients are measured and compared with the trained classifier in order for the source location of the oscillation to be detected. Dynamic time warping is utilized to handle the out-of-sync between testing data sets and training data sets due to the oscillation detection delay. [5]

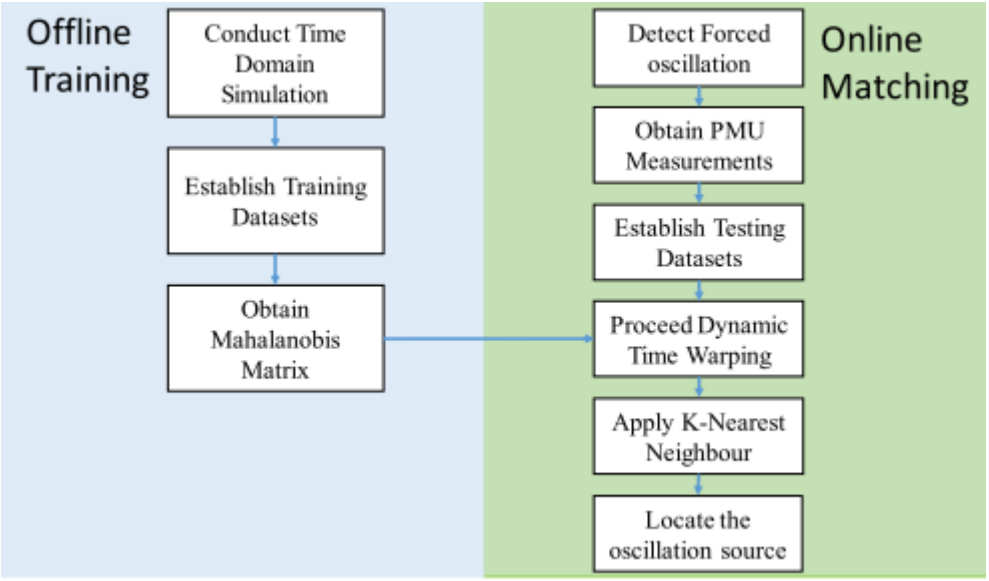

Figure 3. 5: Forced oscillation source identification based on multivariate time series classification

Mahalanobis Distance is a standard measure of the distance, which is characterized by a symmetry Positive Semi-Definite (PSD) matrix M. For two vectors x and y, where $x, y \in R^d$, the squared Mahalanobis distance between x and y is defined as follows:[5]

$$d_M(x, y) = (x - y)^T M (x - y)$$

If M=I, Mahalanobis distance degenerates to the standard Euclidean distance.

Traveling wave-based methods

Traveling wave-based methods need measurements relating to the a few starting periods of the oscillation. In that way, the arrival time or time differences between different locations can be determined. The advantage of this category of methods is their fast response. For making these methods applicable in practice, the detection accuracy of arrival time, the impact from the non-constant wave speed throughout the network and the adaptability to different network topologies should be first investigated and guaranteed.

Traveling wave-based methods use the principle of the electromechanical wave propagation to detect the source of an oscillation. Preferably, in case both the accurate detection of the arrival time of the oscillation at different locations and the actual wave speed map were available, the source location result should be correct and accurate. The earliest detected peak of the oscillation always first appears at the generator with forced oscillation, i.e. oscillation source. Also, this phenomenon is claimed in another way where the oscillation phase of the bus far away from the disturbance is lagging that of the bus close to the disturbance. [6]

Damping torque-based methods

By utilizing the damping torque-based methods, the generator with a negative damping torque coefficient consists the oscillation source. The type of methods and its growth relies on the extension of the damping torque concept from a single-machine-infinite-bus system (SMIB) to a multi-machine system.

The first introduction of the damping torque concept was utilized to offer a physical insight to system stability problem on an SMIB system. In a SMIB system, the damping

torque coefficient can be obtained by using the system response based on the least square method or Kalman filter.

The damping torque-based location methods have clear physical meaning and could be applied locally for each individual generator, i.e. distributed implementation. Thus, this type of methods could be promising for locating the bad damping source. On the other hand, this category of methods may not succeed in working under some forced oscillation cases. Furthermore, the measurements of generator electromagnetic torque, rotor angle and speed are often required for estimating the damping torque from system trajectories; however, these are not always directly measured by present PMUs. [6]

Mode shape estimation-based methods

Mode shape corresponds to the relative magnitude and phasing of the oscillation of the system. Its definition is based on the right eigenvectors of the state matrix of the linearized system model. The accurate system model, though, is rarely easy to get and the model-based mode shape analysis has only been applied to test systems for a better understanding. For using the mode shape information in real systems, many measurement- based methods for estimating the mode shape have been proposed.

This type of methods finds the oscillation source by estimating the mode shape using measurements from different locations. After that, it identifies the source based on the mode shape. In case of a 2-machine, the generator leading in mode shape phase contributes less damping. Then, it can be understood that the oscillation source is the leading generator. In case of large power systems, the leading generator in a leading group is identified as the oscillation source. Despite the fact that this method can recognize the oscillation source in many tested cases, it may possibly fail or provide wrong results. Furthermore, the fundamental location principle has not been thoroughly proved.

The mode shape estimation-based location methods that currently exist always try to be supported by finding a connection to the damping concept. There are no many investigations regarding the conditions under which the estimated mode shape from measurements sends the information for locating the oscillation source. It was testified, though, that under resonance condition the estimated mode shape from measurements could be quite different compared to the one from model-based eigenanalysis; thus, the contribution of mode shape information in locating the forced oscillation source may not be sufficient. [6]

Energy based methods

Transient energy function (TEF) is an application of Lyapunov function in power system stability analysis. It corresponds to the sum of the kinetic and potential energies of all generators in the synchronous coordinate framework.

The energy-based methods have the ability to identify generator-type oscillation source since the energy dissipation is proved to be consistent with the damping toque. When applying the energy-based methods to monitor the energy flows on branches in the network, the directions of the energy flows may be significantly affected by nearby loads such that the results may be misjudged. However, the usage of the characteristics of the oscillations – such as the concentric relaxation phenomenon for forced oscillation – that can lead to the accurate identification of the location of the source, is something that still needs more investigations.

The TEF based method is utilized for analyzing and characterizing the power system oscillations. The transient energy concept can be extended from generators to the branches in the network, which is called branch potential energy (BPE). The first attempt to apply the TEF or BPE for locating the source of forced oscillation was implemented by monitoring the energy flow throughout the network and finding the generator that injects the energy into the network as the source. The energy dissipation has been proven consistent with the damping torque under some assumptions and the source can be identified as the component producing energy, which means a negative contribution to the damping.

In another method, the energy function for generators based on the Port-Controlled Hamiltonian theory is used, which can consider the excitation system and governor models. Then, a location method based on this energy is applied by monitoring the energy injected to the network at each port and identifying the port with positive energy injection as the source. Nevertheless, the location result from the energy-based methods may be significantly affected by the load model, or even misleading. Concentric relaxation is also a phenomenon that could help avoid the erroneous location results for power systems under forced oscillations. So far, this category of methods has been largely applied to power systems in the past five years. [6]

Other methods

There are some other methods which depend on the system model or cannot provide a clear location of the oscillation source.

The *equivalent circuit-based method* is derived from the energy method, which provides another representation of the system under oscillations. It adopts the phasor concept for the deviations of power and frequency, and the ‘‘source’’ in the ‘‘circuit’’ is identified as the source of the oscillation.

The *hybrid dynamic simulation method* locates the oscillation source, which is based on both the system model and the measurement data. The location idea is to first replace part of the differential and algebraic variables, say V_p, with known measurements and perform the time domain simulation for the rest of the variables, say V_r. If the difference between the simulated response and the corresponding measurement data for V_r is larger than a pre-designed threshold, the source is identified to be within the area associated with V_r. Repeating the process will provide a more accurate location for the source.

An *Artificial Intelligence (AI) based method* is also utilized to locate the source of forced oscillation. Based on different operating conditions, the Characteristic ELLipsoid (CELL) is used to offline train a decision tree considering the sources respectively added to different generators or loads. Then, monitoring the parameters of the CELL using PMU measurements can help locate the source of the forced oscillation.

A *graph-theoretic and measurement-based method* is proposed in used for locating the input disturbance in large networked dynamic systems. This method first applies a system identification routine to construct the input-output transfer matrix and calculate the array of nominal localization keys. Then, an estimated localization key from local PMU measurements can be obtained for the corresponding local area. Comparing the estimated key with the nominal keys will indicate the location of the source.

Lastly, in the *generalized linear model-based method*, a generalized linear model for the system is fitted using the measurement data. Then, such fitted model may help

determine variables that have significant effects on mode damping, which might be related to the oscillation source. [6]

3.3 Resonance Phenomena

Resonance is a phenomenon that only occurs when the frequency at which a force is periodically applied is equal or nearly equal to one of the natural frequencies of the system on which it acts. This causes the system to oscillate with larger amplitude than when the force is applied at other frequencies. [11]

The classic resonance theory in physics is the basis for the interpretation of the resonance phenomena in a power system. In the classical theory, a simple spring mass system is considered as a starting point, with a forced undamped oscillation of $\boldsymbol{F_0 \cos(\omega t)}$. The spring mass system is shown in the Fig. 3.6:

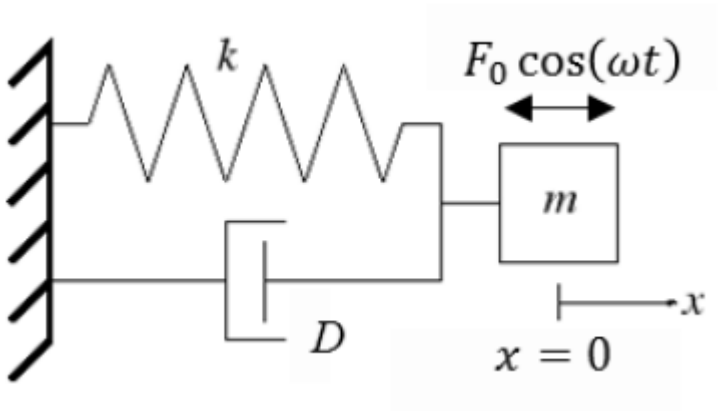

Figure 3. 6: Spring mass system with forced oscillation source [7]

By using the Newton's law and the notation of Figure 3.6, the following equation that describes the system is obtained: [12]

$$\boldsymbol{mX + bX + KX = F_0 \cos(\omega t)} \quad \textbf{(34)}$$

where the system natural frequency $\boldsymbol{\omega_0}$ and damping of the oscillation mode $\boldsymbol{\gamma}$ in the spring mass system are equal to

$$\boldsymbol{\omega_0{}^2 = \frac{K}{m}, \gamma = \frac{D}{m}} \quad \textbf{(35)}$$

and damping ratio is equal to $\boldsymbol{\zeta = {}^{\gamma}/_{2\omega_0}}$.

After rewriting equation (1) in the complex plane and using equation (35), we get

$$\boldsymbol{Z + \gamma Z + \omega_0{}^2 Z = \frac{F_0}{m} e^{j\omega t}} \quad \textbf{(36)}$$

The solution of equation (36) is in the following form:

$$\boldsymbol{Z = A e^{j(\omega t - \delta)}} \quad \textbf{(37)}$$

Thus, after combining equation (36) and (37), the amplitude **A** of the resulting oscillation in the spring mass system is equal to:

$$A = \frac{\frac{F_0}{m}}{\sqrt{({\omega_0}^2 - \omega^2)^2 + (\omega\gamma)^2}} \quad (38)$$

and its phase difference **δ** with the forced oscillation source is

$$\tan\delta = \frac{\omega\gamma}{{\omega_0}^2 - \omega^2} \quad (39)$$

When the amplitude A reaches its maximum value, then resonance happens. In case of an undamped system ($\gamma = 0$) and when the forced frequency equals the natural frequency ($\omega_0 = \omega$) , resonance occurs according to equation (38) and the amplitude of A reaches an infinite value. But in case of a damped system ($\gamma = 0$), then A obtains a finite value according to (38). Practically, the maximum amplitude – which corresponds to resonance – occurs at the maximum frequency value ω_{max} which is smaller than ω_0 (based on the value of damping). [12]

Three cases are of utmost importance:

$$\begin{cases} \omega \to 0 \quad A = \frac{F_0}{K} \quad \delta \to 0 \\ \omega \to \omega_0 \quad A = \frac{F_0}{K} Q \quad \delta \to \frac{\pi}{2} \\ \omega \to \infty \quad A = 0 \quad \delta \to \pi \end{cases} \quad (40)$$

where $Q = {\omega_0}/{\gamma}$.

Therefore, the maximum amplitude can be obtained by calculating the derivative from the first equation in (38) and solving it. The maximum value of amplitude A_{max} and the corresponding frequency ω_{max} are equal to:

$$\begin{cases} A_{max} = \frac{F_0}{K} \frac{Q}{\left(1 - \frac{1}{4Q^2}\right)^{1/2}} \\ \omega_{max} = \omega_0 \left(1 - \frac{1}{4Q^2}\right)^{1/2} \end{cases} \quad (41)$$

In the following figure, the amplitude A, in case of forced external oscillations occurring, is shown for a system with different level of damping.

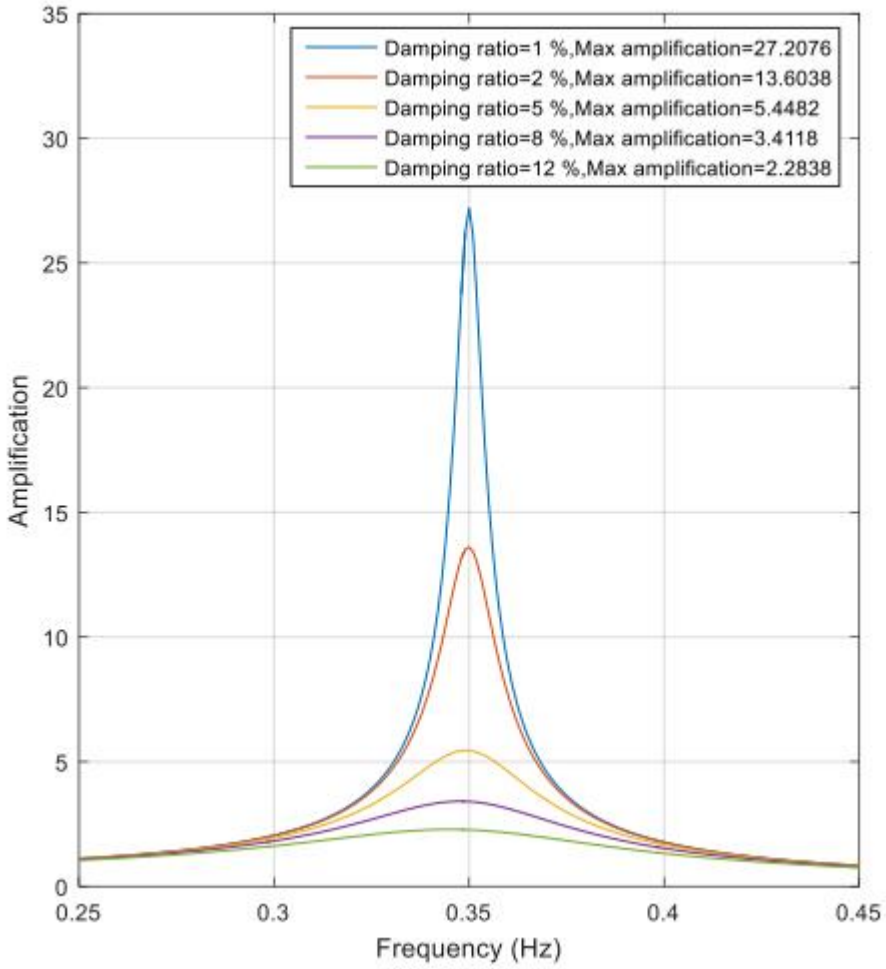

Figure 3. 7: Amplification of the forcing oscillations as a function of frequency in a spring mass mode. The resonance frequency is 0.35 Hz in this case. [7]

From Figure 3.7, the curve with the highest peak corresponds to the lowest damped system (ζ = 1%). At the same time, the curve with the lowest peak corresponds to the most damped system (ζ = 12%). According to the plot, the effect of resonance is minor for well-damped systems while it might be cause serious issues for poorly damped systems.

In addition, as the damping γ increases, then Q decreases. Thus, for higher damped systems, the practical resonance is at peak frequencies ω_{max} that are lower than ω_0 according to equation (40).

3.4 Summary

The importance of inter-area oscillations and forced oscillations is vital for the system's operation. In fact, each of these kinds of oscillations can lead to unexpected system's abnormal operation, as small disturbances affect inter-area modes and forced oscillations often lead to failure. The coupling of these kinds of oscillations, however, leads to a disastrous resonance phenomenon.

In subchapter 3.2, the resonance phenomenon was analyzed in terms of physics. In case of a power network, which is the case of this project, the resonance phenomenon occurrence is closely related to the low frequency of inter-area modes oscillations

calculated in small signal stability analysis. In fact, all the modes of the system are calculated based on the small signal stability analysis (section 2.1) and the inter-area modes are identified. Then, the low frequency electromechanical oscillations which resemble the forced oscillations and result in small signal instability interact with the inter-area oscillations with the same frequency. Therefore, the amplitude of the oscillations of the active power flowing on the tie-lines of the system is increased in a high rate, which actually consists a resonance phenomenon as described in section 3.3. This phenomenon is also called mode coupling and can lead to catastrophic blackouts. [18]

4. Nordic 32 System

The test system used to highlight the resonance phenomenon is a variant of the Nordic 32 system. The system is fictitious but has dynamic properties very similar to the Swedish and Nordic power system. The system is intended for simulations tools, especially for such that are suitable for long term dynamics.

4.1 System Overview

The system is depicted in the following one-line diagram

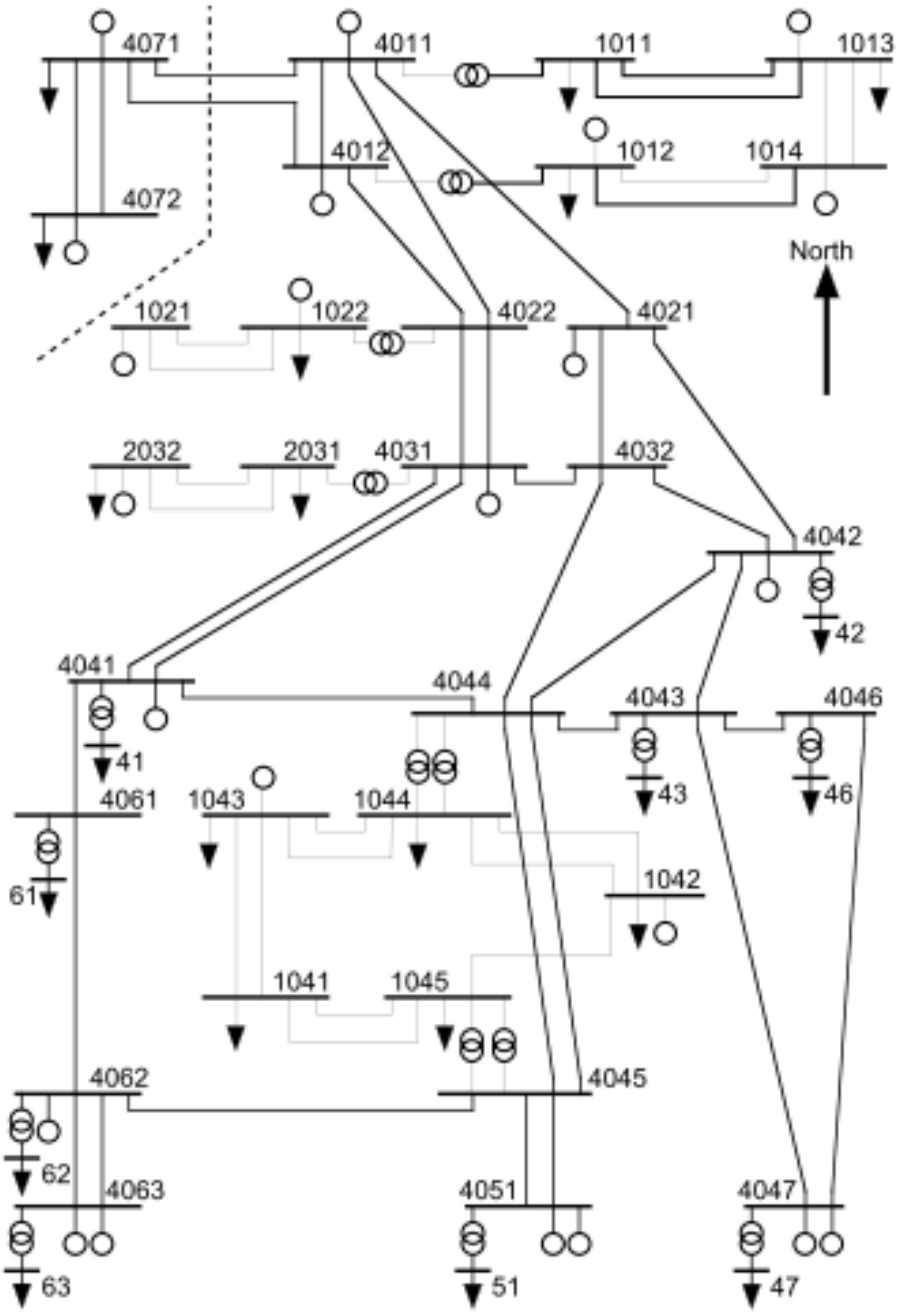

Figure 4. 1: Layout of NORDIC32 with the dashed line representing the Swedish-Finnish border. Buses with two-digit numbers are at 130 kV, while for other buses, the first digit indicates a voltage of 130, 220 or 400 kV. [13]

The network data as well as the models are standardized; for instance, the test system utilizes only one type of excitation model with a few sets of data. The number of nodes and generators is quite limited, 32 and 23 respectively. In addition, there are generator buses and some load buses.

The Nordic 32 test system consists of 4 major geographical areas: [14], [15]

• "**North**" with basically hydro generation and some load

• "**Central**" with much load and thermal power generation

• "**Equiv**" or "**External**" connected to the "North". It has a mixture of generation and load

• "**Southwest**" with thermal generation, rather loosely connected to the rest of the system, and some load

The network is quite long. The major transfer section is from "north" to "central", and the southwest area is rather loosely connected to the rest of the system. The "external" system corresponds to a very simplified network. At peak load, the transfer is basically from the "north" to the "central" part. [14], [15]

The main transmission system is designed for 400 kV. There are also regional systems at 130 kV and 220 kV. The number of nodes corresponding to each voltage level are 19, 11 and 2 respectively.

The generation of the system is modeled with 23 generators i.e. 10 round rotor synchronous generators for the Thermal power plants, 12 salient pole synchronous generators for the Hydro power plants and 1 salient pole synchronous compensator. The main characteristic of the system is the long distances between the production centre (North) and consumption center (Central). The high electrical distance between these areas has been reduced by the usage of series capacitance compensation in the 400kV transmission network. [15]

Nordic 32 test system utilizes 2 power flow scenarios. In the 1st scenario, the load level is at normal load and the transfer from "North" to "Central" is at a normal level. In the 2nd scenario, the system is highly loaded, and transfer from "North" to "Central" is remarkably risen. In this particular project, the 1st scenario of Nordic 32 is implemented.

The network data of the elements (busbars, transmission lines, transformers, loads etc.) are listed in detail in Appendix A.

4.2 Dynamic Analysis

The control models of the generators – which are utilized in Nordic 32 tests system – are presented in this section for the analysis of system's dynamic behavior. The controllers utilized in Nordic 32 are proposed by Svenska Kraftnät. Two types of generators are used in the system; round rotor generators in thermal power stations and salient pole generators in hydro power plants. The controllers implemented in these generators are listed below: [15], [16]

- A simple model for the excitation system with three-time constants
- Power system stabilizers for all the units.
- Governor controllers for the hydro power units.

The PowerFactory block diagrams for the controllers above are presented in the following figures.

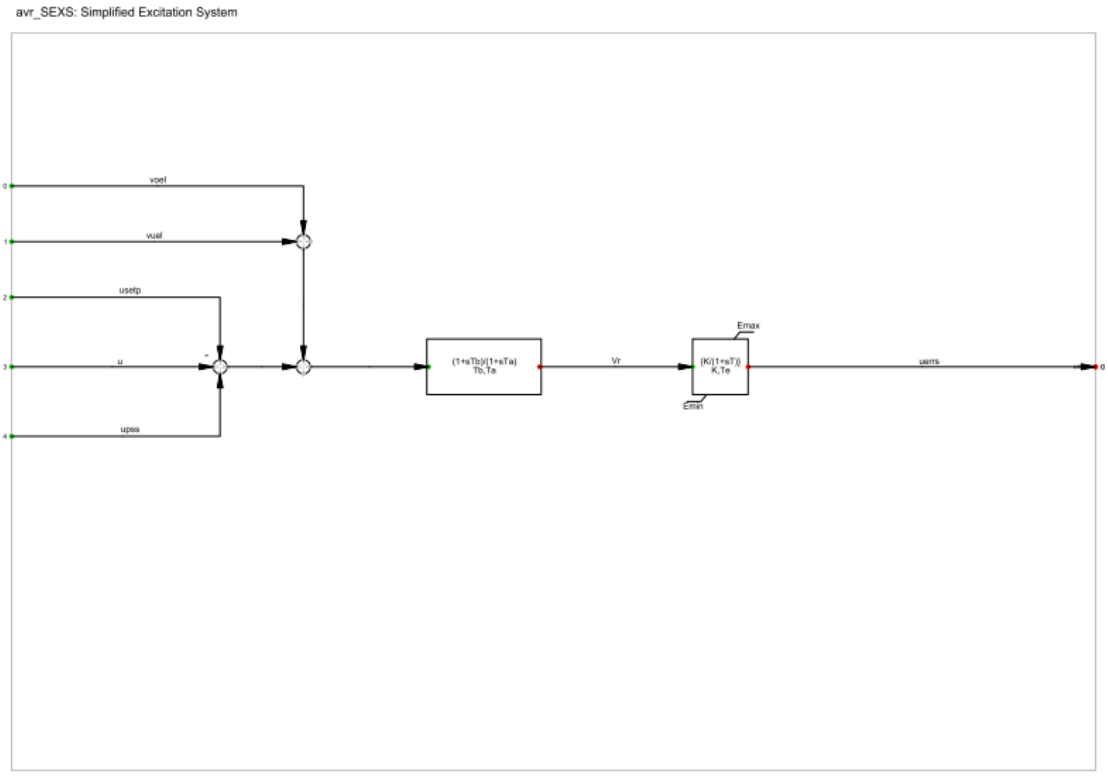

Figure 4. 2: PowerFactory block diagram of the excitation system - SEXS

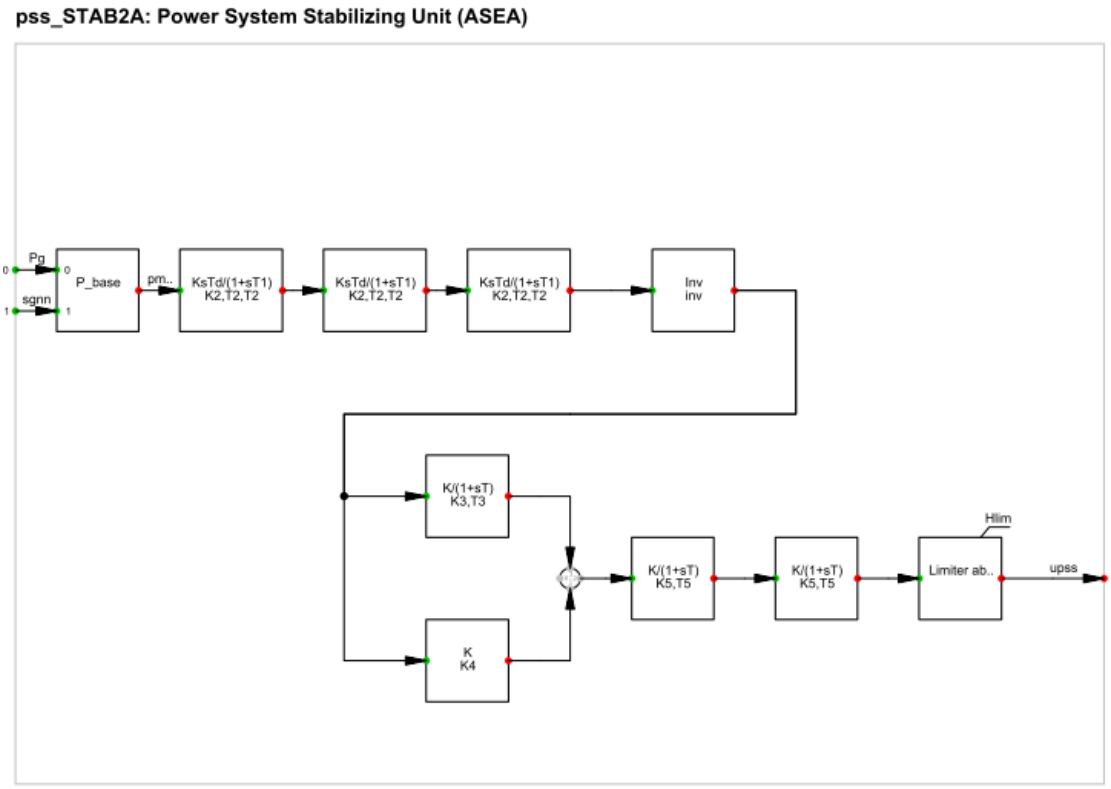

Figure 4. 3: PowerFactory block diagram of the power system stabilizer (PSS) – STAB2A

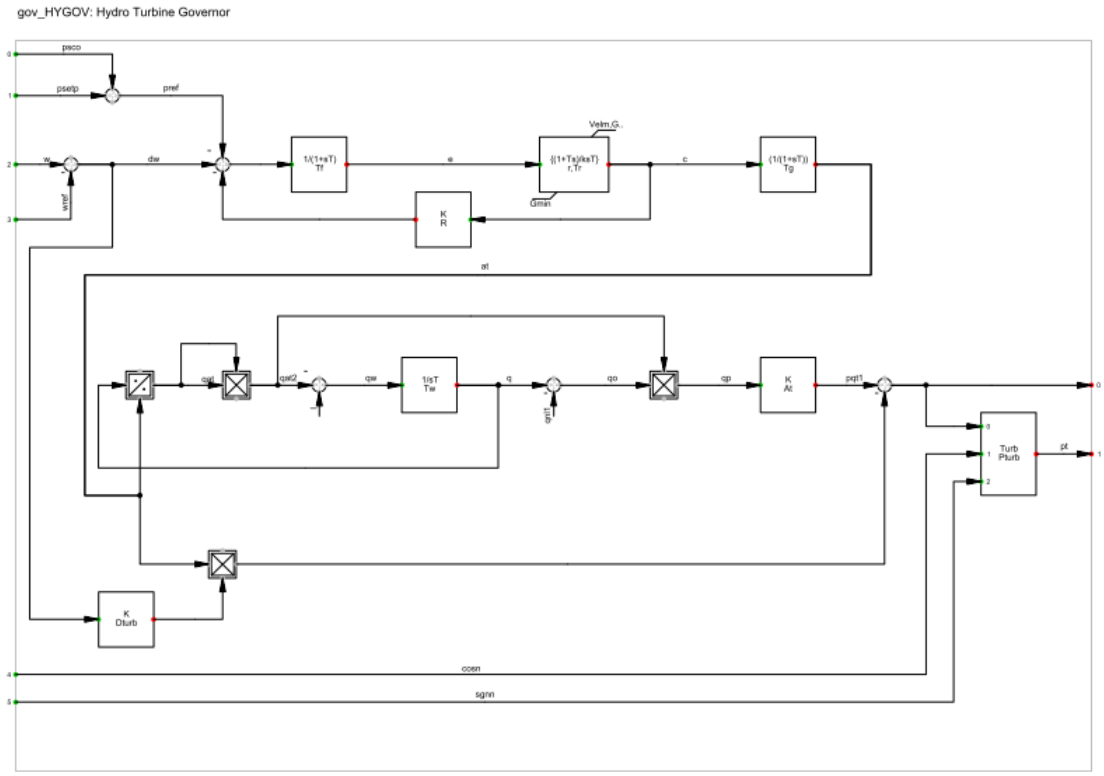

Figure 4. 4: PowerFactory block diagram of the Hydro Governor - HYGOV

The various constant values of the controllers in the Nordic 32 test system utilized for the simulation results are listed in Appendix B.

Therefore, the composite model of the generator model in PowerFactory is also shown below (the model for generator at bus 4072 is utilized as example). The previous dynamic diagrams of the PSS (STAB2A), the Hydro Governor (HYGOV) and the excitation system (SEXS) is depicted in the generator model.

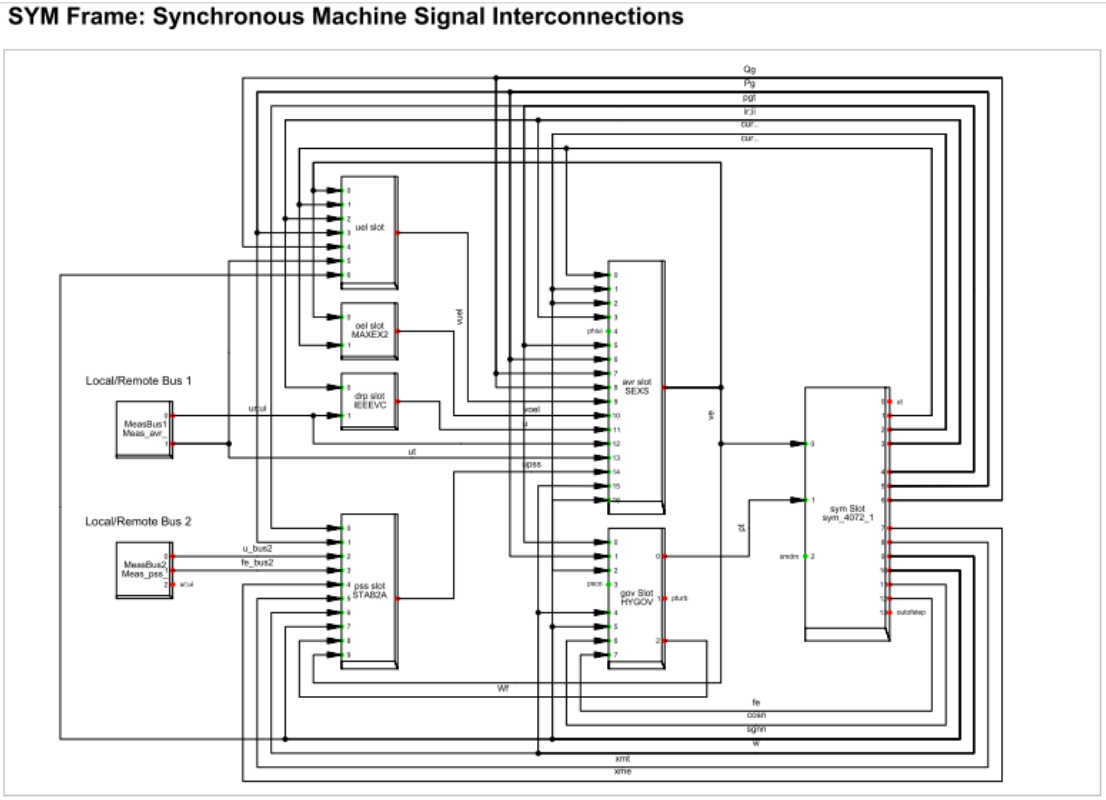

Figure 4. 5: PowerFactory block diagram of the generator at bus 4072 - SYM

5. Simulation results on DigSilent PowerFactory

This chapter presents the simulation results that highlight the resonance impact on inter-area oscillations. The load-flow calculation of the Nordic 32 test system is calculated and then the modal analysis is implemented to obtain the modes of the system and study them.

Next, forced oscillation – simulated by creating load variations with specific frequencies based on the inter-area modes frequencies – are implemented. Different cases are tested in order to analyze the amplification on the tie-lines oscillations and clarify the resonance phenomenon.

The different cases tested depend on several factors – assuming that the forced oscillation frequency is very close to the inter-area mode frequency in all cases. These factors are listed below:

- Change of force oscillation frequency in a value close to the inter-area frequency
- Amplitude of forced oscillations
- Type of load variations that are the source of forced oscillations
- Location of load where variation is implemented

5.1 Software overview

DigSilent PowerFactory is a leading power system analysis software application for use in analyzing generation, transmission, distribution and industrial systems. It covers the full range of functionality from standard features to highly sophisticated and advanced applications including wind power, distributed generation, real-time simulation and performance monitoring for system testing and supervision.

The basic functions and integrated features of PowerFactory software are listed below

- Load Flow Analysis
- Short-Circuit Analysis
- Load Flow Sensitivities
- Basic MV/LV Network Analysis
- Power Equipment Models
- Network Representation
- Network Model Management
- Network Diagrams and Graphic Features
- Results and Reporting
- Data Converter

For the purpose of this project, the load flow calculation method utilized is a full AC Newton-Raphson balanced technique. [16]

5.2 Inter-area modes – observability calculation

The Nordic 32 test system modeled in PowerFactory, which is the basis of this project, is shown in the following figure.

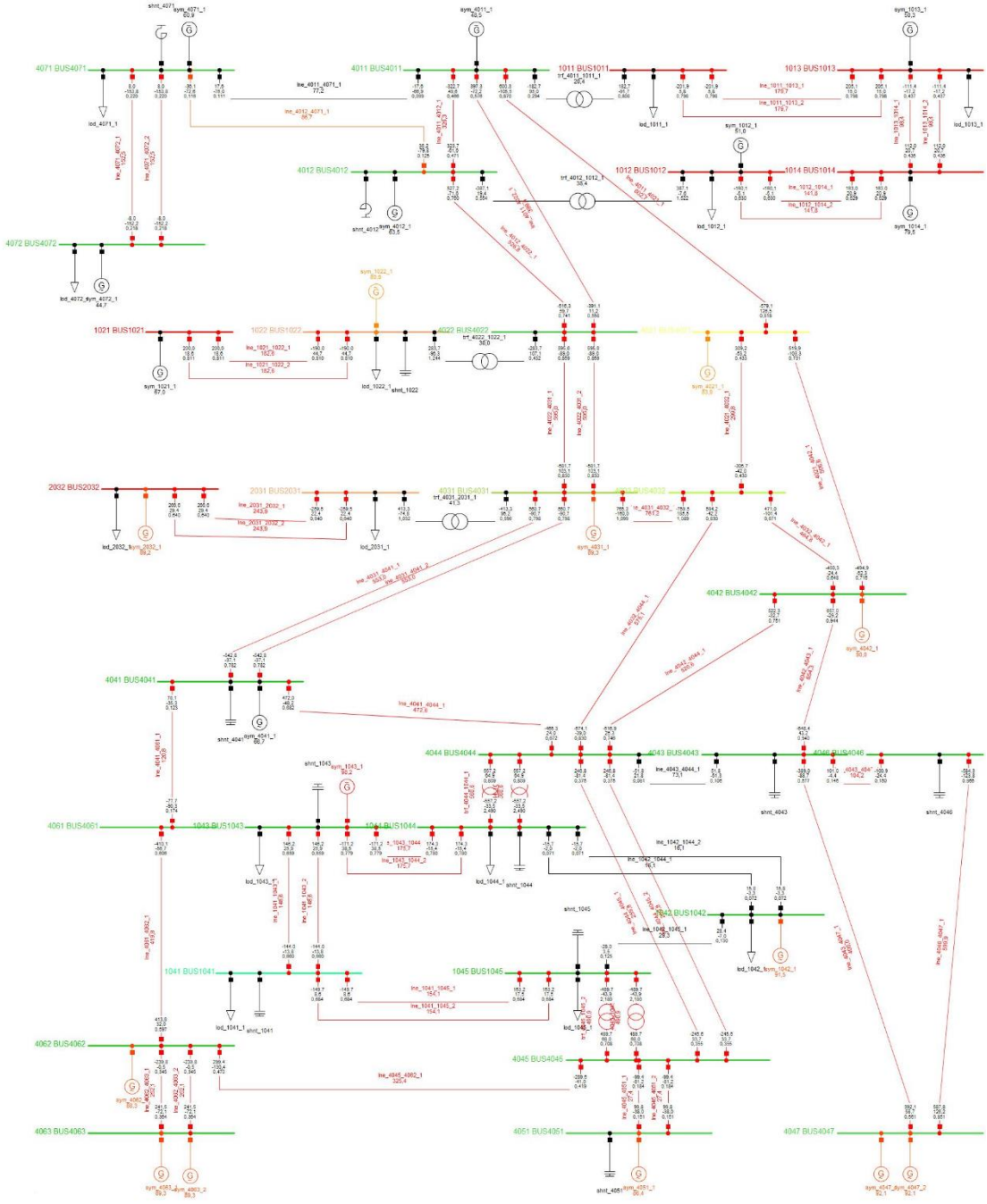

Figure 5. 1: Nordic 32 test system modeled in DigSilent PowerFactory software

Voltage dependency is taken into account for the load flow analysis shown above. The ZIP model, which is utilized for the Nordic 32 test system, is a polynomial based static load model considering voltage dependency and is described by the following formula [20]

$$P_{ZIP} = P_{nom}\left[P_Z\left(\frac{U}{U_0}\right)^2 + P_I\left(\frac{U}{U_0}\right) + P_P\right] \quad (42)$$

From the above formula, the load is separated into parts with constant impedance (Z), constant current (I), and constant power (P). The values of the ZIP model parameters in the load flow calculation of Nordic 32 are equal to the ones utilized by Svenska Krafnat, and are listed below are: [20]

- $\boldsymbol{P_Z}$ **: 40%**
- $\boldsymbol{P_I}$ **: 0%**
- $\boldsymbol{P_P}$ **: 60%**

This system is utilized in all the cases where the resonance impact on the tie-lines is tested.

Small signal stability analysis is performed with the aim to calculate all the eigenvalues and eigenvectors of the system. Based on these calculations, the inter-area modes are identified.

There are **356** eigenvalues (modes) of the system of which **202** are complex and occur in conjugate pairs**.** Each of these **101** pairs corresponds to an **oscillatory mode**. The oscillatory modes that have a damping frequency which is smaller than 1 Hz are selected, as inter-area mode frequency has such a value. Then, from these modes, the first 11 with the lowest damping ratio value are presented in the following table:

Table 1: Oscillatory modes of the Nordic 32 test system for the 1st power flow scenario

Name	*Real Part (1/s)*	*Imaginary part (rad/s)*	*Angle (deg)*	*Damping Frequency (Hz)*	*Damping (1/s)*	*Damping Ratio*
Mode 142	-0.387	6.103	93.633	**0.971**	0.387	**0.063**
Mode 145	-0.431	5.401	94.562	**0.859**	0.431	**0.079**
Mode 149	-0.318	3.924	94.643	**0.624**	0.318	**0.080**
Mode 147	-3.610	4.577	128.261	0.728	3.610	0.619
Mode 188	-2.049	1.584	142.283	0.252	2.049	0.791
Mode 058	-19.517	6.158	162.487	0.980	19.517	0.953
Mode 062	-19.777	6.036	163.027	0.960	19.777	0.956
Mode 064	-19.620	5.983	163.040	0.952	19.620	0.956
Mode 052	-20.405	6.020	163.562	0.958	20.405	0.959
Mode 050	-20.471	6.034	163.574	0.960	20.471	0.959
Mode 066	-19.630	5.749	163.675	0.915	19.630	0.959

From the Table 1, the 3 first modes (*Modes 142, 145 and 149*) are of utmost importance. The reason is that the damping ratio of these three modes is quite small (6.3 %, 7.9% and 8%). So, these are the modes of interests and are further analyzed in the following paragraphs of this subchapter.

The corresponding eigenvalues plot of all the Oscillatory modes of the system is presented below. The three modes of interest are the ones closest to the y-axis and are pointed out on the Figure below.

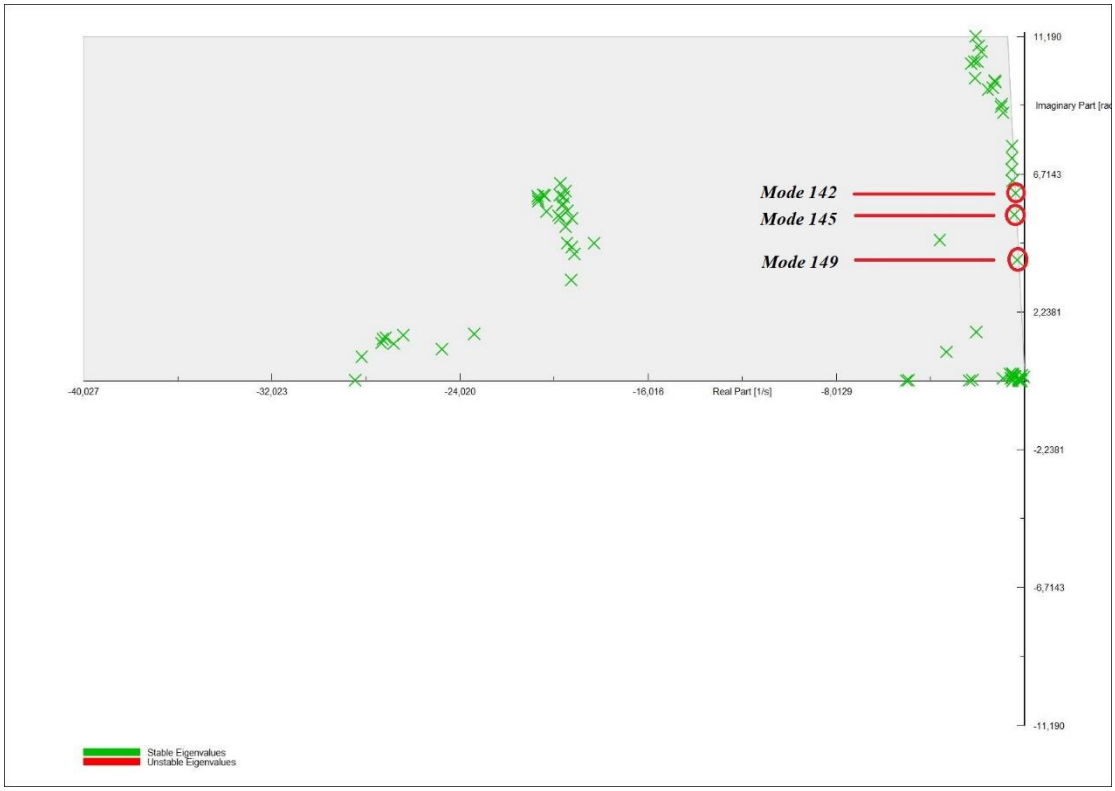

Figure 5. 2: Oscillatory modes of the Nordic 32 test system

Therefore, from both Table 1 and Fig 5.2 the three inter-area modes of interest are pointed out, which are the following:

- **Inter-Area Mode 1: Mode 149**
- **Inter-Area Mode 2: Mode 145**
- **Inter-Area Mode 3: Mode 142**

These modes are identified by checking the values of two parameters. First, the value of the damping frequency in an inter-area mode should be smaller than 1 Hz which is the case for these three modes. In fact, according to Table 1, frequency values corresponding to *Inter-Area Mode 1, 2* and *3* are equal to **0.624 Hz**, **0.859 Hz** and **0.971 Hz** respectively.

Furthermore, these three modes have the smallest damping ratio values; in fact, their damping ration is less than 10%. therefore, a remarkable resonance impact is expected when the frequency of the inter-area oscillations of these modes and forced oscillations are coupled.

In the following table, the modal analysis for the 1st power flow scenario of Nordic 32 test system is implemented. The inter-area modes that correspond to the 3 inter-area modes identified above are shown below.

Table 2: Oscillatory modes of the Nordic 32 test system for the 2nd power flow scenario

Name	*Real Part (1/s)*	*Imaginary part (rad/s)*	*Angle (deg)*	*Damping Frequency (Hz)*	*Damping (1/s)*	*Damping Ratio*
Inter-area mode 3	-0.355	6.096	93.332	**0.970**	0.355	**0.058**
Inter-area mode 2	-0.425	5.498	94.421	**0.875**	0.425	**0.077**
Inter-area mode 1	-0.263	3.726	94.038	**0.593**	0.263	**0.070**

It is obvious from Table 2 that the damping ratio values are a bit lower than those in Table 1. This is logical, as a highly loaded case is tested in this scenario. Since the obtained results are very close for the 2 scenarios, the project will focus only on the 1st power flow scenario.

Beside the parameters mentioned above, the observability plots should also be taken into account. These plots are determined for each mode by calculating the observability matrix from equation (28). From equation (28), observability is linked to the modal matrix $\boldsymbol{V^R}$ that corresponds to the right eigenvector. Therefore, the modal matrix $\boldsymbol{V^R}$ is obtained first in order to finally determine the observability matrix.

All the calculations mentioned above are implemented automatically in PowerFactory for obtaining the observability plot of each mode. In fact, the areas of the Nordic 32 with generators that oscillate in different directions are defined by an inter-area mode and can be depicted in the corresponding observability plot.

In the following plot the observability plot corresponding to *Inter-Area Mode 1* is presented

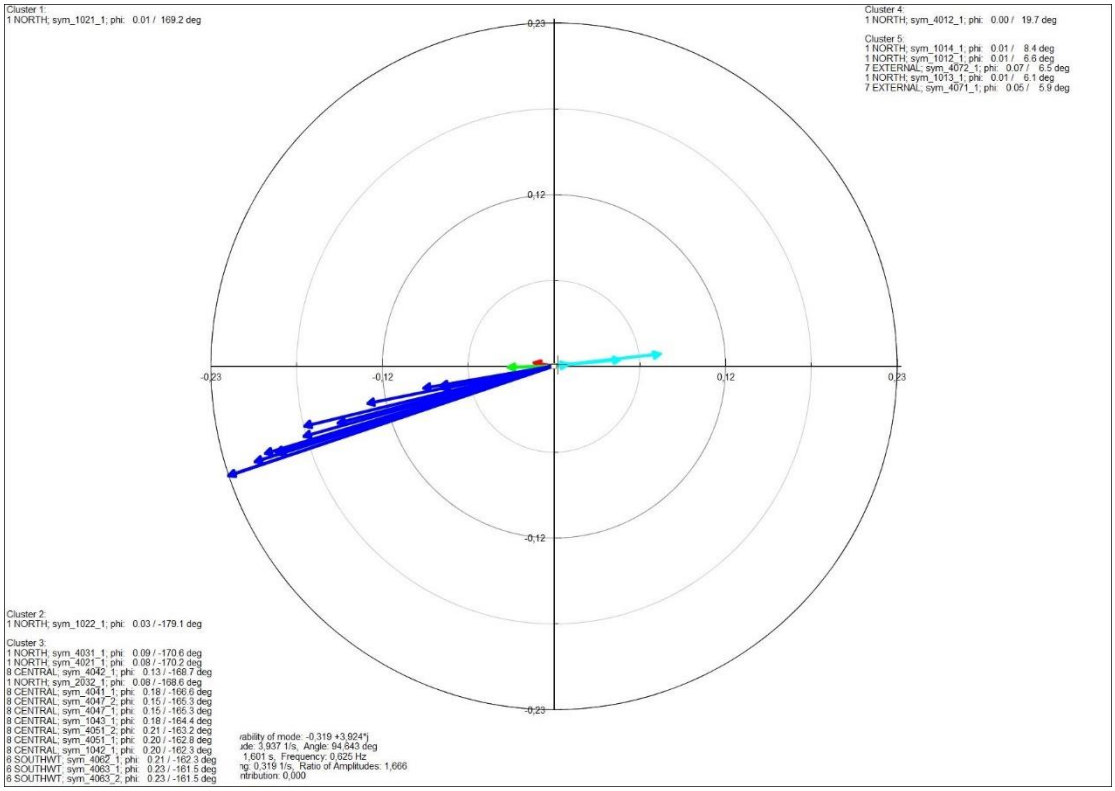

Figure 5. 3: Observability plot for Inter-Area mode 1

From Fig 5.3, it is quite obvious that the generators from the External area of the system oscillate against the generators of the rest areas. This result verifies that Mode 149 is an Inter-area mode.

Similarly, the observability for *Inter-Area Mode 2* can be calculated, as shown below

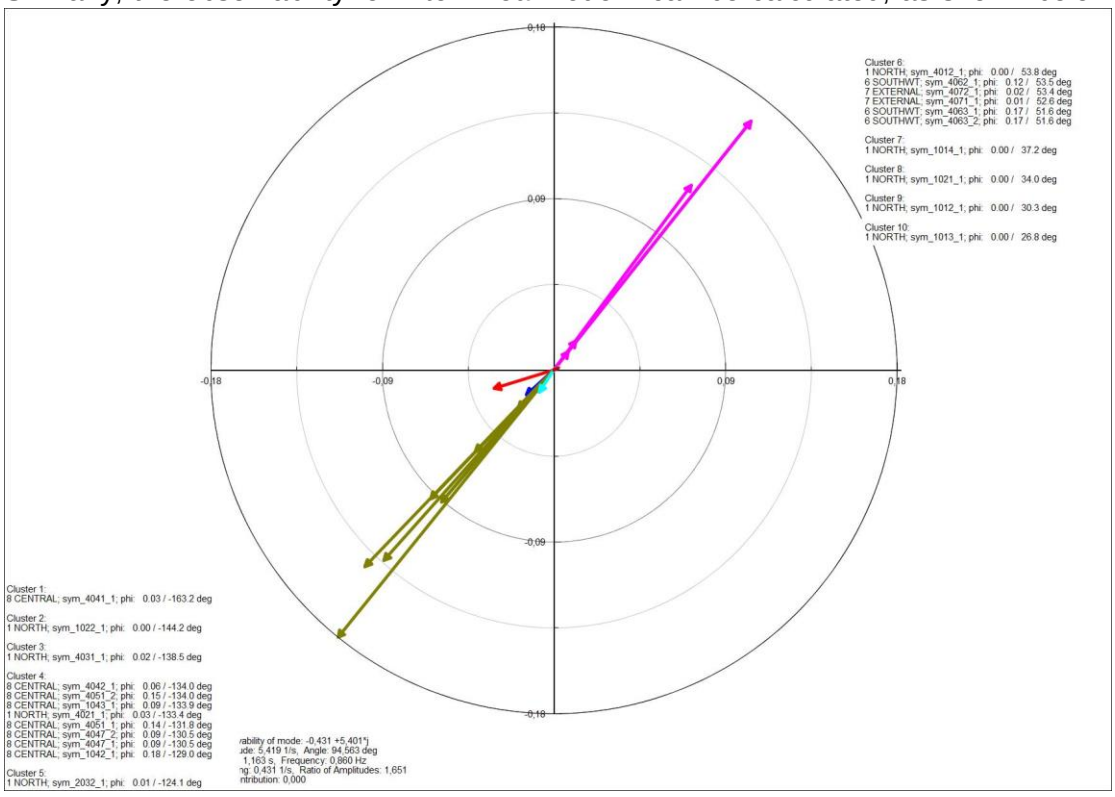

Figure 5. 4: Observability plot for Inter-Area mode 2

From Fig 5.4, it can be figured out that the generators from the Central area of the system oscillate against those of the Southwest Area. This result verifies that Mode 145 is an Inter-area mode.

The observability plot for *Inter-Area Mode 3* is calculated and shown in Fig 5.5. Similarly to the previous cases, it is obvious from this figure that the generators of the Northern Area oscillate against the generators of the rest areas. Thus, this consists an Inter-area mode as well and will be further studied in this project.

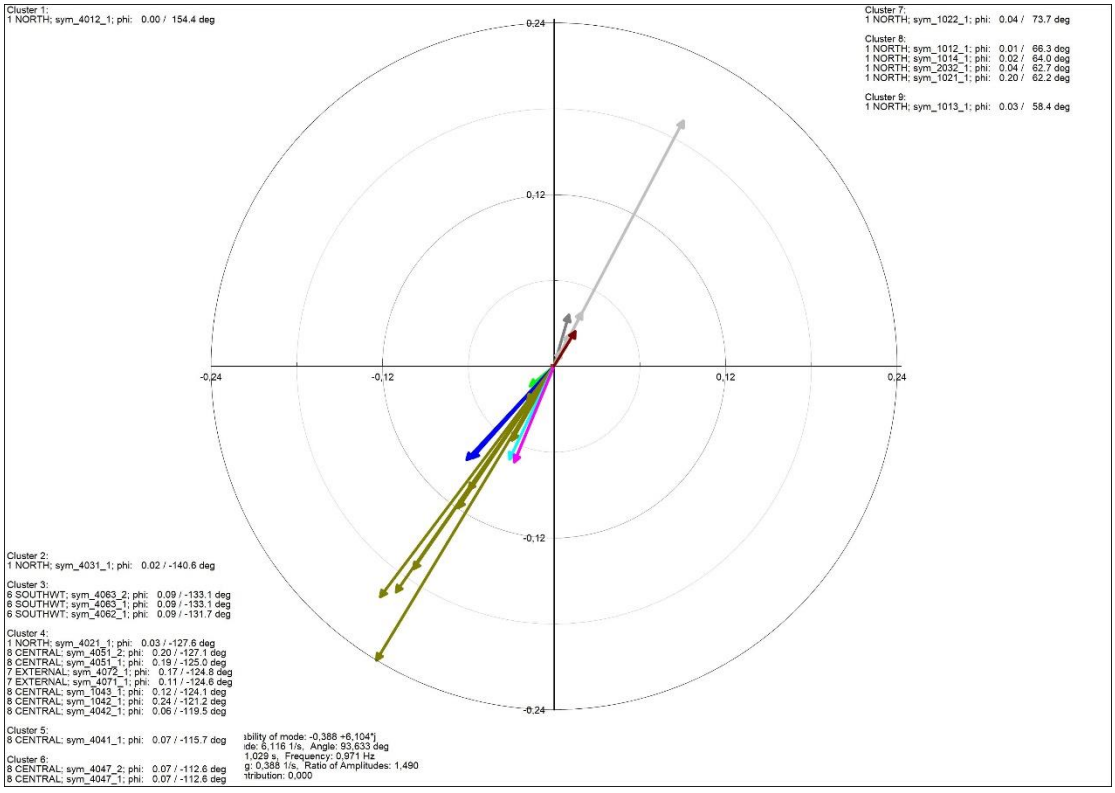

Figure 5. 5: Oscillatory plot for Inter-area mode 3

5.3 Inter-area modes – controllability and participation factor calculation

The location of the forcing oscillation is totally connected to the controllability of the mode. In case an area of the power network has a large surplus generation and a generator located on a bus in that area has high controllability, then the damping of the inter-area modes is improved. However, if a generator – with high controllability - is located on a bus in an area where large amounts of power are imported over ac interconnections, then the damping ratio is decreased to at least some of the inter-area modes. [19]

Therefore, the most critical locations in terms of resonance are locations where the controllability – as well as the participation – of the oscillation mode is the highest and there is power transfer. This is happening at the edge of the Nordic test system, where there is power transfer between the Swedish grid and the rest Nordic power grids.

The controllability and participation of the three Inter-Area modes defines the buses where deployment of control actions is most efficient to damp the oscillations. The loads of these buses are selected for the simulations of this project. In fact, load

variations – that correspond to forced oscillations – will be simulated for highlighting the resonance phenomena.

In the following plots, the controllability corresponding to *Inter-Area Mode 1* for variable phi – which is the machine rotor angle – and for speed is presented. The normalized numerical values for controllability and participation for these variables in all three inter-area mode cases are presented in Appendix C.

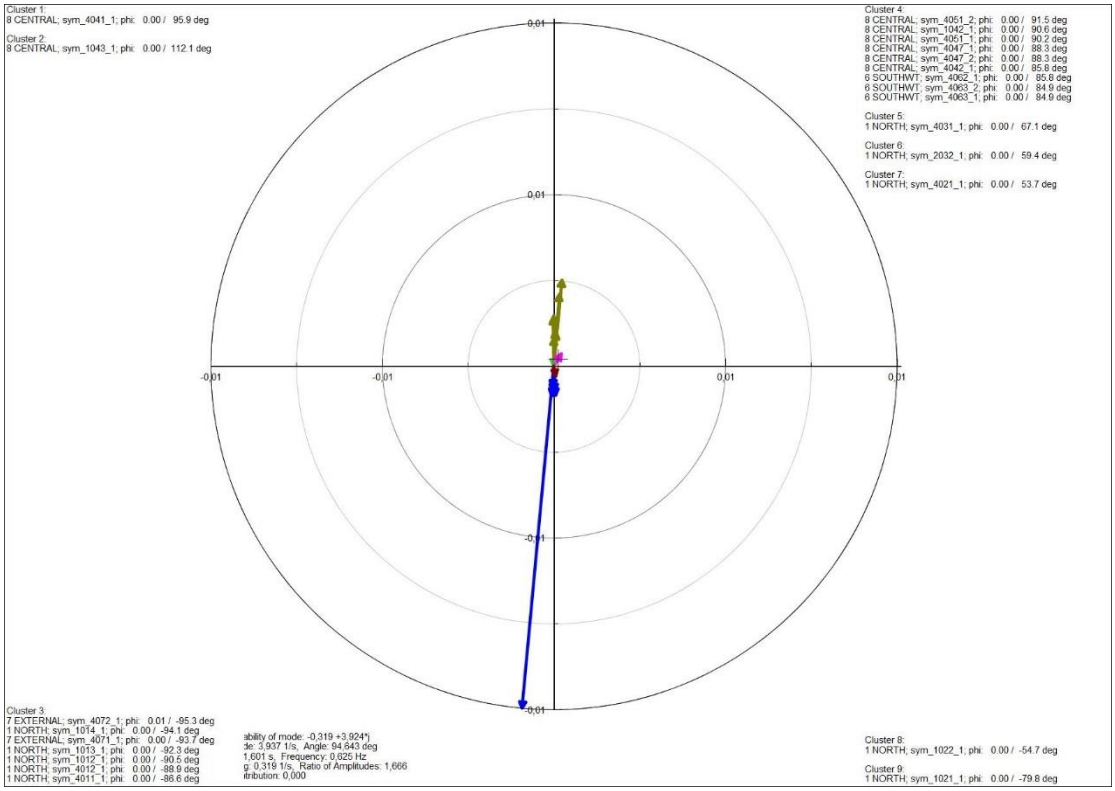

Figure 5. 6: Controllability plot for Inter-Area mode 1 – phi variable

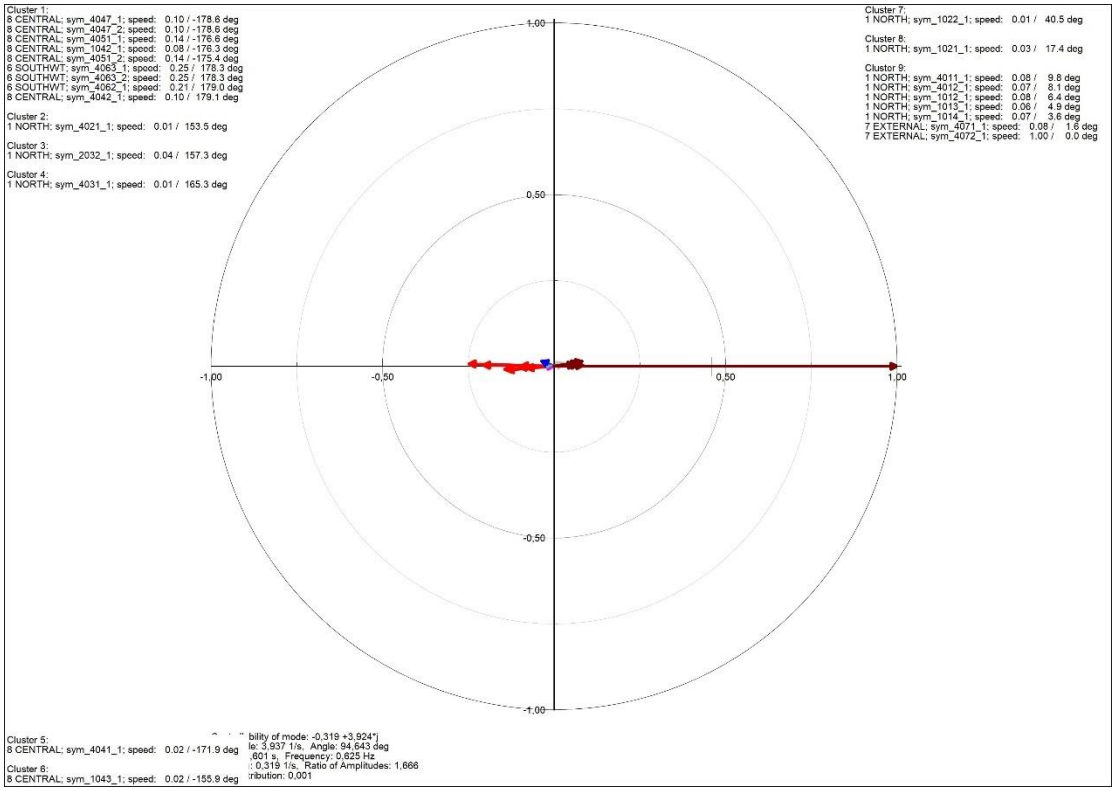

Figure 5. 7: Controllability plot for Inter-Area mode 1 – speed variable

From both the plots above, it can be concluded that generator on 4072 bus in the External Area of the Nordic 32 test system is more controllable – in fact the control actions affecting the speed of the generator on 4072 bus, as concluded by Fig. 5.7. Therefore, the forced oscillation will have the biggest impact – and resonance will occur – if it is tested at the load connected to 4072 bus, as the controllability here is higher, the frequencies of the forced oscillations and natural oscillations are close and the damping of the system is low.

The same conclusion applies for the participation factor plot, for both variables phi and speed. This can easily be concluded, as the modal controllability is related to the left eigenvector (equation 27), modal observability is related to the right eigenvector (equation 28) and the participation factor combines both eigenvectors (equation 23). Thus, the generator participating the most is the one connected at 4072 bus, as shown in the plots below.

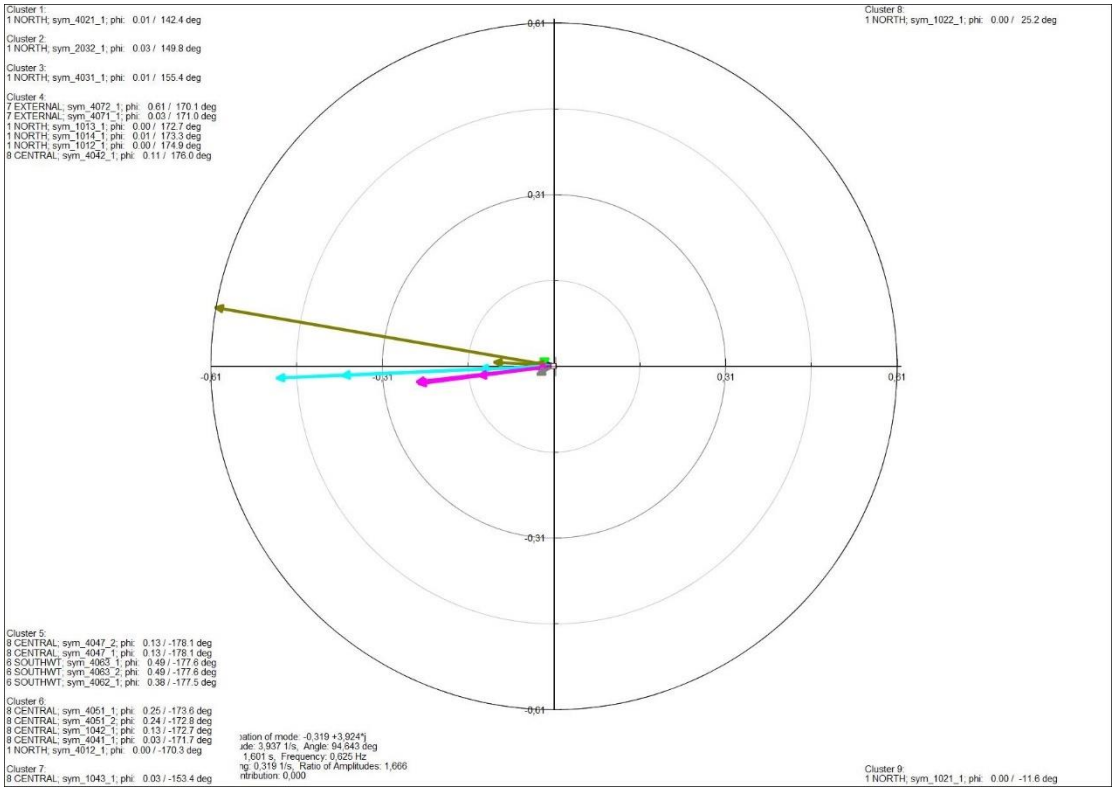

Figure 5. 8: Participation plot for Inter-Area mode 1 – phi variable

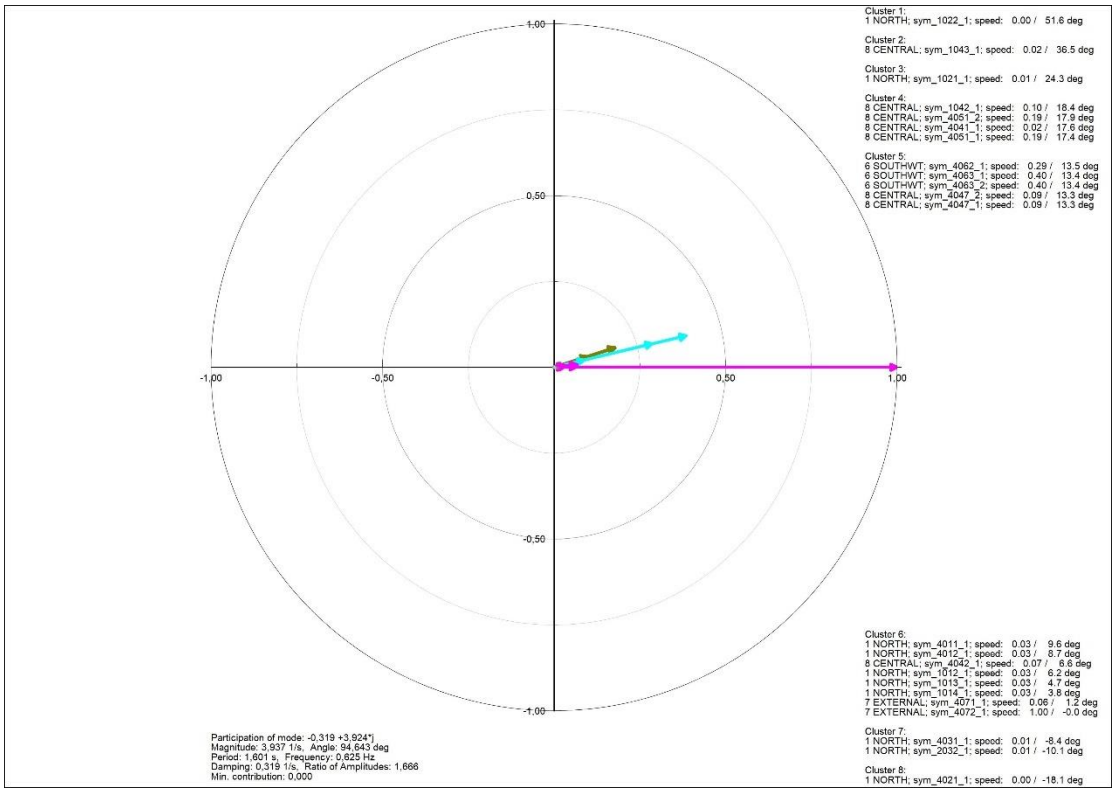

Figure 5. 9 Participation plot for Inter-Area mode 1 – speed variable

The final conclusion for *Inter-area mode 1*- that will be shown in the following subchapters - is that the more controllable the generator of the bus where forced oscillations takes place, the larger its impact will be on the transferred active power at

the tie lines of the system. The tie- lines where this impact is visible connect the two areas of the system presented in the observability plot.

The controllability and participation factor plots for *Inter-Area Mode 2* are similarly calculated and presented in the following figures.

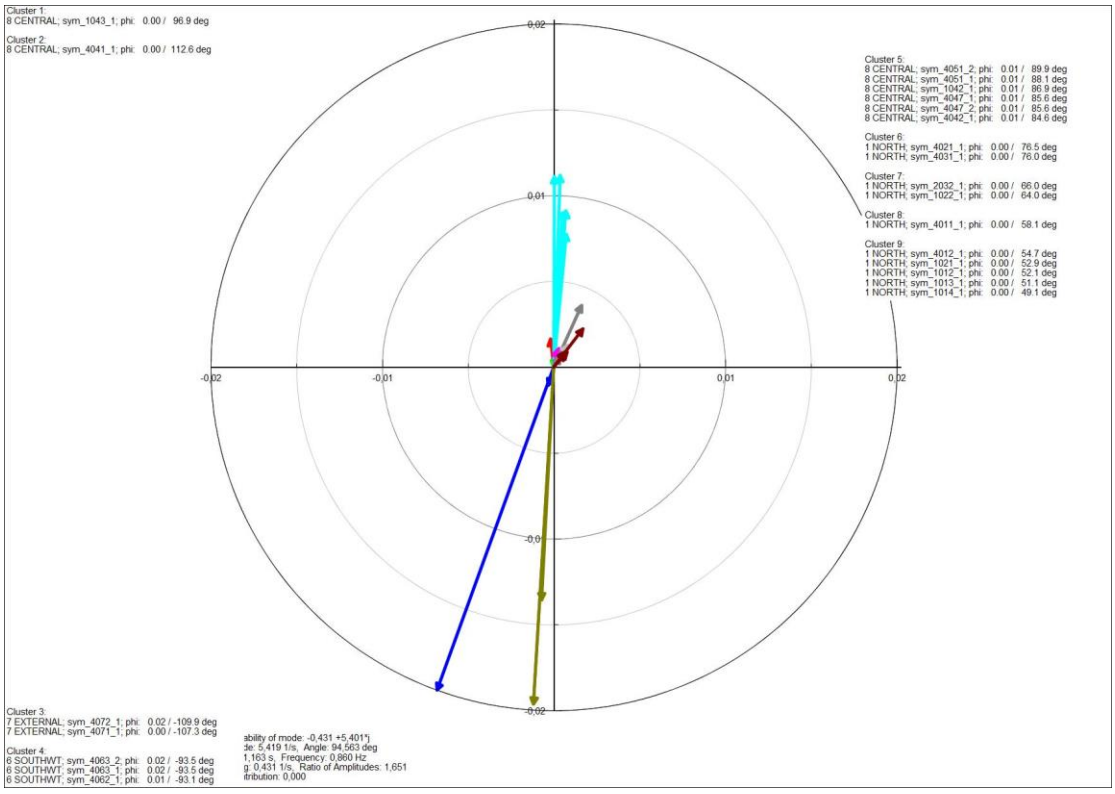

Figure 5. 10: Controllability plot for Inter-Area mode 2 – phi variable

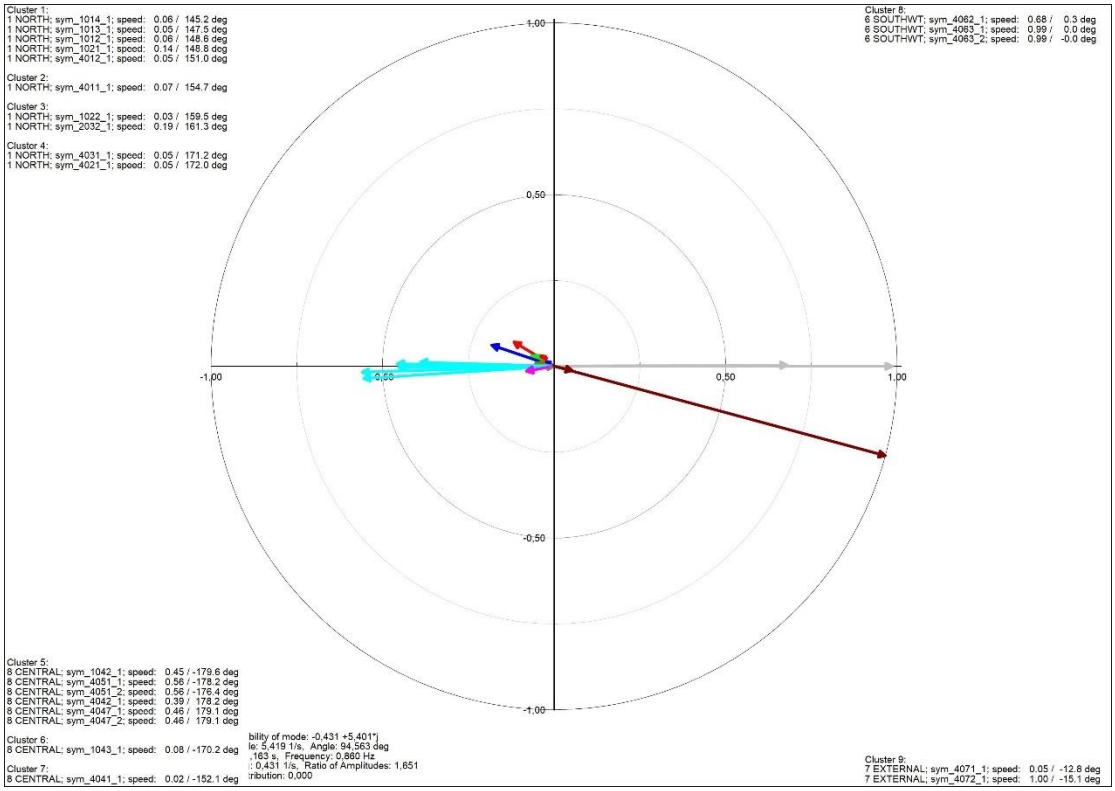

Figure 5. 11: Controllability plot for Inter-Area mode 2 – speed variable

Based on the plots above, generator on 4063 bus in the Southwest Area of the Nordic 32 test system is more controllable. Therefore, the forced oscillation will have the biggest impact – and resonance will occur – if it is tested at the load connected to 4063 bus.

Furthermore, the generator at 4072 bus of the External area also has equal controllability to the generator at 4063 bus – taking into account both variables. However, according to the observability plot of *Inter-Area Mode 2*, the Southwest and the Central Area are of great importance as the generators in these areas oscillate in opposite directions. In that case, the forced oscillation load event is going to be tested at both loads – in the Southwest area and the External area – in section 5.7 in order to highlight the resonance phenomenon in each case.

Interesting results are obtained from the participation factor plot – which is based on the same principles as the one as for Inter-area mode 1 - since the generator participating the most is the one connected at 4063 bus, as shown below.

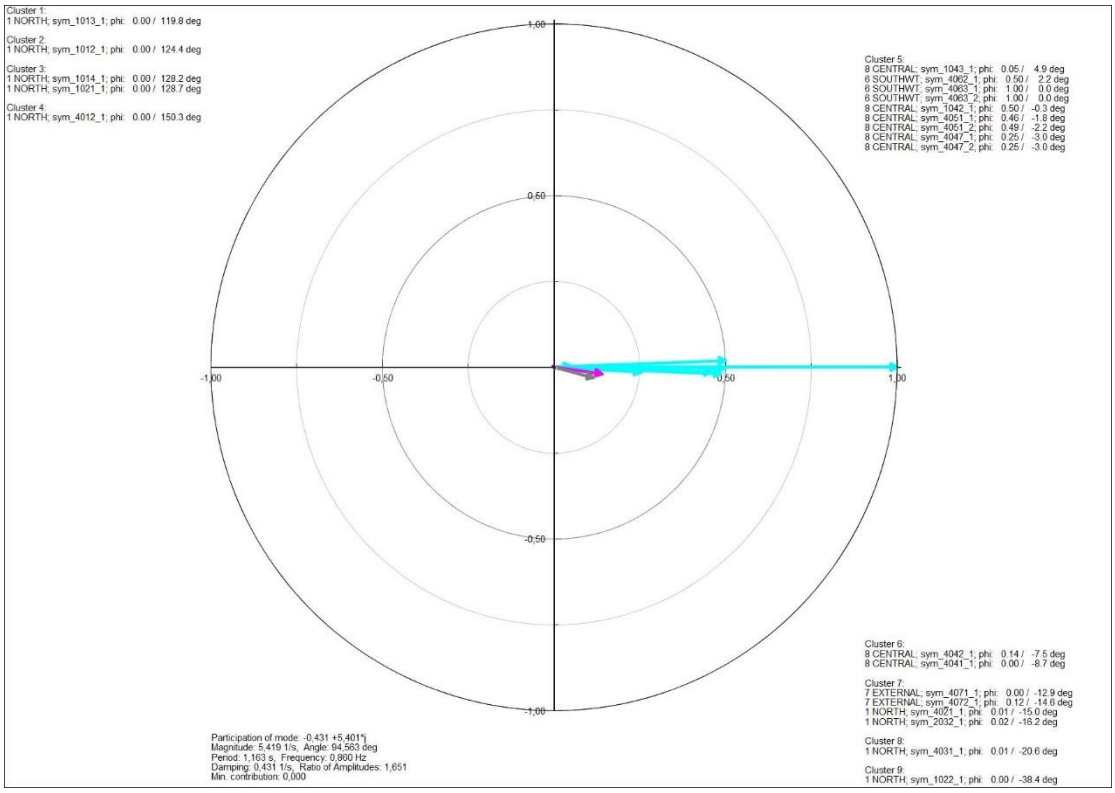

Figure 5. 12: Participation plot for Inter-Area mode 2– phi variable

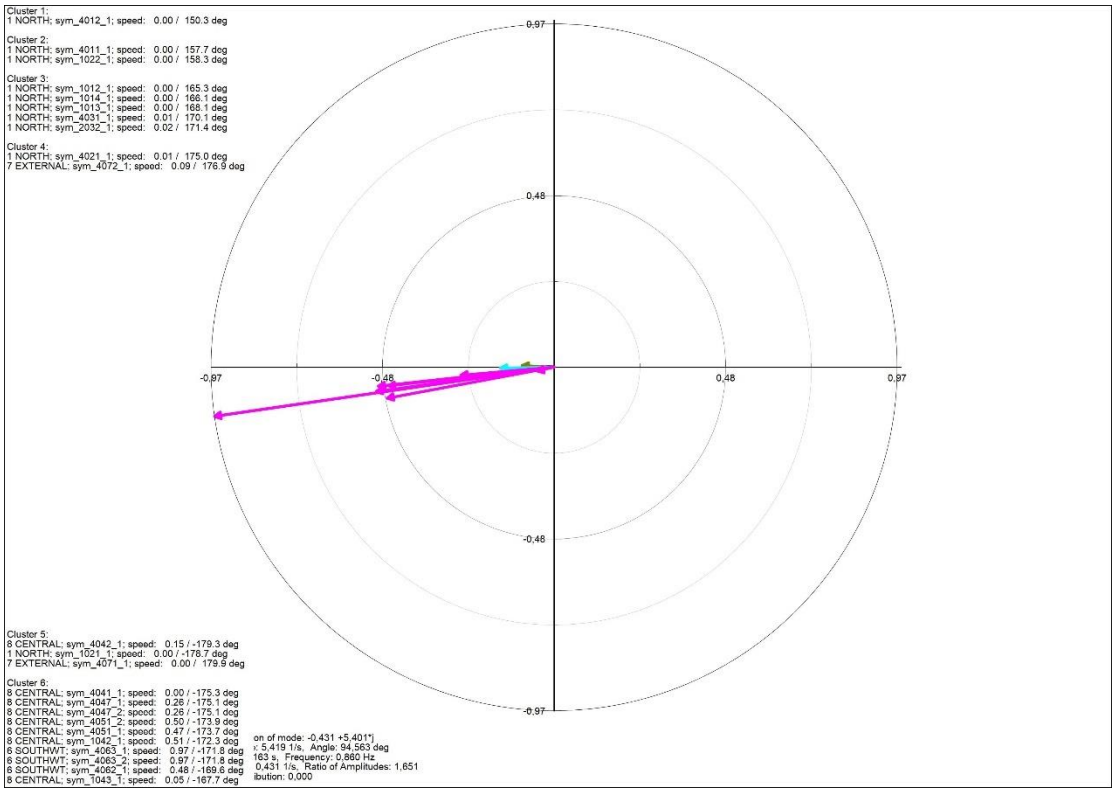

Figure 5. 13: Participation plot for Inter-Area mode 2– speed variable

In fact, regarding variable phi, the participation value for generator at bus 4063 is equal to 1, whereas the participation at bus 4072 is equal to 0.12, according to Table C2 in

Appendix C. So, regarding inter-area mode 2, although these two buses are equally controllable, the generator at bus 4063 is participating 8.3 times more than the one at 4072 bus. This fact influences the resonance simulations that are will be presented in 5.7 section. The same conclusions apply if the participation plot regarding speed is tested.

The controllability plots corresponding to *Inter-Area Mode 3* for variable phi and for all variables are calculated similarly and presented below:

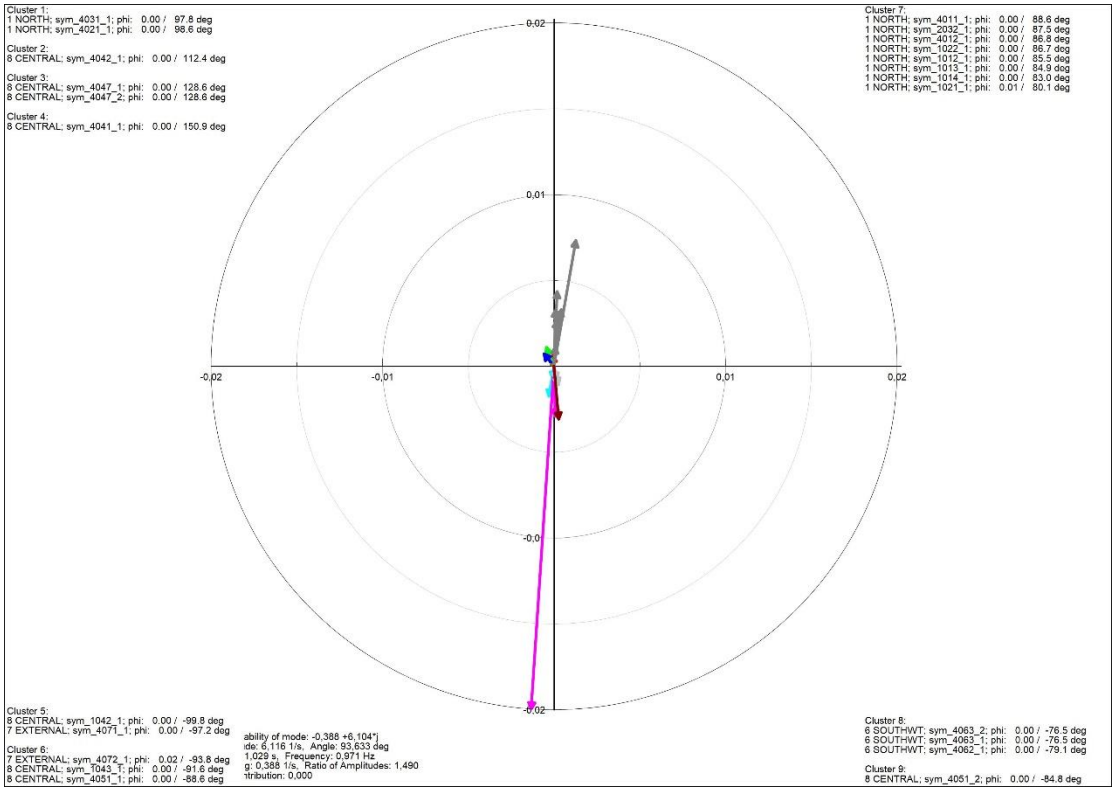

Figure 5. 14: Controllability plot for Inter-Area mode 3 – phi variable

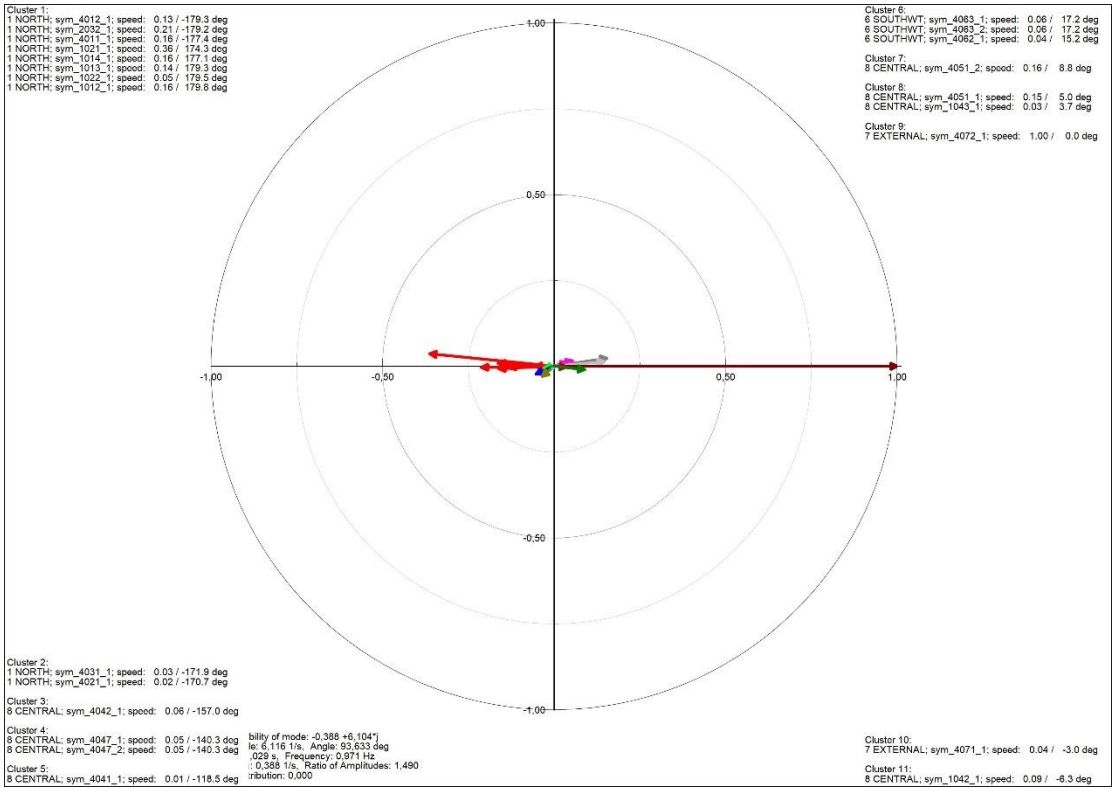

Figure 5. 15: Controllability plot for Inter-Area mode 3 – speed variable

Similarly to the case of *Inter-Area Mode 1*, the generator on 4072 busbar is more controllable – in fact the control actions affecting the speed of the generator on 4072 bus – in the case of *Inter-Area Mode 3*. This outcome comes from both the figures above, where the vector corresponding to generator of 4072 busbar is larger.

The participation of generator on 4072 busbar is also larger compared to the rest generators. This conclusion is extracted after calculating the following participation plot for *Inter-Area Mode 3.*

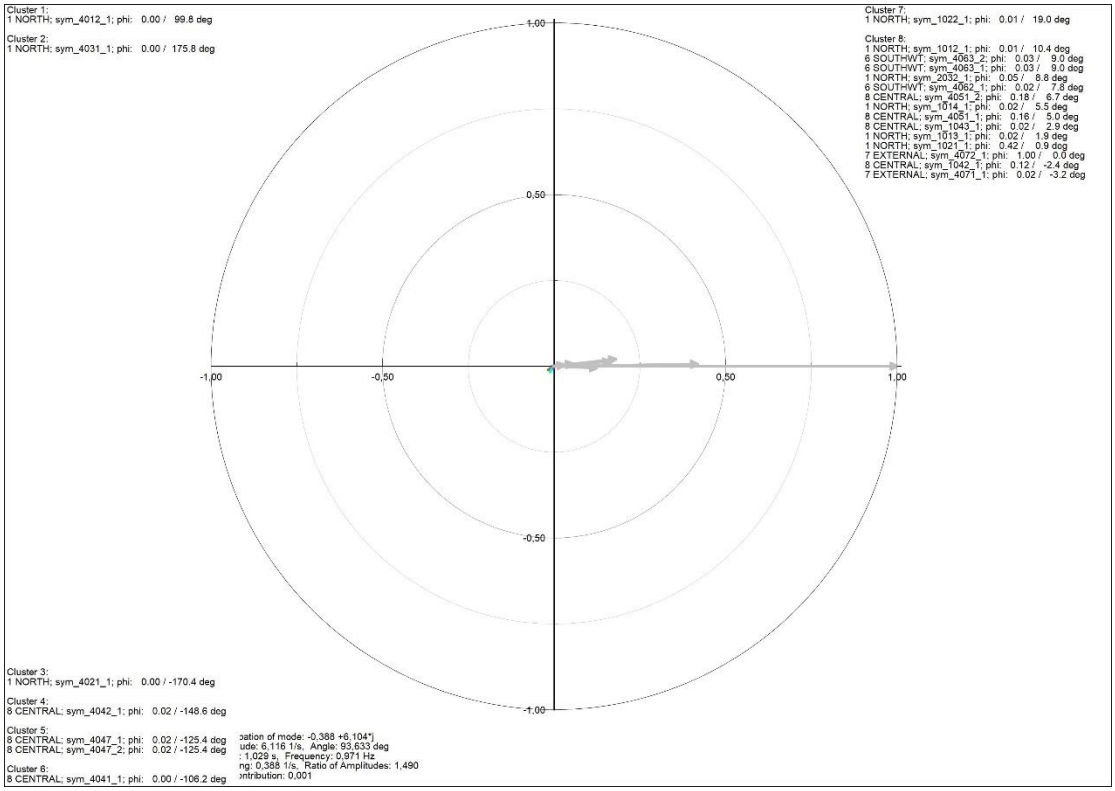

Figure 5. 16: Participation plot for Inter-Area mode 3 – phi variable

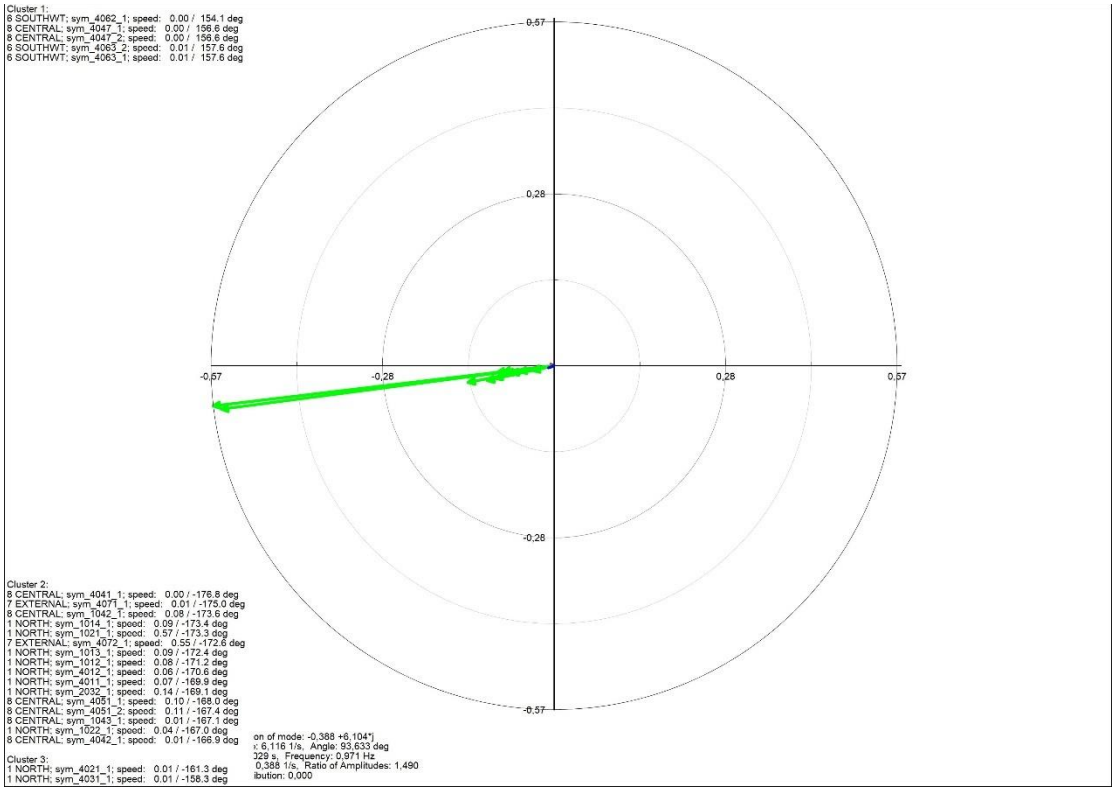

Figure 5. 17: Participation plot for Inter-Area mode 3 – speed variable

So, in case the forced oscillations are tested on the load of busbar 4072, a larger resonance impact is expected, as both the controllability and the participation corresponding to the generator of 4072 busbar are larger. This will be presented in the following simulation results.

5.4 Inter-area modes – resonance impact in tie-lines oscillations

The load variations at the loads of the buses with the highest controllability and participation – as calculated in subsection 5.3 – are then simulated. At the same time, the damping of the inter-area modes is low, and the frequency of inter-area oscillations is equal to the frequency of forced oscillations. These load variations correspond to the forced oscillations studied, and they are simulated in PowerFactory. They consist of repeated load ramp events, and their duration matches to the inter-area mode frequency in order to underline the resonance phenomena. Their amplitude is equal to 20 MW p-p.

In fact, these ramp load events form triangle waves that correspond to sine waves with the same frequency – as the fundamental harmonic frequency has the biggest impact on the formation of triangle waves. According to Fourier analysis, the amplitude of the corresponding sine waves is given below.

$$A_{sine} = \frac{8}{\pi^2} A_{triangle} = \frac{8}{\pi^2}\ 20\ MW \quad (42)$$

So, the forced oscillations simulated with the same frequency as the inter-area modes are shown below

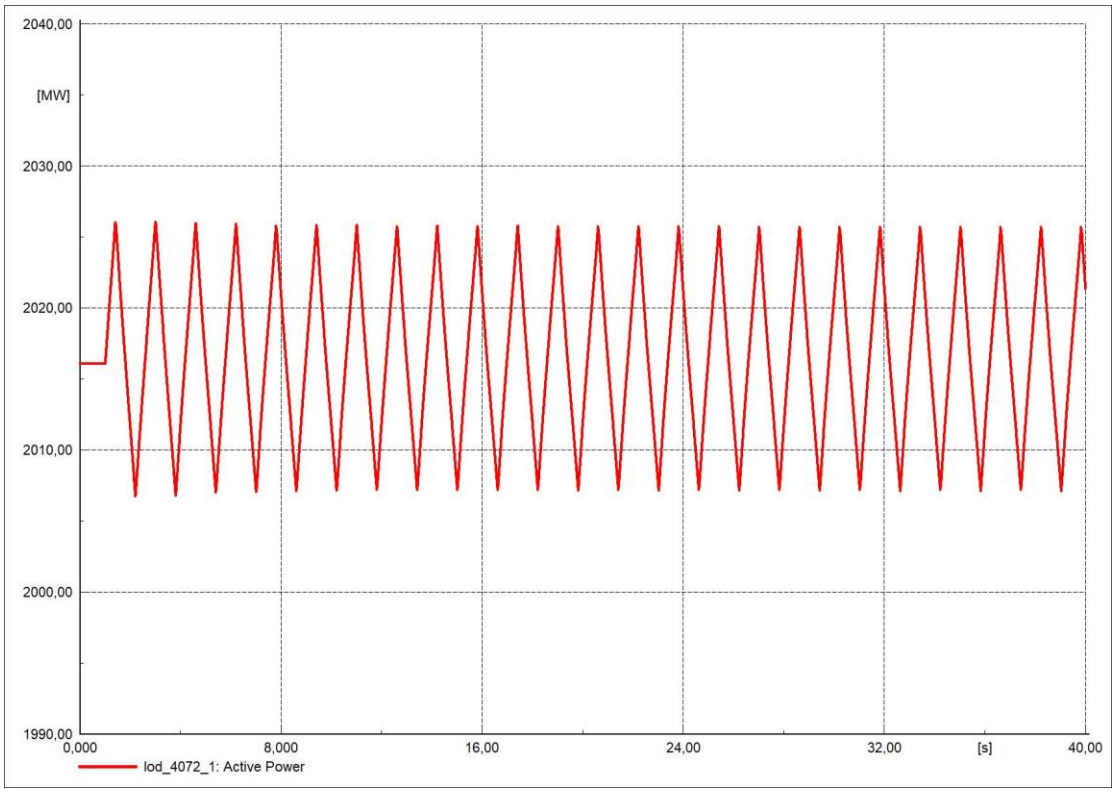

Figure 5. 18: Load Variation Signal – 0.62 Hz (Inter Area mode 1 frequency)

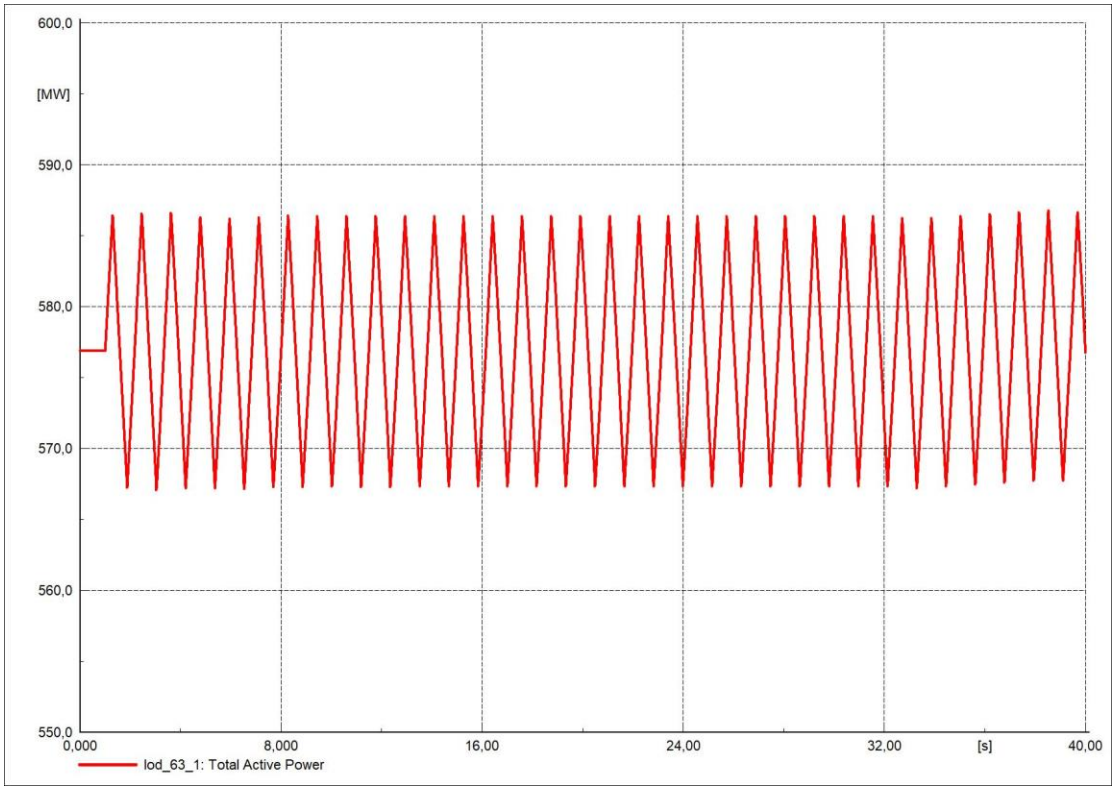

Figure 5. 19: Load Variation Signal – 0.86 Hz (Inter Area mode 2 frequency)

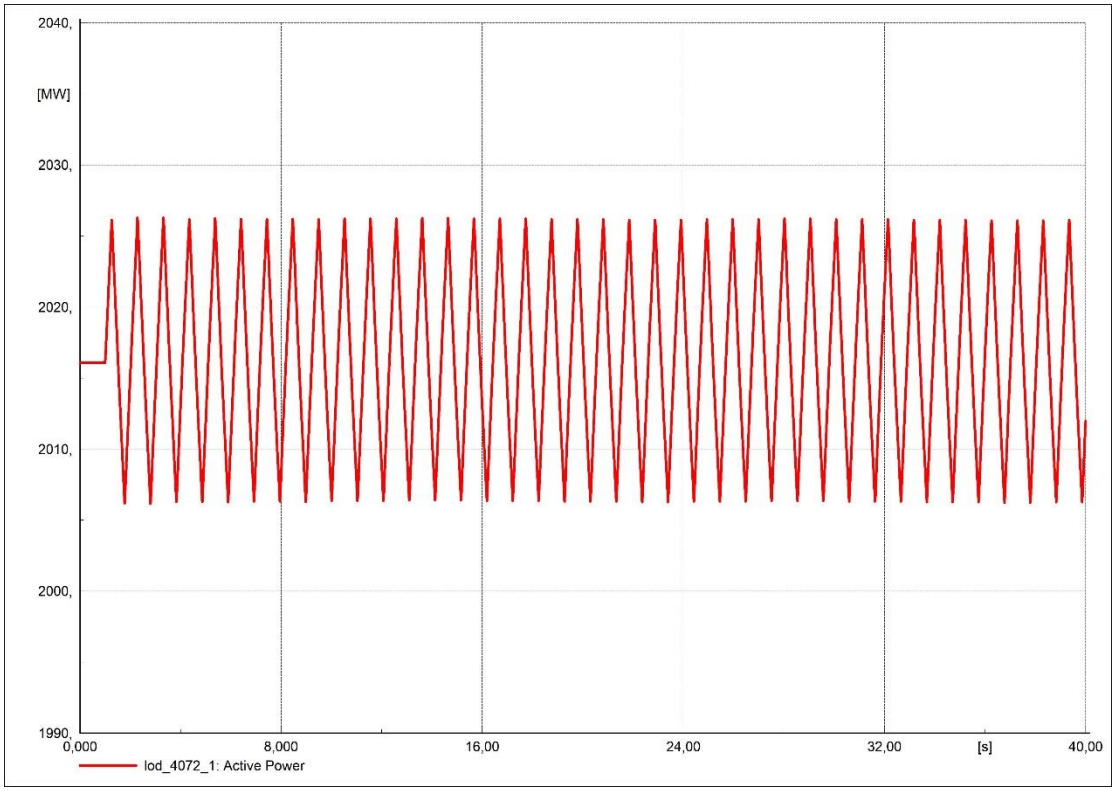

Figure 5. 20: Load Variation Signal – 0.97 Hz (Inter Area mode 3 frequency)

The simulated resulting amplified oscillations on the active power of the tie-lines - that adhere to the resonance phenomenon because of the frequencies coupling – is shown in the following figures (taking into account all the three inter-area modes)

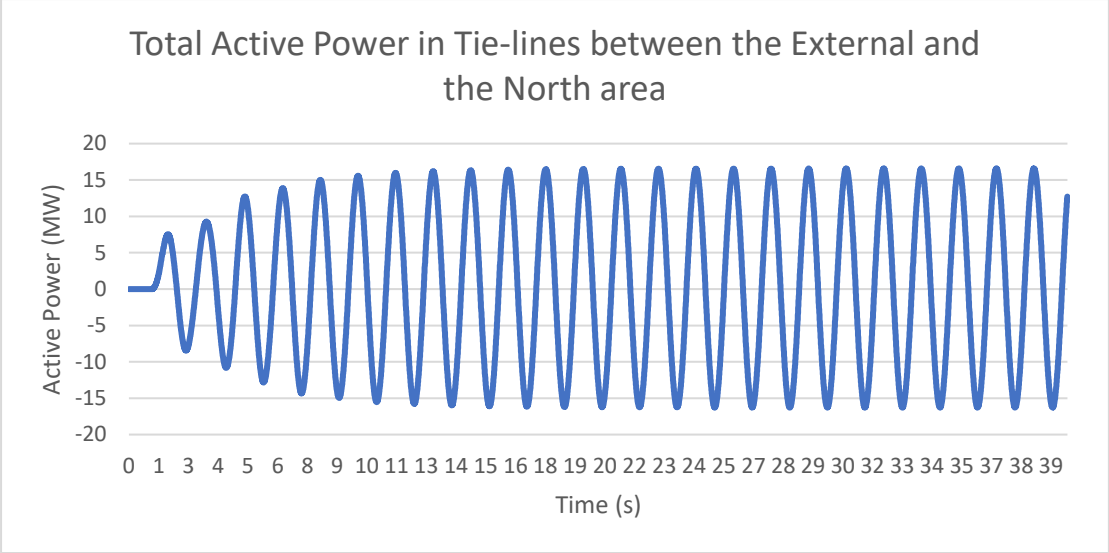

Figure 5. 21: Resonance impact in Tie-lines between the External Area and the North Area of Nordic 32 (Inter-Area mode 1)

As seen in Fig. 5.21, the amplified tie-lines oscillations – when the Forced oscillation frequency is coupled with the frequency of *Inter-Area Mode 1* – have a magnitude equal to 33 MW peak-to-peak. This result corresponds to an amplification factor equal to **1.5** as the peak-to-peak magnitude of the load variations is equal to 20 MW. The frequency of the resulting oscillations is equal to the frequency of the injected signal after the first 4 duty cycles.

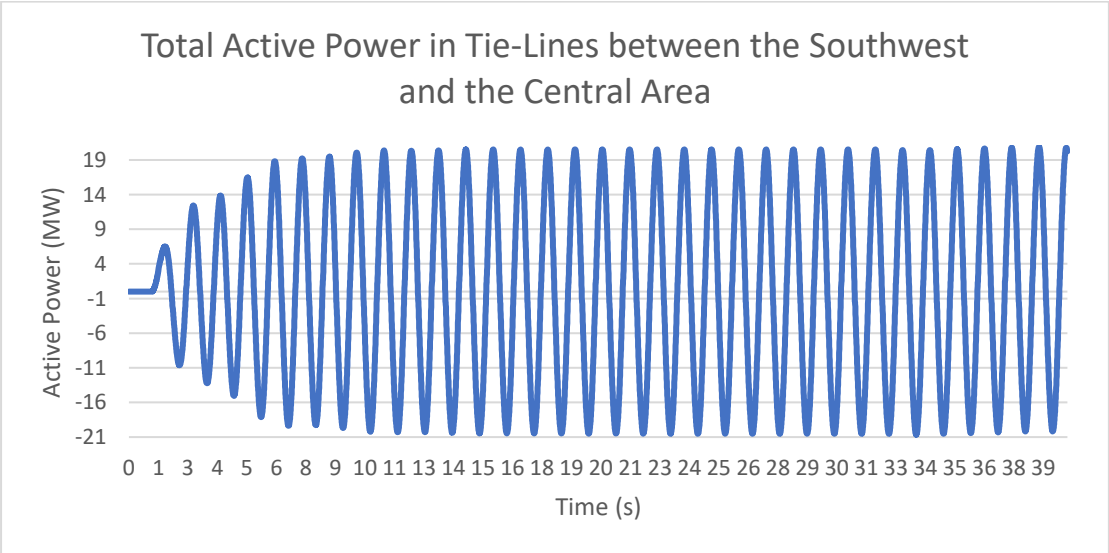

Figure 5. 22: Resonance impact in Tie-lines between the Southwest Area and the Central Area of Nordic 32 (Inter-Area mode 2)

Then, as seen in Fig. 5.22, the amplified tie-lines oscillations – when the Forced oscillation frequency is coupled with the frequency of *Inter-Area Mode 2* – have a magnitude equal to 40.94 MW peak-to-peak. This result corresponds to an amplification factor equal to **2.05** as the peak-to-peak magnitude of the load variations is also equal to 20 MW. The frequency of the resulting oscillations in that case is equal to the frequency of the injected signal after the first 5 duty cycles.

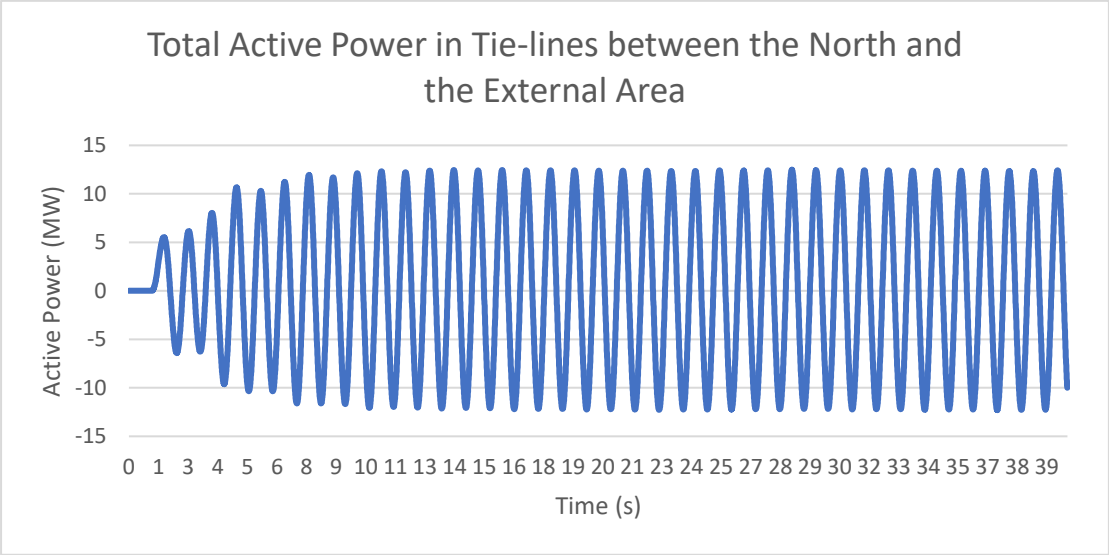

Figure 5. 23: Resonance impact in Tie-lines between the North Area and the External Area of Nordic 32 (Inter-Area mode 3)

According to Fig. 5.23, the amplified tie-lines oscillations – when the Forced oscillation frequency is coupled with the frequency of *Inter-Area Mode 3* – have a magnitude equal to 24.77 MW peak-to-peak. This result corresponds to an amplification factor equal to **1.24** as the peak-to-peak magnitude of the load variations is also equal to 20 MW. The frequency of the resulting oscillations in that case is equal to the frequency of the injected signal after the first 8 duty cycles

5.5 Sensitivity to frequency of forced oscillations

In this subchapter, the results regarding the frequency in which the forced oscillations take place are going to be tested. In fact, the amplification in the transferred active power is estimated when the frequency of the forced oscillation is equal to the inter-area mode frequency. Then, the frequency of forced oscillations is changed to values near the system mode frequencies to test the magnitude of their impact in the tie-line oscillations.

The simulation results when forced oscillations have a frequency equal ***to Inter-Area Mode 1 frequency (0.62 Hz)*** are used as a **reference** (**Fig. 5.21**). Then, the same results are obtained when forced oscillations' frequency is equal to 0.7 Hz and 0.8 Hz and are presented below.

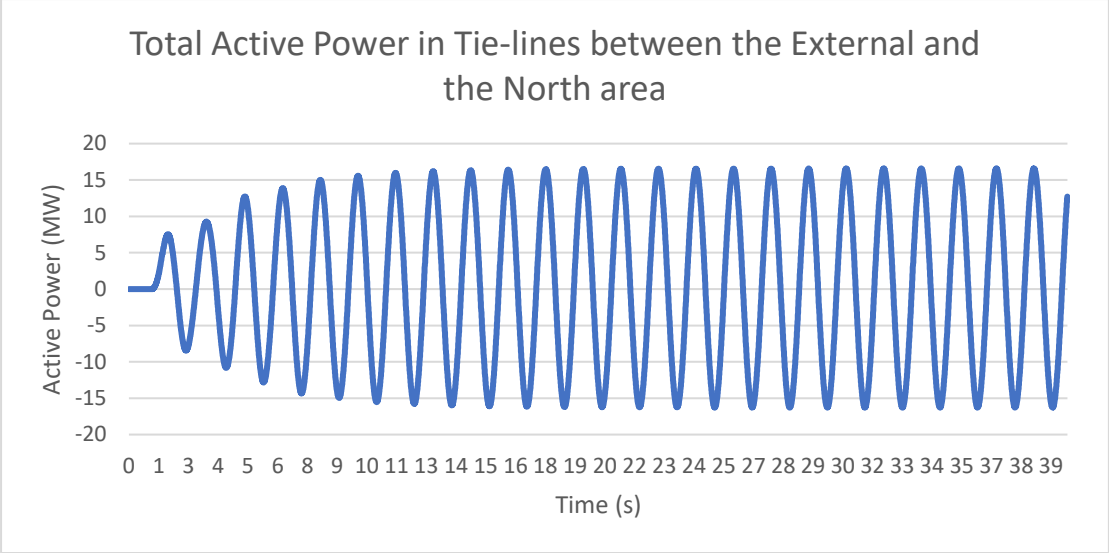

Figure 5. 24: Active Power Oscillations -Forced Oscillations frequency equal to 0.62 Hz (Inter-area mode frequency)

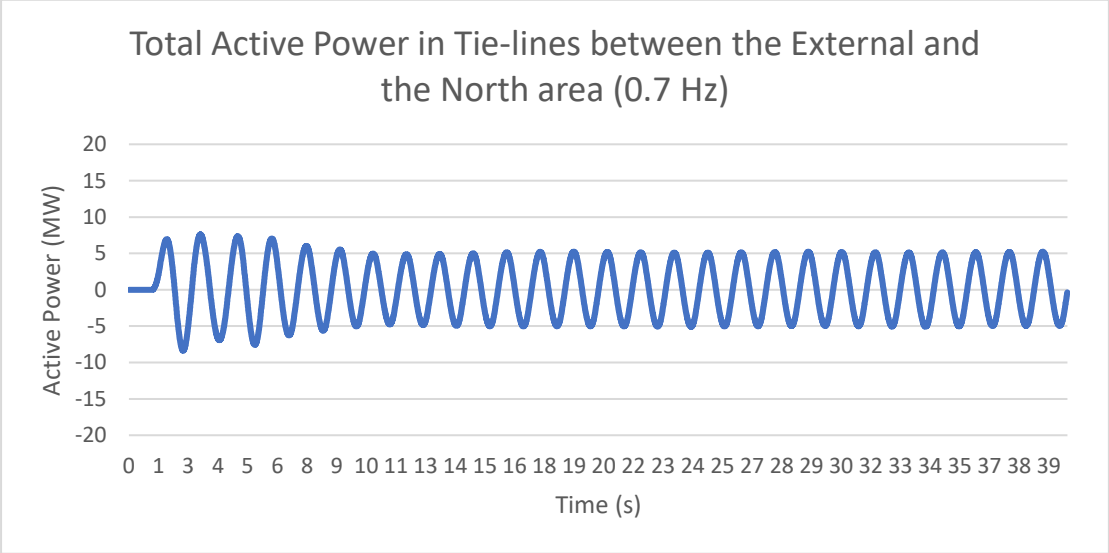

Figure 5. 25: Active Power Oscillations -Forced Oscillations frequency equal to 0.7 Hz

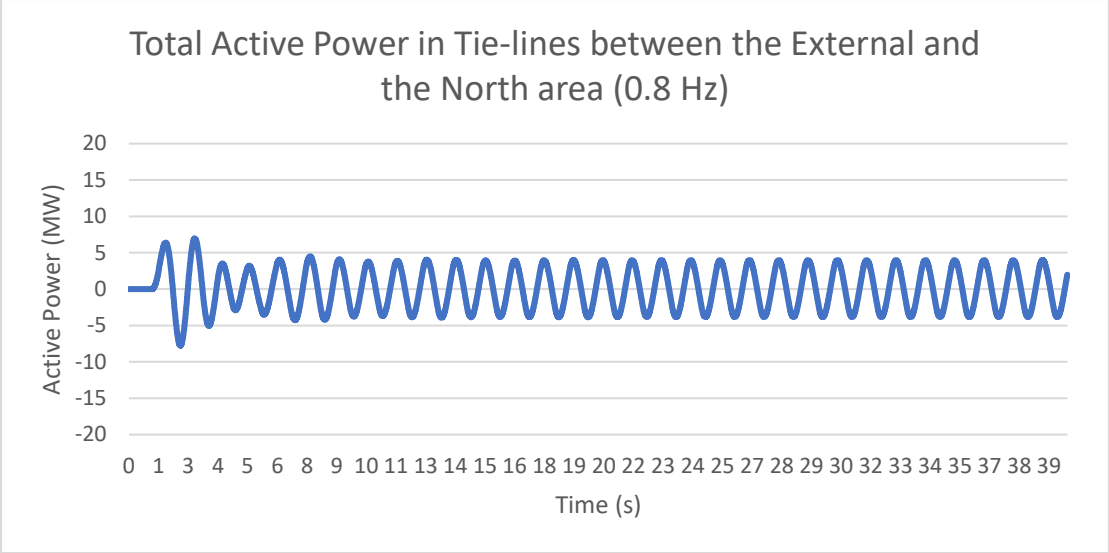

Figure 5. 26: Active Power Oscillations -Forced Oscillations frequency equal to 0.8 Hz

These interesting simulation results obtained in PowerFactory verify the theoretical analysis of the project. In fact, the resulting oscillations on the tie lines have an amplitude of 33 MW p-p in case of forced oscillations with a frequency equal to the inter-area mode frequency (0.62 Hz). However, in case the frequency is slightly increased, the oscillations of the same tie-lines have a significantly decreased amplitude. In fact, in case of a forced oscillation with a frequency equal to 0.7 Hz, the resulting amplitude of the oscillation at tie-lines between the external and the north area at Nordic 32 test system is 10 MW p-p (Fig. 5.25). Also, when the frequency of the forced oscillation has a slightly bigger value - equal to 0.8 Hz – then the resulting amplitude of the oscillation at the same tie-lines is smaller - 8 MW p-p (Fig. 5.26).

The table below shows the amplification of resulting oscillations in accordance with the frequency of forced oscillations on 4072 load.

Table 3: Resonance impact on tie-lines between External and North area regarding frequency of Forced Oscillations

Forced Oscillations (frequency Hz)	*Resulting oscillations (MW)*	*Amplification factor*
0.62	33	1.65
0.7	10	0.5
0.8	8	0.4

Thus, no resonance phenomenon is noticed in the simulation results if there is no coupling of the frequencies between forced and inter-area oscillations.

5.6 Sensitivity to amplitude of forced oscillations

In this subchapter, the results regarding the amplitude of the forced oscillations are going to be tested. The simulation results when forced oscillations have an amplitude equal ***to Inter-Area Mode 1 amplitude (20 MW)*** are used as a **reference**. Then, the same results are obtained when forced oscillations' amplitude is equal to 10 MW and 5 MW. In these simulations, there is a coupling between the frequencies of the Inter-area mode 1 and the forced oscillation. The damping ratio, therefore, is the one of

Inter-area mode 1 and the forced oscillations occur at the generator on bus 4072 which has high controllability.

The obtained simulation results in PowerFactory are shown below.

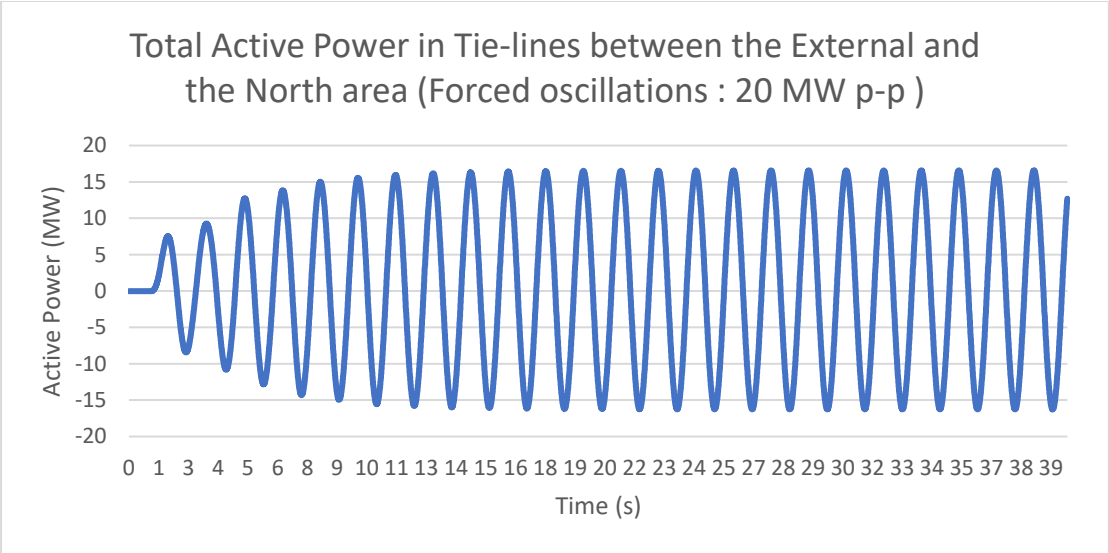

Figure 5. 27: Active Power Oscillations when forced Oscillations amplitude is equal to 20 MW p-p

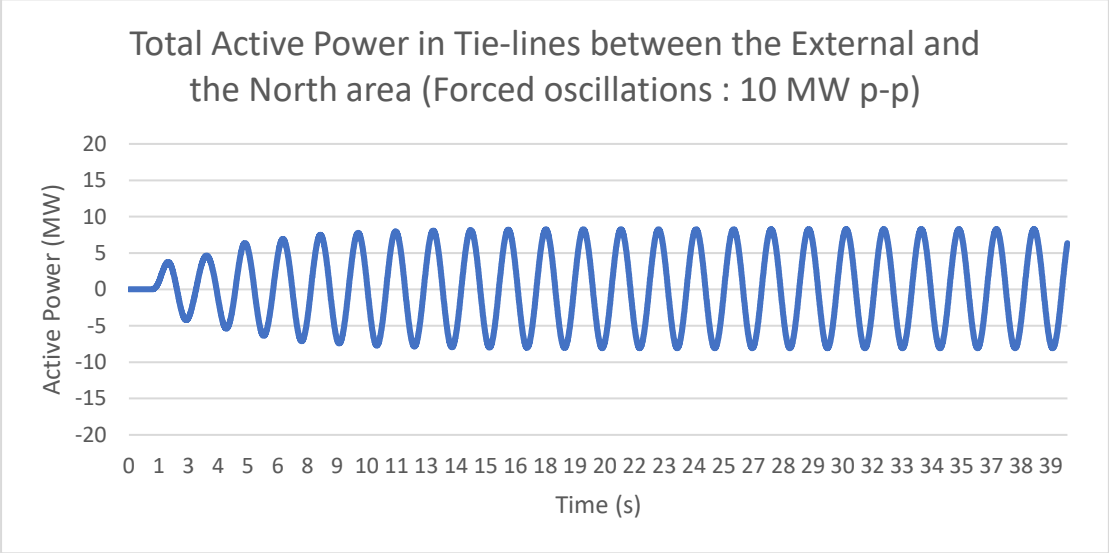

Figure 5. 28: Active Power Oscillations when forced Oscillations amplitude is equal to 10 MW p-p

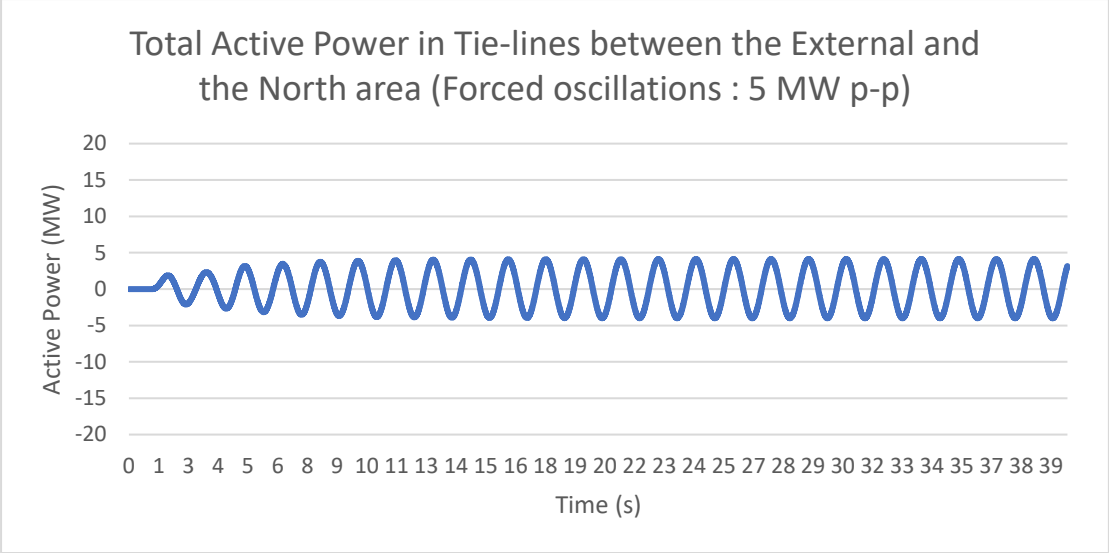

Figure 5. 29: Active Power Oscillations when forced Oscillations amplitude is equal to 5 MW p-p

The table below shows the amplification of resulting oscillations in accordance with the magnitude of forced oscillations on 4072 load.

Table 4: Resonance impact on tie-lines between External and North area regarding magnitude of Forced Oscillations

Forced Oscillations (MW p-p)	*Resulting oscillations (MW)*	*Amplification factor*
20	33	1.65
10	16	1.60
5	8.125	1.625

According to the simulation results, the amplitude of the forced oscillations affects significantly the resonance impact on the tie-lines. In fact, in case the amplitude of the forced oscillations is equal to 20 MW p-p, then the resulting amplitude of the oscillations on the tie-lines between the external and the north area of Nordic 32 test system is equal to 33 MW p-p. If the magnitude of the forced oscillations is decreased in half – 10 MW p-p – then the corresponding resulting amplitude of the oscillations on the same tie-lines also drops to 16 MW p-p. Similarly, in case the magnitude of the forced oscillations is again decreased in half – 5 MW p-p – then the corresponding resulting amplitude of the oscillations on the same tie-lines drops to 8.125 MW p-p as in the previous case.

Therefore, for changes in low amplitude forced oscillations, it can be concluded that the resulting tie-lines oscillations behave almost linearly.

5.7 Sensitivity to controllability – participation factor of forced oscillations location

In this subchapter, the results regarding the location of the forced oscillations are going to be tested. As analyzed in subchapter 5.4, the location where forced oscillations occur is connected to the controllability and the participation factor on that particular bus. Three different cases for each of the inter-area modes are going to be simulated in order to obtain more accurate conclusions.

5.7.1 Simulation results in different forced oscillations location regarding Inter-Area mode 1

The simulation results when there is a coupling between the *Inter-area mode 1* frequency and the forced oscillations frequency of 20 MW p-p are shown in this subchapter. Here, the forced oscillations take place on busbar 4072 where the highest controllability is noticed (Fig. 5.6 and 5.7). Then, the same results are obtained when forced oscillations' location is changed to busbars 63 and 1043, where controllability is less noticeable. The magnitude, as well as the frequency of these forced oscillation remain the same.

Therefore, the obtained simulation results in PowerFactory are shown below.

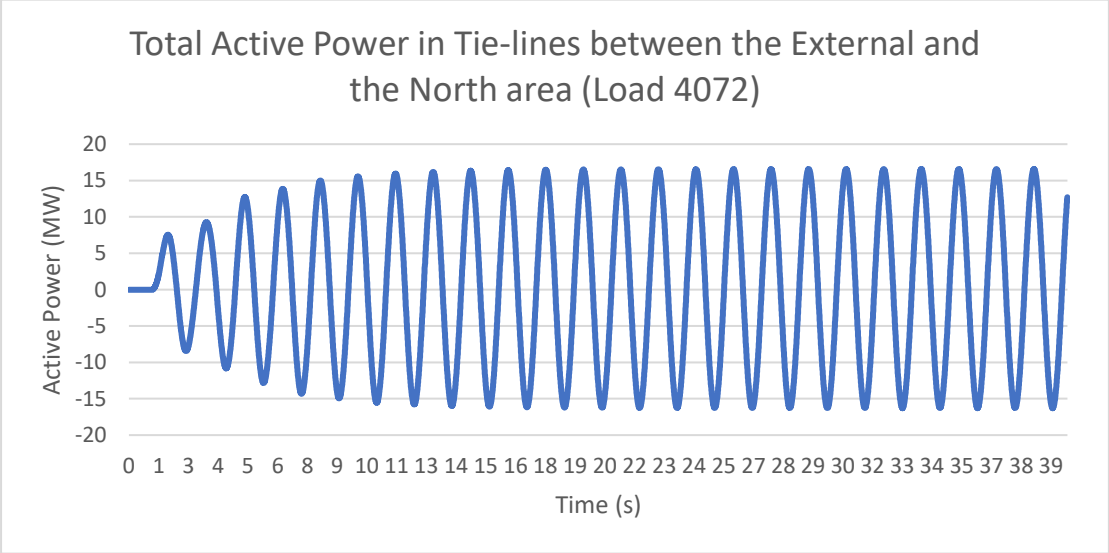

Figure 5. 30: Inter-area mode 1 – Active Power Oscillations when forced Oscillations location is at Bus 4072

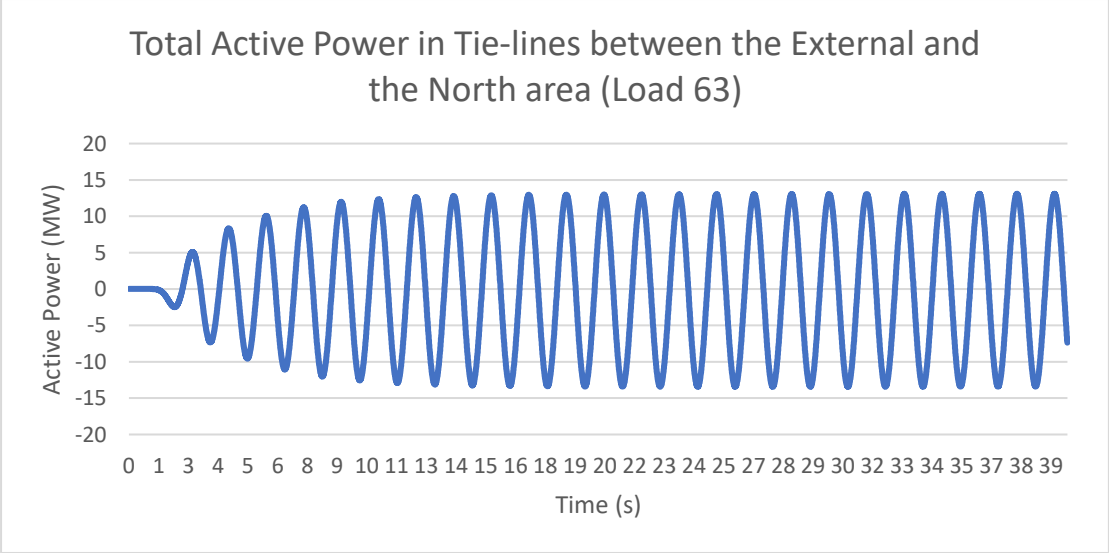

Figure 5. 31: Inter-area mode 1 – Active Power Oscillations when forced Oscillations location is at Bus 63

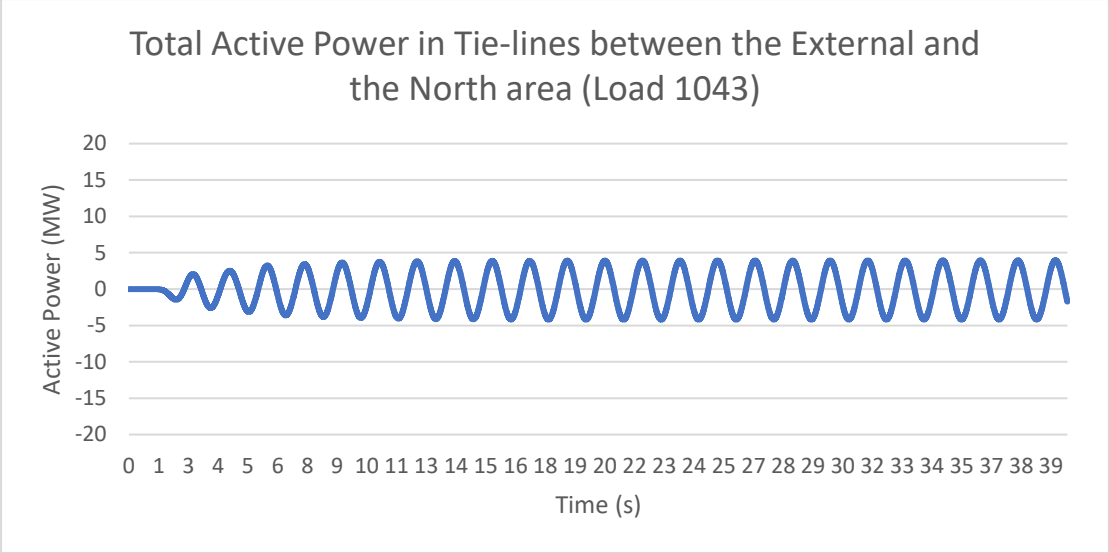

Figure 5. 32: Inter-area mode 1 – Active Power Oscillations when forced Oscillations location is at Bus 1043

The table below shows the normalized participation, controllability and resulting amplification factor in every case simulated, considering machine rotor-angle phi as state variable.

Table 5: Data for mode 149 in specific locations

Busbar/Load	*Amplification factor*	*Controllability*	*Participation*
4072	1.65	1	1
63	1.325	0.25	0.80
1043	0.4	0.02	0.05

As seen in the obtained simulation results, the resulting oscillations have a magnitude of 33 MW p-p in case of forced oscillations with 20 MW magnitude that occur on 4072 bus. However, in case forced oscillations with the same magnitude take place on 63 bus or 1043 bus, which have lower controllability and the rest conditions are exactly the same – frequency coupling, damping ratio – then the resulting oscillations on the same tie-lines have a lower magnitude. The tie-lines oscillations magnitude in these cases is equal to 26.5 MW and 8 MW p-p, which is almost 1.24 and 3.8 times lower than before respectively. This can be noticed in Fig. 5.31 and 5.32 as well as on Table 5.

5.7.2 Simulation results in different forced oscillations location regarding Inter-Area mode 2

Very interesting simulations are obtained in *Inter – area mode 2* case. As mentioned in 5.3 section, there are two busbars – busbar 4063 and busbar 4072 on which the generators are equally controllable (Fig. 5.10 and 5.11). They differ, however, in participation (Fig. 5.12 and 5.13). Forced oscillations of 20 MW p-p due to load variations are taking place with inter-area mode 2 frequency (0.86 Hz) on the corresponding loads on these 2 buses – as well as on load 1043.

The resulting oscillations on the tie-lines between the Southwest area and the Central area of Nordic 32 test system are then calculated and shown below.

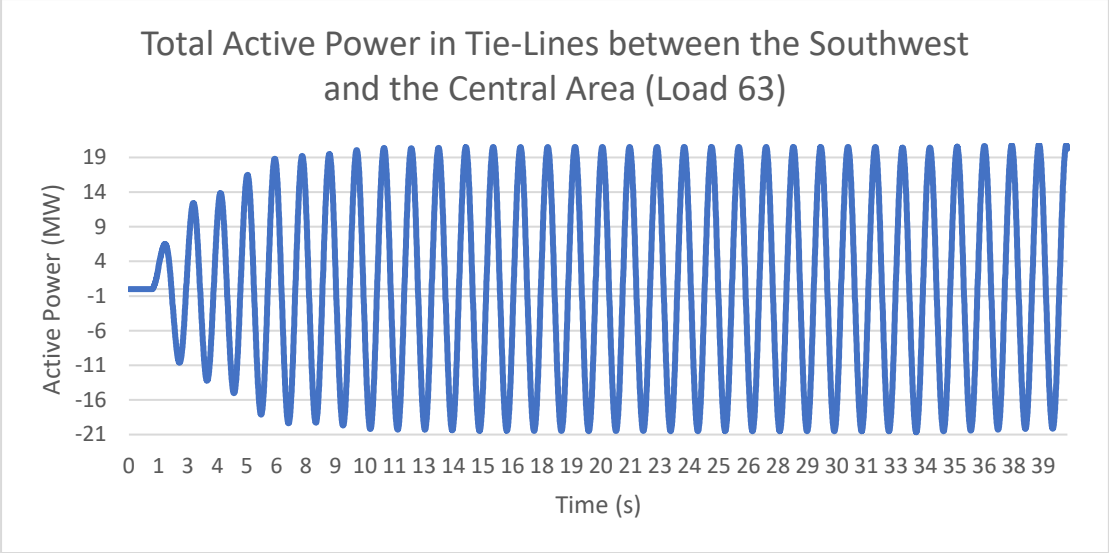

Figure 5. 33: Inter-area mode 2 – Active Power Oscillations when forced Oscillations location is at Bus 63

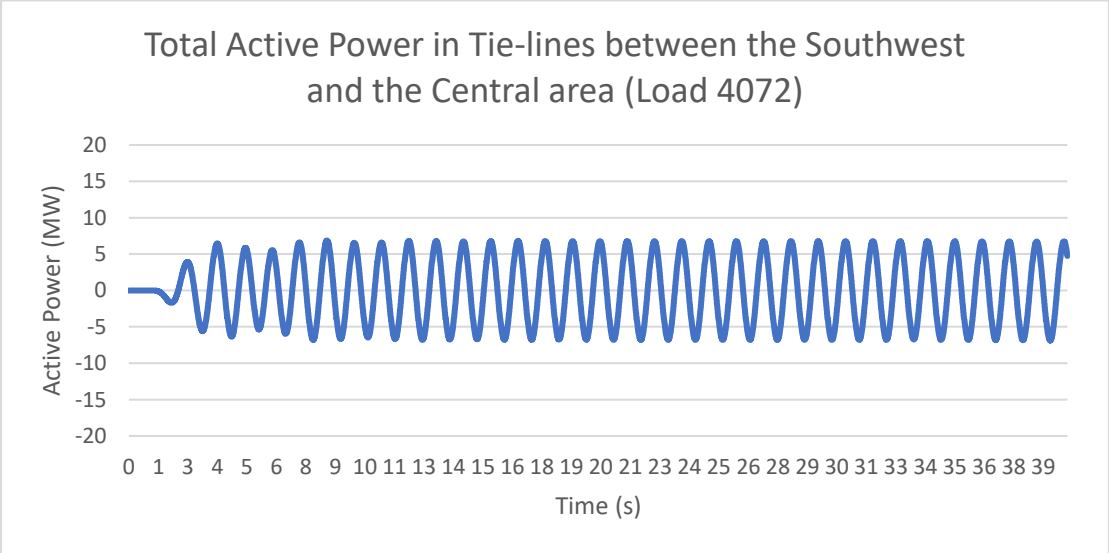

Figure 5. 34: Inter-area mode 2 – Active Power Oscillations when forced Oscillations location is at Bus 4072

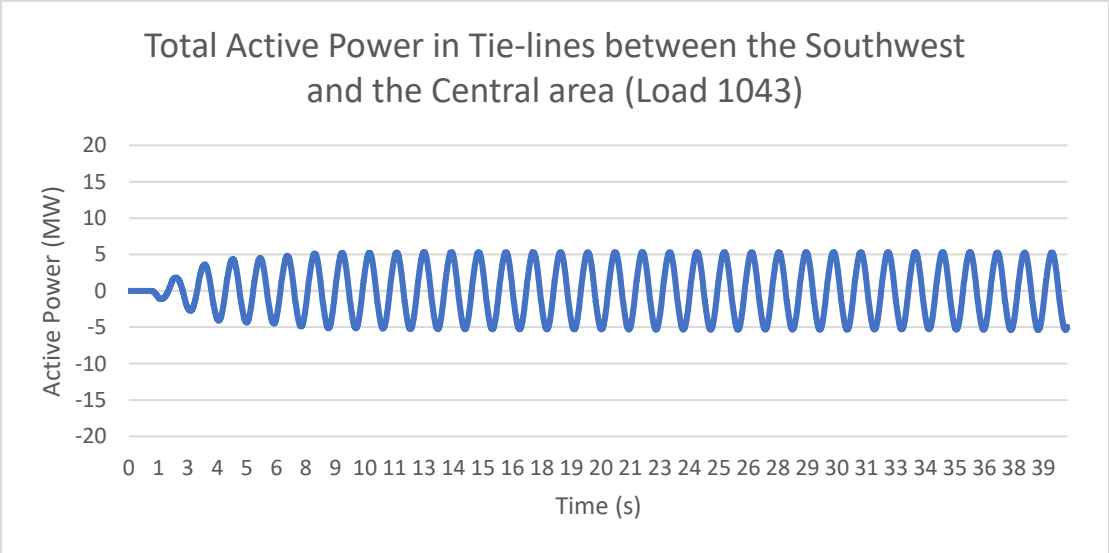

Figure 5. 35: Inter-area mode 2 – Active Power Oscillations when forced Oscillations location is at Bus 1043

The table below shows the normalized participation, controllability and resulting amplification factor in every case simulated, considering machine rotor-angle phi as state variable.

Table 6: Data for mode 145 in specific locations

Busbar/Load	*Amplification factor*	*Controllability*	*Participation*
4072	0.67	1	0.12
63	2.05	0.98	1
1043	0.53	0.08	0.05

As can be seen from graph 5.33, the resonance impact is very high in the resulting oscillation of the tie-lines when the load variations are tested on the load of 4063 bus, which has very high controllability (equal to 0.98) and participation (equal to 1). The magnitude of the resulting oscillations is equal to 40.94 MW p-p.

On the contrary, when the load variations are tested on the load of 4072 bus – which is as controllable as the one on 4063 bus - with the same magnitude and frequency, the resonance impact is negligible. In this case, the magnitude of the resulting oscillations is equal to 13.47 MW p-p (3 times smaller). The controllability is almost the same as in bus 4063 (equal to 1), however the participation is 8.3 times lower (equal to 0.12).

Regarding the resulting oscillations on tie-lines because of forced oscillation on load 1043 (Fig 5.35), they have significantly smaller magnitude compared to those obtained by forced oscillations on load 63 (Fig 5.33). This is reasonable, as generator on busbar 1043 has much smaller controllability and participation magnitude compared to the generator on bus 63, as seen on Table 6.

Therefore, controllability obviously affects the resonance impact on tie-lines oscillations, based on the simulations results. The theoretical background is explained in subchapter 5.3, as controllability is closely connected to the damping ratio of the mode. Since there is a high controllability on 4072 bus – which is located at the edge of the system – and the damping ratio of the *Inter-area mode 1* is low, a significant resonance phenomenon occurs because of the coupling of frequencies between forced and inter-area oscillations. However, in case controllability on a bus is not accompanied with high participation, then the resonance impact on the tie-lines is insignificant as it was proved in the simulations of Fig. 5.34 and 5.35.

5.7.3 Simulation results in different forced oscillations location regarding Inter-Area mode 3

In this subchapter, the simulation results when there is a coupling between the *Inter-area mode 3* frequency and the forced oscillations frequency of 20 MW p-p are shown. Here, the forced oscillations take place on busbar 4072 where the highest controllability is noticed (Fig. 5.14 and 5.15). Then, the same results are obtained when forced oscillations' location is changed to busbars 63 and 1043, where controllability is less noticeable. The magnitude, as well as the frequency of these forced oscillation remain the same.

The obtained simulation results in PowerFactory are shown below.

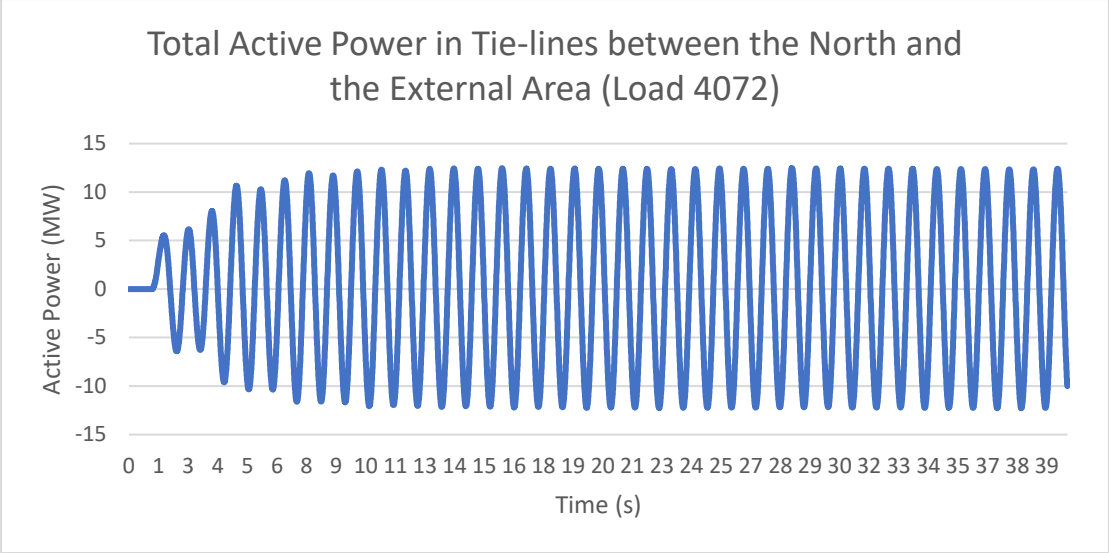

Figure 5. 36: Inter-area mode 3 – Active Power Oscillations when forced Oscillations location is at Bus 4072

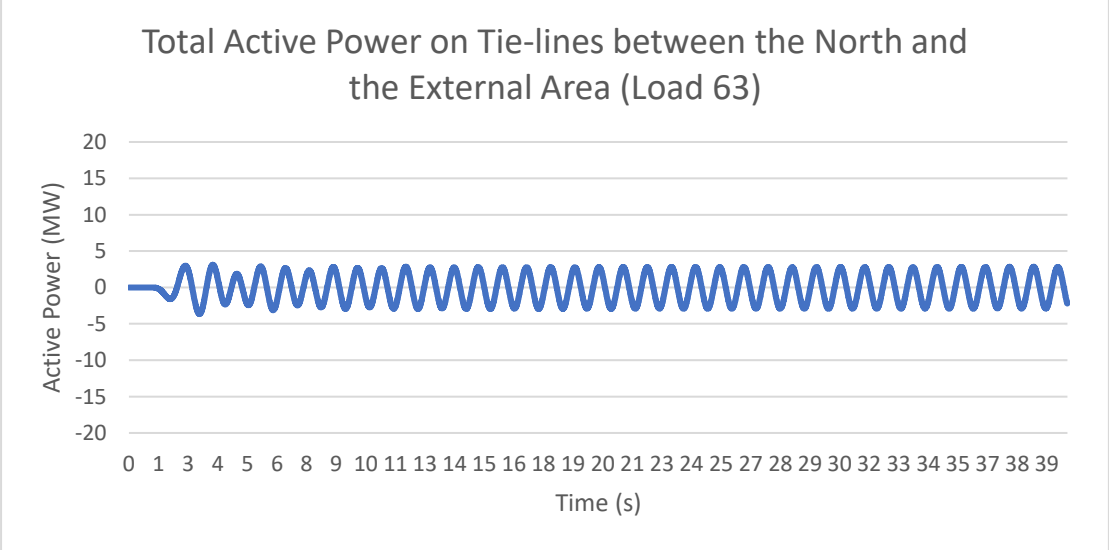

Figure 5. 37: Inter-area mode 3 – Active Power Oscillations when forced Oscillations location is at Bus 63

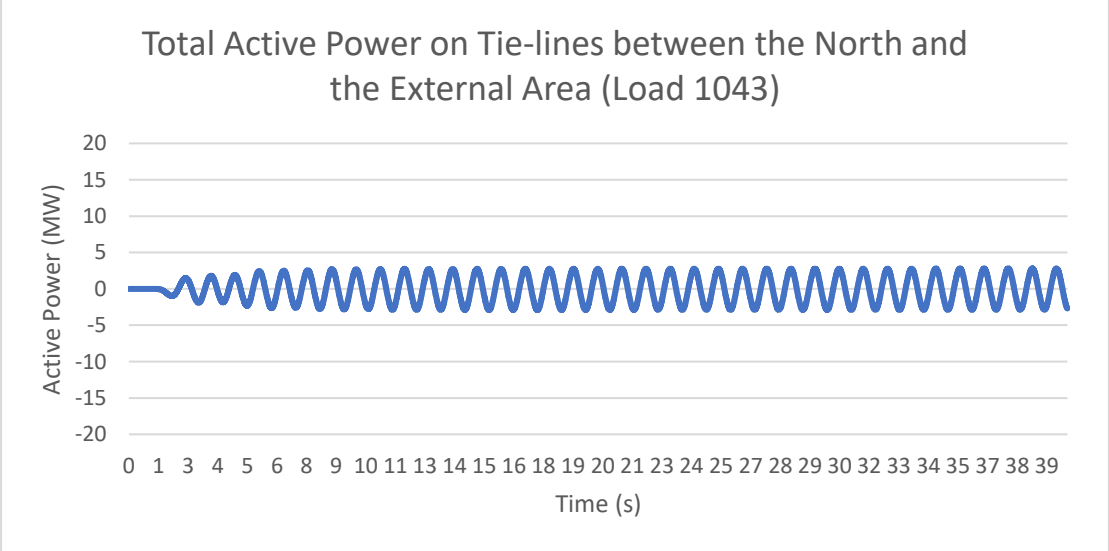

Figure 5. 38: Inter-area mode 3 – Active Power Oscillations when forced Oscillations location is at Bus 1043

The table below shows the normalized participation, controllability and resulting amplification factor in every case simulated, considering machine rotor-angle phi as state variable.

Table 7: Data for mode 142 in specific locations

Busbar/Load	*Amplification factor*	*Controllability*	*Participation*
4072	1.24	1	1
63	0.34	0.06	0.03
1043	0.29	0.03	0.02

The obtained results are very similar to those obtained for Inter-Area mode 1 (section 5.7.1). In fact, based on the obtained simulation results, the resulting oscillations have a magnitude of 24.77 MW p-p in case of forced oscillations with 20 MW magnitude that occur on 4072 bus. However, in case forced oscillations with the same magnitude take place on 63 bus or 1043 bus, which have lower controllability and the rest conditions are exactly the same – frequency coupling, damping ratio – then the resulting oscillations on the same tie-lines have a lower magnitude. The tie-lines oscillations magnitude in these cases is equal to 6.744 MW and 5.713 MW p-p, which is almost 3.67 and 4.33 times lower than before respectively. This can be noticed in Fig. 5.37 and 5.38 as well as on Table 7.

5.7.4 Conclusions on the impact of controllability and participation

The simulation results obtained in the previous subchapters, prove that the location where forced oscillations take place clearly affect the impact of resonance phenomena on the corresponding tie-lines. The magnitude of controllability on the generators of the buses is a major factor for the magnitude of resulting oscillations. However, participation seems to be a more critical factor for the resonance impact, as analyzed in subchapter 5.7.2.

According to the 3 inter-area mode cases analyzed, the participation factor values are somewhat proportional to the amplification of resulting oscillations. It has to be noticed, though, that their relationship appears to be non-linear and needs further research.

An overview table is given below where the whole analysis of subchapter 5.7 is summarized - the amplification factor values are rounded to one decimal place. In that way, the comparison and the understanding of the obtained results is more feasible.

Table 8: Summarized analysis of controllability-participation sensitivity

Busbar/Load	*Mode 1*	*Controllability*	*Participation*	*Amplification Factor*
4072	149	1	1	1.7
63	149	0.25	0.80	1.3
1043	149	0.02	0.05	0.4
Busbar/Load	*Mode 2*	*Controllability*	*Participation*	*Amplification Factor*
4072	145	1	0.12	0.7
63	145	0.98	1	2.1
1043	145	0.08	0.05	0.5
Busbar/Load	*Mode 3*	*Controllability*	*Participation*	*Amplification Factor*
4072	142	1	1	1.2
63	142	0.06	0.03	0.3
1043	142	0.03	0.02	0.3

5.8 Sensitivity to the kind of forced oscillations (ramp load events vs step load events)

In this subchapter, the results regarding the kind of the load variations of the forced oscillations are going to be tested. The simulation results when load variations consist of ramp events with an ***amplitude of 20 MW*** are used as a **reference**. Then, the same results are obtained when load variations consist of step load events.

In fact, these step load events form square waves that correspond to sine waves with the same frequency – as the fundamental harmonic frequency has the biggest impact on the formation of square waves. According to Fourier analysis, the amplitude of the corresponding sine waves is given below.

$$A_{sine} = \frac{4}{\pi} A_{square} = \frac{4}{\pi}\ 20\ MW \quad \textbf{(43)}$$

The default ramp load events that correspond to the forced oscillations and affect Inter-area mode 1 oscillations of the tie-lines are already shown in Fig. 5.18. The step load events – with the same amplitude – that affect the same inter-area mode are shown below.

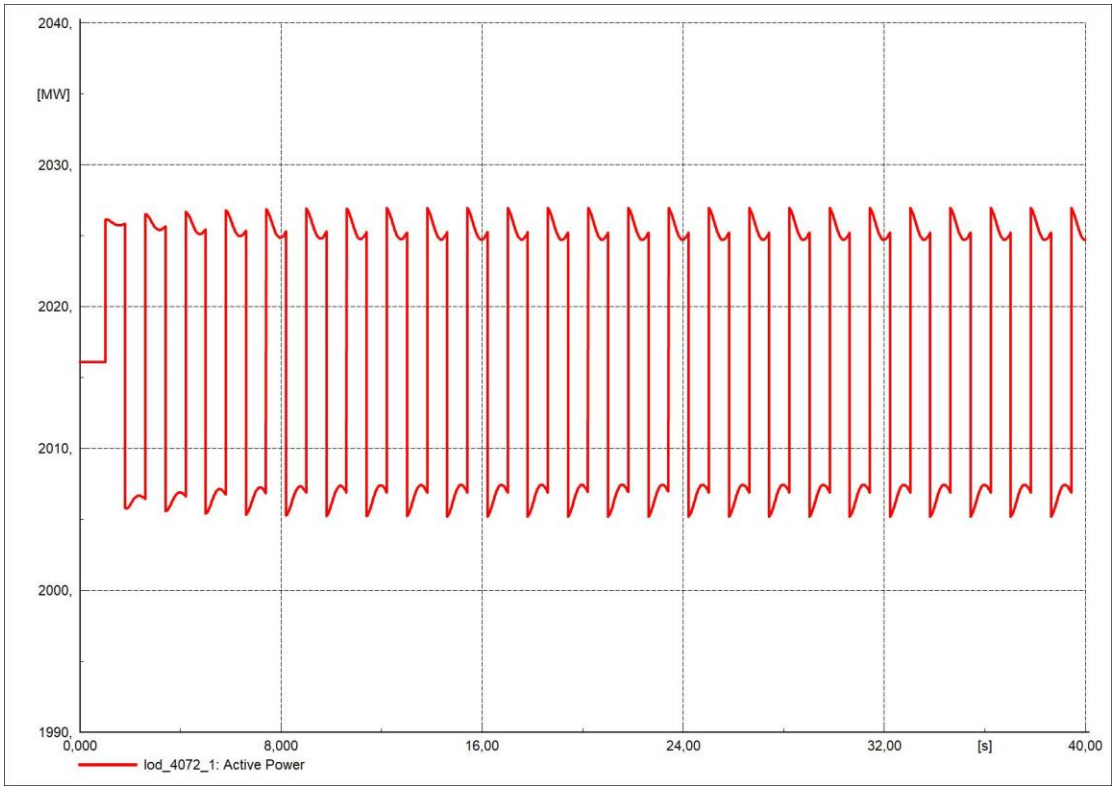

Figure 5. 39: Step Load events that create load variations on 4072 load

The resulting oscillations on the tie-lines between the External area and the North area of Nordic 32 test system – while having the step load events mentioned above – are depicted in the following figure.

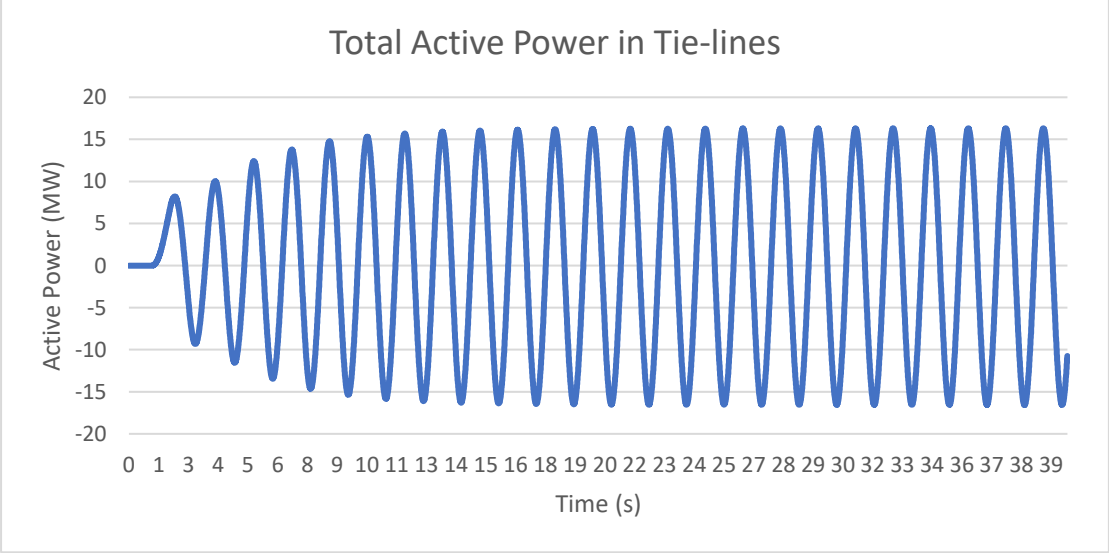

Figure 5. 40: Active Power Oscillations when load variations are created by step load events

By observing the resulting tie-lines oscillations in Fig. 5.40, and after comparing them with the results on the same tie-lines created by ramp load events (Fig. 5.21), it can be concluded that they are almost the same. Resulting tie-lines oscillations created by step load events have a slightly larger amplitude equal to 33.5 MW p-p. The small arcs on the top and bottom of each step in Fig. 5.39 (because of the load model utilized in PowerFactory simulations) are probably the reason of this small difference. But in

general, the comparison of the amplified active power oscillations between these two cases – both of which create a strong resonance phenomenon – does not have very strong differences as the cases of the previous subchapters.

6. Conclusion and Future Work

6.1 Conclusions

This project studied the resonance impact of forced oscillations when interacting with inter-area electromechanical oscillations. Simulation results on several cases were obtained by utilizing the DigSilent PowerFactory software and analyzing the resonance phenomenon on Nordic 32 test system. The resonance analysis was performed based on small signal stability analysis from which the inter-area modes were obtained. Low values of frequency and damping ratio were set as a criterion for identifying the inter-area modes.

The main objectives listed in the introduction of the project are met in a satisfying level through this project. In fact, the information collected while working on the thesis project provides great value to the knowledge of the phenomenon of resonance on inter-area modes oscillations because of forced oscillations. Furthermore, certain scenarios were noticed through the studies performed in the project. In fact, investigations of forced oscillations reasons to buses and areas with significant controllability of the affected mode is highly recommended, as this is a strong case scenario that can lead to resonance phenomena on the power system. Also, in case real measurements can be utilized for identifying the distinct shape of the amplification behavior shown in the simulations, the identification of resonance amplified oscillations by engineers could be simplified.

The main factors affecting the amplitude of oscillations on tie-lines due to forced oscillations were studied in the simulation part. These factors were:

- Frequency value of forced oscillations
- Controllability magnitude of busbar where forced oscillations occured
- Amplitude of forced oscillations

The kind of forced oscillations was also tested in the simulations as the impact of ramp load events and step load events was tested on the resulting oscillations. However, it was shown that the resonance impact was not affected significantly by that factor.

As far as the three factors mentioned above are concerned, simulations proved their importance for the resonance phenomenon in power systems. In case any of these factors was slightly changed, resonance impact was dropped significantly on the corresponding tie-lines oscillations. Especially in case of a slight frequency change on forced oscillations or in case of a smaller controllability amplitude on the bus where these oscillations occurred, the resonance phenomenon was diminished on the tie-lines.

The importance of this phenomenon is vital for future power grids and especially for the Nordic power grid. Therefore, it is suggested to Nordic TSOs to keep studying it, create scenarios in which this phenomenon can occur and come up with ways to prevent it, otherwise it would lead to severe stability issues. These scenarios should be taken into deep consideration when connecting large loads and generators to the power grid. Past resonance phenomena that happened in other countries' power grids should also be studied in order to inherit the knowledge already obtained in such situations.

6.2 Future Work

As mentioned at the beginning of section 5.2, voltage dependency is taken into account for the load flow analysis of the Nordic 32 test system in all the simulations implemented. The ZIP model parameters have the same values in PowerFactory as the ones Svenska Kraftnät utilizes. However, it would be very beneficial to further analyze the impact of changing the parameters of voltage dependency. For instance, if the load model is based solely on constant power ($\boldsymbol{P_P}$: $\mathbf{100}\%$), while keeping the rest parameters of the model same, the resulting oscillations are affected but not in the same way as in the simulation results. Thus, the impact of load modelling on the resonance impact needs further research.

Furthermore, controllability of the modes, its connection with the participation factor of the same modes and their resonance impact is a fact that needs further research. This outcome is based on the simulation results obtained in 5.7 section for *Inter-area mode 2*, where forced oscillations at a high controllable bus of the Nordic 32 test system (bus 4072) with low participation did not result in resonance on the active power of the tie-lines. In case of high participation, controllability is a crucial factor of the resonance impact since it is directly linked to the location of the forced oscillations. However, the level in which controllability of a mode affects the resonance impact in case its participation is low is a fact that should be further investigated. In addition, since participation is the combination of controllability and observability of a mode, the role of observability on the participation, and thus on the resulting resonance impact, is also a matter that must be searched in depth in real-case measurements.

The residues of the transfer function of the system can be further studied, too. In fact, the relationship between the generators and the forced oscillation location – which is described by the corresponding transfer function – may lead to more information about the influence of generators to the resonance impact.

Finally, alterations of operating state, like the level of power flow over tie lines in the system, influences the damping of the modes. Studying several power flow scenarios would be of interest to identify possible additional factors influencing the resonance amplification from forced oscillations. The damping ratio at a certain mode is such a factor, as its value is affected in case of changes in active power flow while the initial power balance on the loads is preserved. However, the frequency of the mode would also be affected. So forced oscillations signals with the new frequency should be injected, otherwise, the frequency coupling will not be obtained, and the study of resonance phenomenon would not be feasible. Altering of PSS parameters have direct impact on one or several modes of the system (both damping and frequency); thus, this would affect the resonance impact. Therefore, addressing PSS controller parameters and their connection with the resonance impact is a task that should be further studied.

Bibliography

[1] Kundur, Prabha, Neal J. Balu, and Mark G. Lauby. Power system stability and control. Vol. 7. New York: McGraw-hill, 1994.

[2] Rogers, Graham. Power system oscillations. Springer Science & Business Media, 2012.

[3] M. Ghandhari, “Stability of Power Systems - An introduction”, Royal Institute of Technology (KTH), Electric Power and Energy Systems, 2018

[4] Vanfretti, Luigi, et al. "Effects of forced oscillations in power system damping estimation." 2012 IEEE International Workshop on Applied Measurements for Power Systems (AMPS) Proceedings. IEEE, 2012.

[5] Meng, Yao, et al. "Forced oscillation source location via multivariate time series classification." 2018 IEEE/PES Transmission and Distribution Conference and Exposition (T&D). IEEE, 2018.

[6] Bin, W. A. N. G., and S. U. N. Kai. "Location methods of oscillation sources in power systems: a survey." Journal of Modern Power Systems and Clean Energy 5.2 (2017): 151-159.

[7] Seppänen, Janne, et al. "Resonance of Forcing Oscillations and Inter-Area Modes in the Nordic Power System." 2018 IEEE PES Innovative Smart Grid Technologies Conference Europe (ISGT-Europe). IEEE, 2018.

[8] Entso-E grid map. Available: https://docstore.entsoe.eu/Documents/Publications/maps/2019/Map_Northern-Europe-3.000.000.pdf

[9] Messina, Arturo Roman, ed. Inter-area oscillations in power systems: a nonlinear and nonstationary perspective. Springer Science & Business Media, 2009.

[10] Chompoobutrgool, Yuwa. Concepts for power system small signal stability analysis and feedback control design considering synchrophasor measurements. Diss. KTH Royal Institute of Technology, 2012.

[11] Resnick and Halliday (1977). Physics (3rd ed.). John Wiley & Sons. p. 324.

[12] Sarmadi, S. Arash Nezam, and Vaithianathan Venkatasubramanian. "Inter-area resonance in power systems from forced oscillations." IEEE Transactions on Power Systems31.1 (2015): 378-386.

[13] Samuelsson, Olof. "Load modulation at two locations for damping of electro-mechanical oscillations in a multimachine system." 2000 Power Engineering Society Summer Meeting (Cat. No. 00CH37134). Vol. 3. IEEE, 2000.

[14] Qi, Le. Modelica driven power system modeling, simulation and validation. Diss. Master’s thesis, Royal Institute of Technology (KTH), 2014.

[15] Walve, Kenneth. "'Nordic32A–A Cigre test system for simulation of transient stability and long-term dynamics." Svenska Kraftnät(1993).

[16] Peppas, Dimitris. "Development and analysis of Nordic32 power system model in PowerFactory." (2008).

[17] User Manual, DIgSILENT Power Factory 2019. "Version 2019" DIgSILENT GmbH, Gomaringen, Germany (2018).

[18] Shim, Jae Woong, et al. "Impact analysis of variable generation on small signal stability." 2014 Australasian Universities Power Engineering Conference (AUPEC). IEEE, 2014.

[19] S. Elenius, K. Uhlen, and E. Lakervi, “Effects of controlled shunt and series compensation on damping in the Nordel system, “IEEE Trans. Power Syst., vol. 20, no. 4, pp. 1946-1957, Nov. 2005.

[20] Hillberg, Emil. "Development of improved aggregated load models for power system network planning in the Nordic power system Part 1: Method development." (2018).

Appendix A

A.1 Busbars

Node	Area	Nominal Voltage (kV)	Active Load (MW)	Reactive Load (MVar)	Active Compensation (MW)	Reactive Compensation (MVar)
1011	North	130	200	80	0	0
1012	North	130	300	100	0	0
1013	North	130	100	40	0	0
1014	North	130	0	0	0	0
1021	North	130	0	0	0	0
1022	North	130	280	95	0	50
1041	Central	130	600	20	0	200
1042	Central	130	300	80	0	0
1043	Central	130	230	100	0	150
1044	Central	130	800	300	0	200
1045	Central	130	700	250	0	200
2031	North	220	100	30	0	0
2032	North	220	200	50	0	0
4011	North	400	0	0	0	0
4012	North	400	0	0	0	-100
4021	North	400	0	0	0	0
4022	North	400	0	0	0	0
4031	North	400	0	0	0	0
4032	North	400	0	0	0	0
4041	Central	400	0	0	0	200
4042	Central	400	0	0	0	0
4043	Central	400	0	0	0	200
4044	Central	400	0	0	0	0
4045	Central	400	0	0	0	0
4046	Central	400	0	0	0	100
4047	Central	400	0	0	0	0
4051	Central	400	0	0	0	100
4061	Southwest	400	0	0	0	0
4062	Southwest	400	0	0	0	0
4063	Southwest	400	0	0	0	0
4071	External	400	300	100	0	-400
4072	External	400	2000	500	0	0
41	Central	130	540	128.28	0	0
42	Central	130	400	125.67	0	0
43	Central	130	900	238.83	0	0
46	Central	130	700	193.72	0	0
47	Central	130	100	45.19	0	0
51	Central	130	800	253.22	0	0
61	Southwest	130	500	112.31	0	0
62	Southwest	130	300	80.02	0	0
63	Southwest	130	590	256.19	0	0

A.2 Transmission Lines

Line name	From	To	Line Number	Resistance (Ω)	Inductance (Ω)	S_{nom} (MVA)
1011-1013	1011	1013	1	1.69	11.83	1400
1011-1013	1011	1013	2	1.69	11.83	1400
1012-1014	1012	1014	1	2.366	15.21	1400
1012-1014	1012	1014	2	2.366	15.21	1400
1013-1014	1013	1014	1	1.183	8.45	1400
1013-1014	1013	1014	2	1.183	8.45	1400
1021-1022	1021	1022	1	5.07	33.8	1400
1021-1022	1021	1022	2	5.07	33.8	1400
1041-1043	1041	1043	1	1.69	10.14	1400
1041-1043	1041	1043	2	1.69	10.14	1400
1041-1045	1041	1045	1	2.535	20.28	1400
1041-1045	1041	1045	2	2.535	20.28	1400
1042-1044	1042	1044	1	6.422	47.32	1400
1042-1044	1042	1044	2	6.422	47.32	1400
1042-1045	1042	1045	1	8.45	50.7	1400
1043-1044	1043	1044	1	1.69	13.52	1400
1043-1044	1043	1044	2	1.69	13.52	1400
2031-2032	2031	2032	1	5.808	43.56	1400
2031-2032	2031	2032	2	5.808	43.56	1400
4011-4012	4011	4012	1	1.6	12.8	1400
4011-4021	4011	4021	1	9.6	96	1400
4011-4022	4011	4022	1	6.4	64	1400
4011-4071	4011	4071	1	8	72	1400
4012-4022	4012	4022	1	6.4	56	1400
4012-4071	4012	4071	1	8	80	1400
4021-4032	4021	4032	1	6.4	64	1400
4021-4042	4021	4042	1	16	96	1400
4022-4031	4022	4031	1	6.4	64	1400
4022-4031	4022	4031	2	6.4	64	1400
4031-4032	4031	4032	1	1.6	16	1400
4031-4041	4031	4041	1	9.6	64	1400
4031-4041	4031	4041	2	9.6	64	1400
4032-4042	4032	4042	1	16	64	1400
4032-4044	4032	4044	1	9.6	80	1400
4041-4044	4041	4044	1	4.8	48	1400
4041-4061	4041	4061	1	9.6	72	1400
4042-4043	4042	4043	1	3.2	24	1400
4042-4044	4042	4044	1	3.2	32	1400
4043-4044	4043	4044	1	1.6	16	1400
4043-4046	4043	4046	1	1.6	16	1400
4043-4047	4043	4047	1	3.2	32	1400
4044-4045	4044	4045	1	3.2	32	1400
4044-4045	4044	4045	2	3.2	32	1400
4045-4051	4045	4051	1	6.4	64	1400
4045-4051	4045	4051	2	6.4	64	1400
4045-4062	4045	4062	1	17.6	128	1400
4046-4047	4046	4047	1	1.6	24	1400
4061-4062	4061	4062	1	3.2	32	1400
4062-4063	4062	4063	1	4.8	48	1400
4062-4063	4062	4063	2	4.8	48	1400
4071-4072	4071	4072	1	4.8	48	1400
4071-4072	4071	4072	2	4.8	48	1400

A.3 Transformers

Transformer Name	HV Busbar	LV Busbar	Number	Area	Rating (MVA)	HV Side (kV)	LV Side (kV)
4011-1011	4011	1011	1	North	1000	400	130
4012-1012	4012	1012	1	North	1000	400	130
4022-1022	4022	1022	1	North	1000	400	130
4031-2031	4031	2031	1	North	1000	400	220
4044-1044	4044	1044	1	Central	1000	400	130
4044-1044	4044	1044	2	Central	770	400	130
4045-1045	4045	1045	1	Central	1430	400	130
4045-1045	4045	1045	2	Central	100	400	130
4041-41	4041	41	1	Central	100	400	130
4042-42	4042	42	1	Central	100	400	130
4043-43	4043	43	1	Central	100	400	130
4046-46	4046	46	1	Central	1000	400	130
4047-47	4047	47	1	Central	250	400	130
4051-51	4051	51	1	Central	1430	400	130
4061-61	4061	61	1	Southwest	770	400	130
4062-62	4062	62	1	Southwest	500	400	130
4063-63	4063	63	1	Southwest	1000	400	130

A.4 Generators

Busbar	Rating (MVA)	Xd	Xq	Xd’	Xq’	Xd’’	Xq’’	Td’	Tq’	Td’’	Tq’’
1012	800	1.1	0.7	0.25	-	0.2	0.2	1.13636	-	0.04	0.0285714
1013	600	1.1	0.7	0.25	-	0.2	0.2	1.13636	-	0.04	0.0285714
1014	700	1.1	0.7	0.25	-	0.2	0.2	1.13636	-	0.04	0.0285714
1021	600	1.1	0.7	0.25	-	0.2	0.2	1.13636	-	0.04	0.0285714
1022	250	1.1	0.7	0.25	-	0.2	0.2	1.13636	-	0.04	0.0285714
1042	400	2.2	2	0.3	0.4	0.2	0.2	0.954545	0.3	0.03333	0.025
1043	200	2.2	2	0.3	0.4	0.2	0.2	0.954545	0.3	0.03333	0.025
2032	850	1.1	0.7	0.25	-	0.2	0.2	1.13636	-	0.04	0.0285714
4011	1000	1.1	0.7	0.25	-	0.2	0.2	1.13636	-	0.04	0.0285714
4012	800	1.1	0.7	0.25	-	0.2	0.2	1.13636	-	0.04	0.0285714
4021	300	1.1	0.7	0.25	-	0.2	0.2	1.13636	-	0.04	0.0285714
4031	350	1.1	0.7	0.25	-	0.2	0.2	1.13636	-	0.04	0.0285714
4041	300	1.55	1	0.3	-	0.2	0.2	1.35484		0.03333	0.02
4042	700	2.2	2	0.3	0.4	0.2	0.2	0.954545	0.3	0.03333	0.025
4047	600	2.2	2	0.3	0.4	0.2	0.2	0.954545	0.3	0.03333	0.025
4047	600	2.2	2	0.3	0.4	0.2	0.2	0.954545	0.3	0.03333	0.025
4051	700	2.2	2	0.3	0.4	0.2	0.2	0.954545	0.3	0.03333	0.025
4051	700	2.2	2	0.3	0.4	0.2	0.2	0.954545	0.3	0.03333	0.025
4062	600	2.2	2	0.3	0.4	0.2	0.2	0.954545	0.3	0.03333	0.025
4063	600	2.2	2	0.3	0.4	0.2	0.2	0.954545	0.3	0.03333	0.025
4063	600	2.2	2	0.3	0.4	0.2	0.2	0.954545	0.3	0.03333	0.025
4071	500	1.1	0.7	0.25	-	0.2	0.2	1.13636	-	0.04	0.0285714
4072	4500	1.1	0.7	0.25	-	0.2	0.2	1.13636	-	0.04	0.0285714

A.5 Loads

Load name	Busbar	Active Consumption (MW)	Reactive Consumption (MVar)	Rating (MVA)
Load 1011	1011	200	80	100
Load 1012	1012	300	100	100
Load 1013	1013	100	40	100
Load 1022	1022	280	95	100
Load 1041	1041	600	20	100
Load 1042	1042	300	80	100
Load 1043	1043	230	100	100
Load 1044	1044	800	300	100
Load 1045	1045	700	250	100
Load 2031	2031	100	30	100
Load 2032	2032	200	50	100
Load 4071	4071	300	100	100
Load 4072	4072	2000	500	100
Load 41	41	540	128.28	100
Load 42	42	400	125.67	100
Load 43	43	900	238.83	100
Load 46	46	700	193.72	100
Load 47	47	100	45.19	100
Load 51	51	800	253.22	100
Load 61	61	500	112.31	100
Load 62	62	300	80.02	100
Load 63	63	590	256.19	100

Appendix B

B.1 Excitation System

	Round Rotor (Thermal plants)	Salient Pole (Hydro Plants)	Salient Pole (Synchronous Compensator)
K	120	50	50
TA	5	4	4
TB	50	20	20
TE	0.1	0.1	0.1
EMAX	5	4	4
EMIN	0	0	0

B.2 Hydro-Governor System

Permanent droop (R)	0.04
Temporary droop (r)	5
Velocity limits (pu)	max 0.1
Position limits (pu)	min 0 - max 0.95
Governor time constant $\boldsymbol{T_r}$ (s)	5
Filter time constant $\boldsymbol{T_f}$ (s)	0.05
Servo time constant $\boldsymbol{T_g}$ (s)	0.2
Water time constant $\boldsymbol{T_W}$ (s)	1

- Permanent droop (R): At buses 4071 and 4072, the value of Permanent droop (R) is 0.08
- Temporary droop (r): At buses 4071 and 4072, the value of Temporary droop (r) is 0.16

B.3 Power System Stabilizer

Washout factor (K2) (pu)	1
Washout time constant (T2) (s)	4
Signal Transducer 1st factor (K3) (pu)	1
Signal Transducer Time constant (T3) (s)	2
Output Filter factor (K5) (s)	1
Output Filter Time constant (T5) (s)	0.05
Signal Transducer 2nd factor (K4) (pu)	0.3

Appendix C

C.1 Normalized controllability and participation in *Inter-area mode 1* for all generators in Nordic 32 tests system

Generator	Controllability (State Variable: phi)	Controllability (State Variable: speed)	Participation (State Variable: phi)	Participation (State Variable: speed)
sym_4072_1	1	1	1	1
sym_4063_1	0.251632793	0.248208177	0.80747301	0.395439866
sym_4063_2	0.251632793	0.248208177	0.80747301	0.395439866
sym_4062_1	0.210084003	0.206639628	0.616006157	0.293890563
sym_4051_1	0.147147646	0.144221154	0.400377894	0.186320463
sym_4051_2	0.140555689	0.137589059	0.396550733	0.186126241
sym_4047_1	0.102650619	0.100523396	0.214111537	0.090389531
sym_4047_2	0.102650619	0.100523396	0.214111537	0.090389531
sym_4042_1	0.097510628	0.095503145	0.173124793	0.067331904
sym_4071_1	0.085360234	0.08448112	0.052893053	0.064767565
sym_4011_1	0.083343157	0.083234626	0	0.032170478
sym_1042_1	0.081440814	0.079787324	0.219664493	0.101991212
sym_1012_1	0.076099103	0.075997517	0.00661855	0.033428315
sym_1014_1	0.072358483	0.070516205	0.0092729	0.03279543
sym_4012_1	0.071413469	0.070351828	0.002639247	0.028744933
sym_1013_1	0.059914874	0.059950032	0.007432224	0.027733226
sym_2032_1	0.041453633	0.039948218	0.043926645	0.010685214
sym_1021_1	0.029564515	0.028869513	0.005622355	0.007998454
sym_1043_1	0.02148516	0.019913646	0.052172606	0.022108032
sym_4041_1	0.019571908	0.018715986	0.046939463	0.020381299
sym_4031_1	0.015224155	0.014581991	0.018802127	0.005430129
sym_4021_1	0.009505694	0.009045916	0.010179889	0.002463003
sym_1022_1	0.007848115	0.007188838	0.00338291	0.000902914

C.2 Normalized controllability and participation in *Inter-area mode 2* for all generators in Nordic 32 tests system

Generator	Controllability (State Variable: phi)	Controllability (State Variable: speed)	Participation (State Variable: phi)	Participation (State Variable: speed)
sym_4072_1	1	1	0.118574224	0.093043906
sym_4063_1	0.982404646	0.985127011	1	1
sym_4063_2	0.982404646	0.985127011	1	1
sym_4062_1	0.677348727	0.678225298	0.500794878	0.494798602
sym_4051_1	0.55932348	0.559883306	0.457576217	0.485810721
sym_4051_2	0.555619868	0.55625094	0.485782018	0.514730889
sym_4047_1	0.456609624	0.456626244	0.253632905	0.273234812
sym_4047_2	0.456609624	0.456626244	0.253632905	0.273234812
sym_1042_1	0.451880299	0.452322358	0.497511879	0.523660223
sym_4042_1	0.389649155	0.389159291	0.141435188	0.156063582
sym_2032_1	0.197715858	0.191254161	0.016702778	0.022024336
sym_1021_1	0.140074233	0.136942686	0.002892596	0.001282634
sym_1043_1	0.082948463	0.08172092	0.04738429	0.050225147
sym_4011_1	0.074053534	0.072930783	0	0.002101609
sym_1012_1	0.058909508	0.05797331	0.000787292	0.00093441
sym_1014_1	0.057381259	0.055772475	0.001082717	0.000570019
sym_4021_1	0.056063471	0.054697453	0.00942622	0.002617652
sym_4071_1	0.054944362	0.054125412	0.004094534	0.010891513
sym_4012_1	0.053415725	0.052089407	0.000513471	0.000993769
sym_4031_1	0.052129735	0.050162876	0.006147126	0.000805904
sym_1013_1	0.050859101	0.049975976	0.000711532	0.007478579
sym_1022_1	0.034600599	0.033368653	0.000618037	0.001566188
sym_4041_1	0.020506981	0.01991228	0.004117929	0.004607203

C.3 Normalized controllability and participation in *Inter-area mode 3* for all generators in Nordic 32 tests system

Generator	Controllability (State Variable: phi)	Controllability (State Variable: speed)	Participation (State Variable: phi)	Participation (State Variable: speed)
sym_4072_1	1	1	1	0.978029376
sym_1021_1	0.371686349	0.364557219	0.417850527	1
sym_2032_1	0.217832147	0.21186929	0.053435898	0.254991032
sym_1014_1	0.166587757	0.162881887	0.023625273	0.166492921
sym_4011_1	0.163471328	0.161390855	0	0.12518068
sym_1012_1	0.158599263	0.156560662	0.01095363	0.1400936
sym_4051_2	0.154275806	0.155703098	0.180663342	0.199146195
sym_4051_1	0.145812083	0.14704178	0.162955518	0.174130994
sym_1013_1	0.144329915	0.142599205	0.023862701	0.151904363
sym_4012_1	0.133167654	0.13063307	0.001289427	0.100996436
sym_1042_1	0.088974423	0.089442441	0.123857116	0.149167849
sym_4042_1	0.059187578	0.057446294	0.020388158	0.010476924
sym_1022_1	0.056230485	0.056095838	0.012165005	0.010162599
sym_4063_1	0.055422288	0.056095838	0.028722436	0.010162599
sym_4063_2	0.055422288	0.054550453	0.028722436	0.062287085
sym_4047_1	0.046536564	0.045045279	0.019565392	0.007423493
sym_4047_2	0.046536564	0.045045279	0.019565392	0.007423493
sym_4062_1	0.038893526	0.039664439	0.0194125	0.005590253
sym_4071_1	0.035531809	0.035493116	0.021633765	0.010367635
sym_4031_1	0.031917691	0.030314578	0.004023825	0.017163097
sym_1043_1	0.026471492	0.026877225	0.018353092	0.011835276
sym_4021_1	0.025288209	0.024120292	0.004471882	0.011244274
sym_4041_1	0.010160025	0.008577874	0.004245918	0.001082826